

Pyruvate sensing and transport in
Escherichia coli



Ivica Krištofičová

Dissertation der Fakultät für Biologie
der Ludwig-Maximilians-Universität München

München

6.11.2017

Erstgutachter: Prof. Dr. Kirsten Jung

Zweitgutachter: Prof. Dr. Marc Bramkamp

Datum der Abgabe: 6.11.2017

Datum der mündlichen Prüfung: 14.12.2017

Eidesstattliche Erklärung

Ich versichere hiermit an Eides statt, dass die vorgelegte Dissertation von mir selbstständig und ohne unerlaubte Hilfe angefertigt wurde. Des Weiteren erkläre ich, dass ich nicht anderweitig ohne Erfolg versucht habe, eine Dissertation einzureichen oder mich der Doktorprüfung zu unterziehen. Die folgende Dissertation liegt weder ganz, noch in wesentlichen Teilen einer anderen Prüfungskommission vor.

München, 6.11.2017

Ivica Kristoficova

Statutory Declaration

I declare that I have authored this thesis independently, that I have not used other than the declared sources/resources. As well I declare, that I have not submitted a dissertation without success and not passed the oral exam. The present dissertation (neither the entire dissertation nor parts) has not been presented to another examination board.

München, 6.11.2017

Ivica Kristoficova

Contents

Abbreviations	vii
Publications and manuscripts originating from this thesis	viii
Contributions to publications presented in this thesis	ix
Summary	xi
Zusammenfassung	xiii
1 Introduction	15
1.1 Two-component systems	16
1.2 Signal transduction in histidine kinases	17
1.3 Signal transmission by response regulators	19
1.4 LytS/LytTR-like two-component systems	20
1.5 TCS YehU/YehT in <i>Escherichia coli</i>	21
1.6 Transporter YjiY of <i>Escherichia coli</i>	24
1.7 Role of the TCS YehU/YehT	25
1.8 Aims of this thesis	26
2 Identification of a high-affinity pyruvate receptor in <i>Escherichia coli</i>	27
3 BtsT - a novel and specific pyruvate/H⁺ symporter in <i>Escherichia coli</i>	38
4 A single-cell view of the BtsSR/YpdAB pyruvate sensing network in <i>Escherichia coli</i> and its biological relevance	71
5 Concluding discussion	85
5.1 Role of the TCS BtsS/BtsR upon carbon starvation	86
5.2 Function of the histidine kinase BtsS	88

5.3	Importance of the pyruvate transporter BtsT	90
5.4	Role of the TCS BtsS/BtsR	92
5.5	Conclusion and outlook	94
	References (Chapter 1. and 4.)	104
	Supplemental Material - Chapter 2	105
	Supplemental Material - Chapter 3	111
	Supplemental Material - Chapter 4	125
	Acknowledgements	131
	Curriculum Vitae	132

Abbreviations

APC amino acid-polyamine-organocation superfamily

APEC avian pathogenic *Escherichia coli*

ATP adenosine- 5'-triphosphate

CA catalytic and ATP binding domain

cAMP cyclic adenosine-5'-monophosphate

CM cytoplasmic membrane

CP cytoplasm

DHp dimerization and histidine phosphotransfer domain

DRaCALA differential radial capillary action of ligand assay

GAF protein domain in cGMP specific phosphodiesterases, adenylyl cyclases and FhlA

HAMP protein domain in histidine kinases, adenylyl cyclases, methyl accepting proteins and phosphatases

HK histidine kinase

HTH helix-turn-helix motif

MFS major facilitator superfamily

OAA oxaloacetate

OFA oxalate/formate antiporter family

PAS Per- Arn- Sim

PP periplasm

REC receiver domain

RR response regulator

TCA tricarboxyacid

TCS two-component system

TM transmembrane domain

UPEC uropathogenic *Escherichia coli*

wHTH winged helix-turn-helix motif

Publications and manuscripts originating from this thesis

Chapter 2:

Behr, S., **Kristofcova, I.**, Witting, M., Breland, E. J., Eberly, A. R., Sachs, C., Schmitt-Kopplin, P., Hadjifrangiskou, M., Jung, K. (2017). Identification of a high-affinity pyruvate receptor in *Escherichia coli*. *Sci Rep*, 7, 1388. <http://doi.org/10.1038/s41598-017-01410-2>

Chapter 3:

Kristofcova, I., Vilhena, C., Behr, S., Jung, K. (2017). BtsT - a novel and specific pyruvate/H⁺ symporter in *Escherichia coli*. *J Bacteriol*, in press.
<http://doi.org/10.1128/JB.00599-17>

Chapter 4:

Vilhena, C., Kaganovitch, E., Shin, JY., Grünberger, A., Behr, S., **Kristofcova, I.**, Brameyer, S., Kohlheyer, D., Jung, K. (2017). A single-cell view of the BtsSR/YpdAB pyruvate sensing network in *Escherichia coli* and its biological relevance. *J Bacteriol*, in press. <http://doi.org/10.1128/JB.00536-17>

Contributions to publications presented in this thesis

Chapter 2:

Stefan Behr, Michael Wittig, Philippe Schmitt-Kopplin, Maria Hadjifrangiskou and Kirsten Jung designed the experiments. Stefan Behr and Corinna Sachs performed *in vivo* expression studies. Ivica Kristoficova produced the proteins in membrane vesicles as well as right-side-out vesicles, and conducted protein-ligand interaction studies. Michael Wittig carried out the hydrophilic interaction liquid chromatography for determination of compounds concentration. Erin Breland and Allison R. Eberly performed the murine infections. Stefan Behr, Ivica Kristoficova, Maria Hadjifrangiskou and Kirsten Jung wrote the manuscript.

Chapter 3:

Ivica Kristoficova, Cláudia Vilhena, Stefan Behr and Kirsten Jung designed the experiments. Stefan Behr performed comparative genomic studies. Ivica Kristoficova carried out the transport measurements with intact cells and proteoliposomes. Ivica Kristoficova and Cláudia Vilhena conceptually developed experimental conditions for transport assays. Ivica Kristoficova and Kirsten Jung wrote the manuscript.

Chapter 4:

Cláudia Vilhena, Jae Yen Shin, Stefan Behr, and Kirsten Jung designed the experiments. Cláudia Vilhena performed all the experimental work presented on the publication. Cláudia Vilhena and Jae Yen Shin performed statistical analysis of the data. Ivica Kristoficova drew the model. Ivica Kristoficova and Cláudia Vilhena performed reporter assays for the elucidation of the crosstalk between the systems during the development of the manuscript. Eugen Kaganovitch, Alexander Grünberger and Dietrich Kohlheyer help conceptualizing microfluidic experiments during the development of the manuscript. Sophie Brameyer performed plasmid-based experiments during the development of the manuscript. Cláudia Vilhena,

Eugen Kaganovitch, Jae Yen Shin, Alexander Grünberger, Stefan Behr, Ivica Kristoficova, Sophie Brameyer, Dietrich Kohlheyer and Kirsten Jung wrote and corrected the manuscript.

We hereby confirm the above statements:

Ivica Kristoficova

Kirsten Jung

Summary

Two-component systems (TCS) represent a prevalent bacterial mechanism to respond to changing environmental conditions. They comprise an often membrane-integrated histidine kinase (HK) and a soluble response regulator (RR), which regulates target genes expression. The TCS YehU/YehT is found in all commensal and pathogenic representatives within the *Enterobacteriaceae*. In *Escherichia coli* the TCS YehU/YehT contributes to carbon scavenging before entry into stationary phase. The system belongs to the LytS/LytTR family and regulates the expression of *yjiY*, encoding a putative peptide transporter belonging to the CstA family and APC superfamily of secondary transporters. This thesis focuses on the functional characterization of the components involved in the TCS YehU/YehT.

In the first part, the chemical stimulus perceived by the TCS YehU/YehT has been investigated (Chapter 2). It was found out that activation of the TCS YehU/YehT is dependent on the concomitant nutrient starvation and the extracellular availability of pyruvate. Via hydrophilic liquid chromatography, it was demonstrated the extracellular pyruvate is generated from overflow metabolism. Furthermore, the extracellular binding of pyruvate to YehU in vitro was proved by a differential radial capillary action of ligand assay (DRaCALA) and it indeed showed that YehU is a high affinity sensor for extracellular pyruvate.

The second part of the study focused on the identification of the function of the transporter YjiY (Chapter 3). YjiY is composed of 18 transmembrane helices, and no representative of the CstA family has been functionally characterized thus far. Transport studies with intact cells provided first evidence that YjiY is a specific transporter for pyruvate. Furthermore, reconstitution of the purified YjiY into proteoliposomes revealed that YjiY is a pyruvate/H⁺ symporter.

In the third part, we aimed at understanding the biological relevance of the TCS YehU/YehT (Chapter 4). A single-cell analysis of the *yjiY* activation demonstrated cell-to-cell variability that is influenced by external pyruvate availability upon nutrient limiting conditions. Depending on the demand of the individual cells, the TCS YehU/YehT as a part of a functional network with a TCS YpdA/YpdB, ensures an optimization of the physiological state of all cells within the population to withstand upcoming metabolic stress.

In summary, this thesis identified the TCS YehU/YehT to be involved in pyruvate sensing

and transport in order to optimize the physiological state within the whole population of *E. coli*. To indicate their role, the HK YehU, the RR YehT and the transporter YjiY were renamed to BtsS, BtsR and BtsT, for Brenztraubensäure, respectively.

Zusammenfassung

Zwei-Komponenten-Systeme (TCS) stellen einen weit verbreiteten bakteriellen Signaltransduktion-mechanismus dar, um auf wechselnde Umweltbedingungen zu reagieren. TCSs bestehen meist aus einer Membran-integrierten Histidinkinase (HK) und einem löslichen Antwortregulator (response regulator, RR), der die Expression von Zielgenen reguliert. Das TCS YehU/YehT ist in allen kommensalen und pathogenen Vertretern innerhalb der *Enterobacteriaceae* vorhanden. In *Escherichia coli* trägt das TCS YehU/YehT vor dem Eintritt in die stationäre Phase zur Aufnahme von Kohlenstoffverbindungen bei. Das System gehört zur LytS/LytTR-Familie und reguliert die Expression von *yjiY*, welches einen mutmaßlichen Peptidtransporter der CstA-Familie und der APC-Superfamilie von Sekundärtransportern kodiert. Diese Arbeit konzentriert sich auf die Aufklärung der Funktion der beteiligten Komponenten des TCSs YehU/YehT.

Im ersten Teil wurde der durch das TCS YehU/YehT wahrgenommene chemische Reiz untersucht (Kapitel 2). Es wurde gezeigt, dass die Aktivierung des TCS YehU/YehT gleichzeitig von Nährstoffmangel und der extrazellulären Verfügbarkeit von Pyruvat abhängig ist. Mittels hydrophiler Flüssigkeitschromatographie wurde gezeigt, dass das extrazelluläre Pyruvat ein Produkt des Überflusmetabolismus ist. Darüber hinaus wurde die extrazelluläre Bindung von Pyruvat in vitro durch den Liganden-Assay DRaCALA (differential radial capillary action of ligand assay) nachgewiesen, und es zeigte sich tatsächlich, dass YehU ein hochaffiner Sensor für die extrazelluläre Pyruvatkonzentration ist.

Der zweite Teil der Studie konzentrierte sich auf die Aufklärung der Funktion des Transporters YjiY (Kapitel 3). YjiY besteht aus 18 Transmembran-Helices, und bisher wurde noch kein Vertreter der CstA-Familie funktionell charakterisiert. Transportstudien mit intakten Zellen lieferten erste Hinweise darauf, dass YjiY ein spezifischer Transporter für Pyruvat ist. Darüber hinaus zeigte die Rekonstitution des gereinigten YjiY in Proteoliposomen, dass YjiY ein Pyruvat/H⁺ Symporter ist.

Im dritten Teil wollten wir die biologische Relevanz des TCS YehU/YehT (Kapitel 4) verstehen. Eine Einzelzellanalyse der *yjiY*-Aktivierung zeigte eine Zell-zu-Zell-Variabilität, die von der externen Pyruvatkonzentration beeinflusst wird. Das TCS YehU / YehT sorgt als Teil eines funktionellen Netzwerks mit TCS YpdA/YpdB je nach Bedarf der einzelnen

Zellen für eine Optimierung des physiologischen Zustands aller Zellen in der Population, um dem anstehenden Stoffwechselstress standzuhalten.

Zusammenfassend wurde in dieser Arbeit festgestellt, dass TCS YehU/YehT am Detektion und Transport von Pyruvate beteiligt ist, um den physiologischen Zustand innerhalb der gesamten Population von *E. coli* zu optimieren. Um die Funktion der HK YehU, des RRs YehT und des Transporters YjiY im Namen zu verantern, wurden diese Proteine in BtsS, BtsR und BtsT, für Brenztraubensäure, umbenannt.

Chapter 1

Introduction

Bacterial diversity is driven by an almost unlimited number of different environmental habitats where bacteria experience various fluctuations in physical and chemical parameters. In order to colonize, replicate and survive, bacteria need to respond to e.g. limitations of carbon and nitrogen or pH- and osmotic stress. Hence, bacteria evolved strategies for life-threatening situations by adjusting their metabolism to match the resource availability.

Prokaryotes are capable of persisting in diverse environments thanks to **signal transduction systems** (Boor, 2006) and fast cellular response mechanisms, e.g. acid (Haneburger *et al.*, 2012) or heat shock (Schumann, 2012). They as well depend on synchronizing processes, like biofilm formation (Njoroge and Sperandio, 2009), bioluminescence (Anetzberger *et al.*, 2012) and the expression of virulence genes (Rumbaugh *et al.*, 2009).

The simplest and the most predominant form of the bacterial signal transduction represent an one-component system (Ulrich *et al.*, 2005). One single protein contains both input and output domains. Another type of the signaling mechanism is an extracytoplasmic function σ factor with its cognate anti σ factor (Staron *et al.*, 2009). Last but not least, the signal transduction is achieved by **two-component systems** (TCS), which comprise an often membrane-integrated histidine kinase (HK) and a soluble response regulator (RR) (Jung *et al.*, 2012). The HK senses an intra- and/or extracellular stimulus and transfers the information to the cognate RR. Upon activation, the RR mediates the cellular reaction, mainly by adjusting a gene expression profile.

1.1 Two-component systems

TCSs are one of the most widespread transducers of extracellular stimuli in prokaryotes and lower eukaryotes. The number of HK/RR systems differs enormously from species to species, and correlates with the genome size (larger genome encode more TCSs) (Beier and Gross, 2006) as well as the number of different environmental and ecological niches (Alm *et al.*, 2006). Thereby, the number of HK/RR ranges from zero in *Mycoplasma genitalium*, an intracellular parasite living in constant environment, over 36/34 in *Bacillus subtilis* to 136/127 in *Myxococcus xanthus*, an extreme case of a bacterium inhabiting rapidly changing environments (Heermann and Jung, 2010; Capra and Laub, 2012). TCSs occur also in eukaryotes, as one TCS has been found in the yeast *Saccharomyces cerevisiae* and four in the plant *Arabidopsis thaliana* (Barrett and Hoch, 1998). Interestingly, TCSs are as a whole absent in the animal kingdom, as yet no gene encoding a HK or a RR is present in the genome of *Drosophila melanogaster*, *Homo sapiens* or any other animal cell (Wolanin *et al.*, 2002).

In the genome of *Escherichia coli*, the most investigated prokaryote, there are described 30 HKs and 30 RRs (**Fig. 1.1**). Recent years have seen an expansion of research about many of these TCSs however some still await characterization of their stimulus or their function. So far the well-characterized TCSs are e.g. a TCS CheA/CheY in the context of the bacterial chemotaxis (Thakor *et al.*, 2011), a TCS KdpD/KdpE with its importance in keeping potassium balance (Schramke *et al.*, 2017) and a TCS NarQ/NarP with its role in nitrate/nitrite sensing (Gushchin *et al.*, 2017).

Since TCSs are highly homologous between organisms (Grebe and Stock, 1999), the research of various TCSs are of a great importance. And so the basic principles of the signal transduction are providing us with further insights into bacterial virulence and pathogenicity (Gotoh *et al.*, 2010). For example, the TCS AgrA/AgrC is involved in regulation of *Staphylococcus aureus* virulence (Novick, 2003). As far as the future perspectives of TCSs are concerned, metabolic engineering would like to use TCSs to develop novel genetic networks (Salis *et al.*, 2009) and pharmacology to produce novel antimicrobial agents (Gotoh *et al.*, 2010).

usually composed of six TMs recognizing either a membrane interface (DesK) or create a hydrophobic pocket for signal binding (AgrC); (iii) cytoplasmic sensing HKs, both soluble and membrane integrated, responding to an intracellular signal (Krell *et al.*, 2010), (Mascher, 2014).

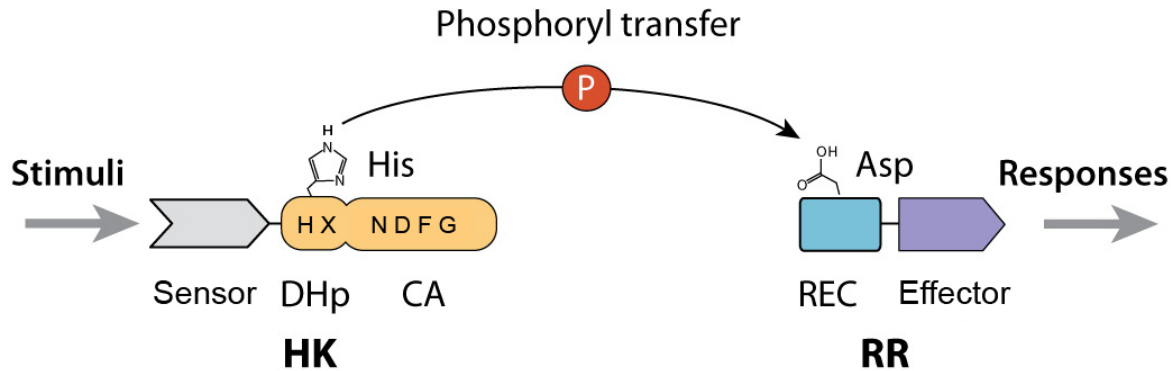


Figure 1.2: Signal transduction by two-component systems. Histidine kinase (HK) perceives the extra- or intracellular stimulus that results in the autophosphorylation of a conserved histidine residue. The phosphoryl group is then transferred to a conserved aspartate residue of the response regulator (RR) which in turn mediates the cellular response. The picture summarizes the domain architecture of HK (sensor and transmitter (DHp and CA) domain) and RR (receiver (REC) and effector domain). Conserved amino residues are written in an one-letter-code. Figure adopted and modified from (Gao and Stock, 2009).

The C-terminal transmitter domain is composed of a dimerization and histidine phospho-transfer domain (DHp, PFAM: HisKA) and the catalytic and ATP binding domain (CA, PFAM:HATPase_c) that are connected by a linker region (**Fig. 1.2**). The DHp domain is usually the site of homodimerization and harbors a conserved histidine residue that represents a phosphorylation site. The CA domain has a catalytic activity to autophosphorylate the HK using the γ -phosphate of ATP. Additionally, CA contains the highly conserved N, D, F and G boxes with corresponding amino acid residues, that are essential in ATP binding, catalysis and phosphotransfer (Stewart, 2010) (Wolanin *et al.*, 2002).

According to all six different amino acid motifs (H, X, N, D, F and G), the histidine kinases can be grouped in 11 families based on a comparative sequence analysis (Grebe and Stock, 1999). Some of these families contain a very distinct sequence similarity that clearly separates them from all other HKs, e.g. chemotaxis kinases. Other families do not show such clear

boundaries. Interestingly, the kinase subfamilies tend to group with regulator subfamilies; suggesting an independent co-evolution of different classes of His-Asp phosphorelay systems (Grebe and Stock, 1999).

A signal conversion in HKs is sometimes also achieved by additional domains, like HAMP, PAS, S-helices and GAF. They are located at the C-terminal part directly after the transmembrane region (Mascher, 2014). HAMP domain (present in histidine kinases, adenylyl cyclases, methyl accepting proteins and phosphatases) mediates the conversion of an extracellular stimulus into the cytoplasmic response by a conformational change (Barakat *et al.*, 2011). PAS (first discovered in proteins Per- Arnt- Sim) and GAF (present in cGMP specific phosphodiesterases, adenylyl cyclases and FhlA proteins) domains are additional sensor and interaction interfaces (Henry and Crosson, 2011) (Mascher, 2014). Last but not least, S-helices (from signaling helix) are preventing a constitutive activation of downstream signaling domains (Anantharaman *et al.*, 2006).

1.3 Signal transmission by response regulators

The major role of a RR is to transfer the signal received by the HK towards a downstream target, which is in the most cases a promoter sequence of a gene. Thereby, the response regulators usually acts as transcription factors with a DNA binding capability (Mizuno, 1997).

RR harbors two domains, a highly conserved receiver domain (REC) at the N-terminus and a variable effector domain at the C-terminus (**Fig. 1.2**). The REC typically contains the conserved aspartate residue able to acquire the phosphoryl group from the His~P of the HK. The Asp~P mediates a conformational change that subsequently effects the activity of the effector domain. In general, effector domains are very diverse. Most of them regulate the transcription of the genes (25 of 32 RR in *E. coli*) and these can be divided into three families represented by OmpR, NarL and NtrC (Stock *et al.*, 2000) (Mizuno, 1997). The OmpR family is the most abundant one with 14 members in *E. coli* that use a winged helix-turn-helix (wHTH) motif to bind DNA. The NarL family consisting of 7 members harbors a typical helix-turn-helix (HTH) motif. The third family, NtrC, has 4 members and its effector part is composed of both an ATPase domain and HTH motif.

1.4 LytS/LytTR-like two-component systems

A detailed understanding of the components, layout and mechanism of bacteria’s TCS provides us with an opportunity for bioengineering or disturbing the bacterial pathogenicity. The main advantages of TCSs are a total absence in the animal kingdom, a relatively simple layout and a high degree of homology between organisms. We can therefore focus on constructing novel signaling circuits, e.g. to improve production yields or stop the production of virulence factors.

In agreement with this, the search for systems regulating toxin production in several bacterial pathogens started with a genome sequencing. Soon after, an unusual response regulator has been found in *Staphylococcus aureus* and some other pathogens. The RR contains a non-HTH DNA binding domain (rather than HTH or wHTH motif typical in RRs) named as **LytTR** after RR LytT in *B. subtilis* and RR LytR in *S. aureus* (Nikolskaya and Galperin, 2002).

In several bacterial genomes, the gene coding for the LytTR-like RR is in an operon with a gene coding for **LytS**-like HK (Anantharaman and Aravind, 2003). These HKs harbor a typical 5 TM Lyt domain (called also Lyts-Yhck, PFAM: 5MTR-LYT), with the N-terminal helix located in a periplasm. In addition, the 5TM domain is combined with the C-terminal signaling domain, which very often is GAF. According to a bacterial sequence alignment, LytS-like HKs are part of the HPK8 family **Table 1.1**. They contain the conserved histidine residue in their H-box, however proline is found preceding the H-box rather to be 5 residues downstream of the box. The first residue after the H-box is phenylalanine instead of an acidic residue. In addition, N- and F- boxes are not conserved (Grebe and Stock, 1999).

Table 1.1: Selection of LytS-containing histidine kinases (HKs)

HK	Organism	Stimulus	RR	Reference
AlgZ	<i>Pseudomonas aeruginosa</i>	unknown	AlgR	(Yu <i>et al.</i> , 1997) (Okkotsu <i>et al.</i> , 2014)
LytS	<i>Staphylococcus aureus</i> , <i>Bacillus subtilis</i>	unknown	LytT	(Brunskill and Bayles, 1996)
YehU	<i>Escherichia coli</i>	Peptides or amino acids	YehT	(Kraxenberger <i>et al.</i> , 2012)
YesM	<i>Bacillus subtilis</i>	unknown	YesN	(Fabret <i>et al.</i> , 1994)
YpdA	<i>Escherichia coli</i>	Extracellular pyruvate	YpdB	(Fried <i>et al.</i> , 2013)
YwpD	<i>Bacillus subtilis</i>	unknown		

Actually, only around 2.7% proteins of all prokaryotic RRs contain the LytTR motif (Galperin, 2006). Even though this represents just around 1 to 2 proteins per genome, these RRs regulate virulence factors like bacteriocins, fimbriae, toxins and extracellular polysaccharides (**Table 1.2**).

Table 1.2: Selection of characterized LytTR-containing response regulators (RRs)

RR	Organism	Regulated process	Reference
AlgR	<i>Pseudomonas aeruginosa</i>	Alginate biosynthesis	(Deretic <i>et al.</i> , 1989)
AgrA	<i>Staphylococcus aureus</i>	Production of toxins and hemolysins	(Novick <i>et al.</i> , 1995)
CbaR	<i>Carnobacterium piscicola</i>	Carnobacteriocin A production	(Quadri <i>et al.</i> , 1997)
ComE	<i>Streptococcus pneumoniae</i>	Competence for genetic transformation	(Pestova <i>et al.</i> , 1996)
EntR	<i>Enterococcus faecium</i>	Enterocin A production	(O’Keeffe <i>et al.</i> , 1999)
FasA	<i>Streptococcus pyogenes</i>	Fibronectin-binding adhesin production	(Kreikemeyer <i>et al.</i> , 2001)
LytR	<i>Staphylococcus aureus</i>	Autolysis	(Brunskill and Bayles, 1996)
MrkE	<i>Klebsiella pneumoniae</i>	Expression of type 3 fimbriae	(Allen <i>et al.</i> , 1991)
PlnC	<i>Lactobacillus plantarum</i>	Plantaricin A production	(Diep <i>et al.</i> , 1996)
SppR	<i>Lactobacillus sakei</i>	Sakacin P production	(Huhne <i>et al.</i> , 1996)
VirR	<i>Clostridium perfringens</i>	Production of perfringolysin O, collagenase, hemagglutinin	(Shimizu <i>et al.</i> , 1994)
YpdB	<i>Escherichia coli</i>	Carbon starvation control	(Behr <i>et al.</i> , 2016)

All in all, LytS/LytTR TCSs play a significant role in bacterial virulence and represent a good target to decrease bacterial infections. For example, in *S. aureus* a modification of an autoinducing peptide (a stimulus for HK AgrC) resulted in inhibition of the LytTR-like RR AgrA virulent response (Lyon *et al.*, 2000). Unfortunately, still several LytS/LytTR TCSs are not well characterized and their perceived stimuli by HK are unknown.

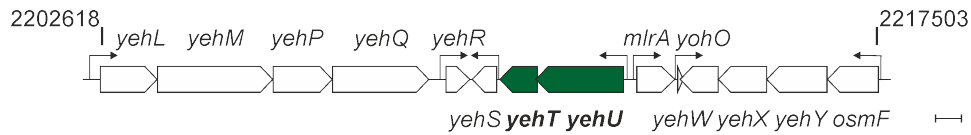
1.5 TCS YehU/YehT in *Escherichia coli*

In Gram-negative bacteria, little is known about the LytS/LytTR-like two-component system YehU/YehT in *Escherichia coli*.

The *yehU* and *yehT* genes are clustered in an operon localized at 47.638 centisomes in *E. coli* MG1655 genome (**Fig. 1.3A**) (Kraxenberger *et al.*, 2012). The genes are 4 bp overlapping. Upstream of the coding region of *yehU* is *mlrA*, a regulator responsible of a curli production in *E. coli* (Brown *et al.*, 2001), *yohO* coding for a small unidentified protein (Hemm *et al.*, 2008) and an operon of *osmF-yehYXW* encoding a putative ABC transporter

(Checroun and Gutierrez, 2004). Downstream of *yehT* is *yehS*, *yehR*, *yehQ*, *yehP*, *yehM* of unknown function and *yehL* which defines a MoxR AAA⁺ family (Snider *et al.*, 2006).

A



B

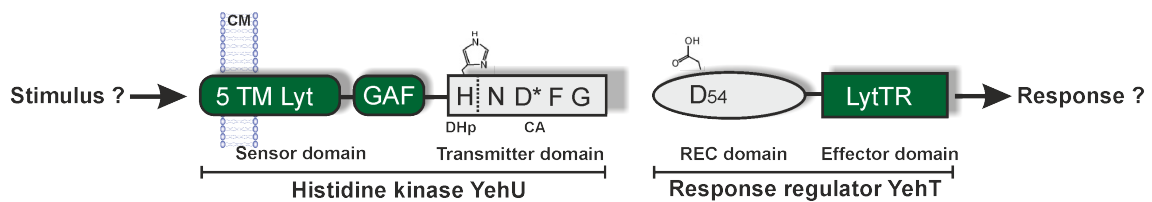


Figure 1.3: The YehU/YehT system in *E. coli*. (A) Chromosomal region between 47.48 and 47.77 centisomes around *yehUT* operon in *E. coli* MG1655. Adopted and modified from (Kraxenberger *et al.*, 2012). (B) Domain organization of YehU and YehT. HK YehU contains a 5TM Lyt domain, GAF domain and transmitter domain with conserved boxes (H, N, D*, F, G). D* box of YehU is not complete. YehT is composed of a receiver domain with the conserved aspartate residue and a LytTR effector domain. CM, cytoplasmic domain. The figure was provided by Stefan Behr, adopted and modified.

The HK YehU (561 amino acids, 62.1 kDa) contains the 5TM Lyt-like sensor domain, transmitter domain and an additional GAF domain (**Fig. 1.3B**). The bioinformatic analysis has revealed an additional transmembrane domain at the N-terminus. The RR YehT (289 amino acids, 27.4 kDa) contains a CheY-like receiver domain with the conserved aspartate residue at position 54 and LytTR effector domain (**Fig. 1.3B**). Up to now, the autophosphorylation of HK YehU or the transfer of the phosphoryl group to YehT was not experimentally detected (Yamamoto *et al.*, 2005).

The YehT RR activates the expression of *yjiY*, which is the only target regulated by the YehU/YehT TCS (Kraxenberger *et al.*, 2012). In *E. coli* MG1655 genome, *yjiY* is located at 98.87 centisomes disconnected from the *yehUT* operon. Interestingly, in other bacterial genomes (e.g. *Shewanella*, *Clostridium* and *Vibrio* species), the *yjiY* is colocalized with the *yehUT* operon. It was determined that YehT binds with the K_d of 75 nM to the *yjiY* promoter

within positions -112 and -13 upstream of the transcriptional start site of *yjiY*. Specifically, the binding occurs at two repeats of the sequence motif ACC(G/A)CT(C/T)A separated by a 13 bp spacer in the promoter of *yjiY*. The third repeat motif of the same sequence probably stabilize the YehT-DNA complex (Kraxenberger *et al.*, 2012).

In vivo reporter studies revealed that the activation *yjiY* promoter occurs at the mid- to late- exponential phase in amino acid rich media, such as LB, peptone and casamino acids (**Fig. 1.4**). Furthermore, the *yjiY* promoter activation was observed in minimal media containing amino acids, acetate, glucuronic acid, gluconic acid or pyruvate as a carbon source (Kraxenberger *et al.*, 2012). At the same time as activation of the *yjiY* promoter is observed ($OD_{600} = 0.6$), the cells initiate production of *yjiY* mRNAs (Behr *et al.*, 2014).

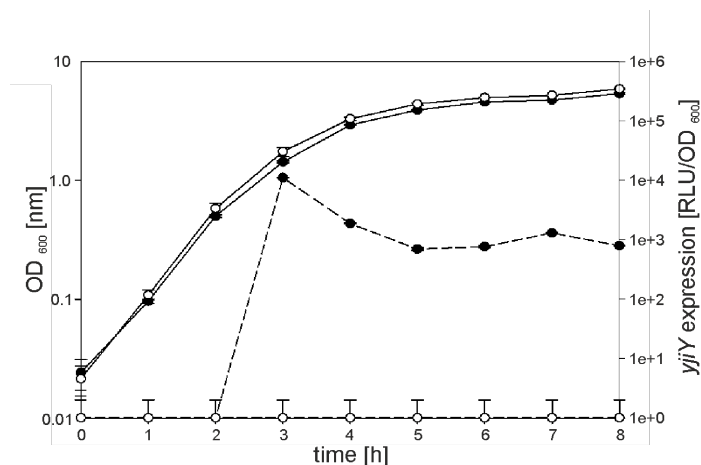


Figure 1.4: *In vivo* reporter assay of *yjiY* promoter activation. *E. coli* MG1655 (●) and *E. coli* MG1655 $\Delta yehUT$ (○) transformed with pBBR *yjiY-lux* were grown in LB, and their growth and luminescence were recorded over time. Figure was adopted from (Kraxenberger *et al.*, 2012).

The expression of *yjiY* requires cAMP and cAMP receptor protein (CRP). The CRP consensus sequence is upstream of the *yjiY* promoter. The mutation of this motif or *crp* deletion reduced the induction of *yjiY* (Kraxenberger *et al.*, 2012). Additionally, the carbon storage regulator A (CsrA), a protein blocking the ribosome binding to mRNA or influencing mRNA stability, is downregulating the expression of *yjiY* at the posttranscriptional level (Kraxenberger *et al.*, 2012). The levels of *yjiY* mRNA are dependent also on the 50S ribosomal protein L4 and the endonuclease RNase E (Singh *et al.*, 2009). Interaction between L4 protein and RNase E on *E. coli* transcripts leads to an increase of *yjiY* mRNA.

1.6 Transporter YjiY of *Escherichia coli*

The target gene of the TCS YehU/YehT *yjiY* codes for a putative transporter with 16 to 18 predicted TMs of yet unknown function.

A bacterial membrane is highly permeable for small molecules (e.g. water, N₂, O₂) and apolar solutes (e.g. glycerol). However, transporters in *E. coli* play an important role in metabolism due to impermeability of the bacterial membrane for polar solutes and charged molecules (e.g. ions and amino acids (Krämer, 1999)). They maintain balance between availability (influx) and loss (efflux) of the substrates. An energy-independent transport, a facilitated diffusion, is catalyzed by channels. Active transport is driven by cell energy and there are three types: primary (ATP), secondary (ions/solute gradients) and group translocation systems (phosphoryl group).

YjiY belongs to the amino acid-polyamine-organocation (APC) superfamily of secondary transporters (Wong *et al.*, 2012; Vastermark *et al.*, 2014). APC contains 18 families and most of their members exhibit a common 5+5 TMs topology (**Table 1.3**).

Table 1.3: Established families in the APC superfamily. Adopted from (Vastermark *et al.*, 2014).

TC#	Family name	Abbreviation	Topology
2.A.3	Amino Acid-Polyamine-Organocation	APC	5+5+2 TMs
2.A.15	Betaine/Carnitine/Choline Transporter	BCCT	2+5+5 TMs
2.A.18	Amino Acid/Auxin Permease	AAAP	11 TMs
2.A.21	Solute:Sodium Symporter	SSS	5+5+4 TMs
2.A.22	Neurotransmitter:Sodium Symporter	NSS	5+5+2 TMs
2.A.25	Alanine or Glycine:Cation Symporter	AGCS	11 TMs
2.A.26	Branched Chain Amino Acid:Cation Symporter	LIVCS	5+5+2 TMs
2.A.30	Cation-Chloride Cotransporter	CCC	12 TMs
2.A.31	Anion Exchanger	AE	7+7 TMs
2.A.39	Nucleobase:Cation Symporter-1	NCS1	5+5+2 TMs
2.A.40	Nucleobase:Cation Symporter-2	NCS2	7+7 TMs
2.A.42	Hydroxy/Aromatic Amino Acid Permease	HAAAP	11 TMs
2.A.46	Benzoate:H ⁺ Symporter	BenE	7+7 TMs
2.A.53	Sulfate Permease	SulP	8-13 TMs
2.A.55	Metal Ion (Mn ²⁺ -iron) Transporter	NRAMP	5+5+2 TMs
2.A.72	K ⁺ Uptake Permease	KUP	5+5+2 TMs
2.A.114	Peptide Transporter Carbon Starvation CstA	CstA	13 - 18 TMs
2.A.120	Putative Amino Acid Permease	PAAP	5+5 TMs

APC is the second largest family of secondary transporters, being smaller only than the Major Facilitator Superfamily (MFS). Functionally characterized transporters of APC superfamily transport amino acids, peptides, inorganic anions or cations (Vastermark *et al.*, 2014).

Furthermore, YjiY belongs to the Peptide Transporter Carbon Starvation CstA family, consisting of proteins of various sizes and topologies. None of them has been biochemically analyzed. Characterized member of this family, the protein CstA, is postulated to be a peptide transporter. The evidence is derived from an observed lower growth rate on peptides of *cstA opp* double mutant compared to *opp* mutant (Schultz and Matin, 1991). In *Campylobacter jejuni*, the *cstA* mutant had a lower growth rate on peptides as nitrogen sources (Rasmussen *et al.*, 2013). In *Salmonella enterica*, the function as a peptide transporter is proposed to both CstA and YjiY (Garai *et al.*, 2015).

1.7 Role of the TCS YehU/YehT

It is worth to mention, that the TCS YehU/YehT is functionally interconnected with the LytS/LytTR-like TCS named YpdA/YpdB (Behr *et al.*, 2014). Both HKs and RRs share the same arrangement of structural domains and their amino acid sequences are over 30% identical (Behr *et al.*, 2017). YpdA/YpdB system responds to media supplemented with pyruvate (Fried *et al.*, 2013). The only target gene of the YpdA/YpdB TCS is *yhjX*, encoding the transporter YhjX, belonging to the the oxalate/formate antiporter (OFA) family and MFS. However, the function of YhjX is not yet elucidated.

It was proposed that these two TCSs, YehU/YehT and YpdA/YpdB, coordinate carbon scavenging and adjustments of bacterial metabolism in preparation for stationary phase (Behr *et al.*, 2014). The transporters YjiY and YhjX replenish carbon resources in order to circumvent the nutrient limitation, e.g. by taking up peptides/amino acids or other carbon sources from available resources. In order to get further insights in the role of both TCSs in *E. coli*, the stimuli of both histidine kinases and function of the regulated transporters need to be addressed. This thesis focuses primarily on the function of the TCS YehU/YehT and its target protein YjiY.

1.8 Aims of this thesis

Two-component systems in prokaryotes and lower eukaryotes have been investigated over 30 years. At the moment, many members in bacterial genomes have been identified, and their molecular details are being described. Despite all the new information, there is still a gap to be filled up. This project focuses on LytS/LytTR-like two component-system YehU/YehT in *E. coli*. The aim is to unravel the function of the TCS YehU/YehT and its target protein YjiY by *in vivo* and *in vitro* studies.

i **Characterization of stimulus perceived by HK YehU**

Based on the previous *in vivo* studies, it is suggested that YehU is an amino acid sensor. However, it is unclear, if the HK works as a direct sensor, and if so, which ligand is binding to it. After elucidating the stimulus identity by additional *in vivo* studies, a ligand binding assay will be carried out.

ii **Identification of the substrate transported by the CstA-like transporter YjiY**

The YehU/YehT system controls expression of *yjiY*, which codes for a transporter belonging to CstA family and APC superfamily of secondary transporters. It is proposed that YjiY is a peptide transporter, however without further characterization. Here, the substrate will be identified and then transport assays will be performed to determine the substrate specificity and mode of energization.

iii **Investigation of the biological relevance of the TCS YehU/YehT**

The promoter of the target gene *yjiY* will be analyzed at the single-cell level to obtain further insights into the biological significance of the TCS YehU/YehT. Then the different cellular fates (ranging from growing to dormant persister cells) will be analyzed.

Chapter 2

Identification of a high-affinity pyruvate receptor in *Escherichia coli*

Behr, S., **Kristofcova, I.**, Witting, M., Breland, E. J., Eberly, A. R., Sachs, C., Schmitt-Kopplin, P., Hadjifrangiskou, M., Jung, K.

Sci Rep, 2017, 7:1388

<http://doi.org/10.1038/s41598-017-01410-2>

SCIENTIFIC REPORTS

OPEN

Identification of a High-Affinity Pyruvate Receptor in *Escherichia coli*

Stefan Behr¹, Ivica Kristofcova¹, Michael Witting², Erin J. Breland³, Allison R. Eberly⁴, Corinna Sachs¹, Philippe Schmitt-Kopplin², Maria Hadjifrangiskou^{4,5} & Kirsten Jung¹

Two-component systems are crucial for signal perception and modulation of bacterial behavior. Nevertheless, to date, very few ligands have been identified that directly interact with histidine kinases. The histidine kinase/response regulator system YehU/YehT of *Escherichia coli* is part of a nutrient-sensing network. Here we demonstrate that this system senses the onset of nutrient limitation in amino acid rich media and responds to extracellular pyruvate. Binding of radiolabeled pyruvate was found for full-length YehU in right-side-out membrane vesicles as well as for a truncated, membrane-integrated variant, confirming that YehU is a high-affinity receptor for extracellular pyruvate. Therefore we propose to rename YehU/YehT as BtsS/BtsR, after “**B**renzt**r**aubens**ä**ure”, the name given to pyruvic acid when it was first synthesized. The function of BtsS/BtsR was also assessed in a clinically relevant uropathogenic *E. coli* strain. Quantitative transcriptional analysis revealed BtsS/BtsR importance during acute and chronic urinary-tract infections.

Exponential growth of bacteria in complex, nutrient-rich media usually ends when at least one nutrient has been used up. We recently reported that the histidine kinase/response regulator system YehU/YehT of *E. coli*, belongs to the LytS/LytTR family and presumably plays a role in tuning bacterial exploitation of available carbon sources¹. Strikingly, the YehU/YehT system is the most widespread representative of its family found in γ -proteobacteria – and many LytS/LytTR-type systems regulate crucial host-specific mechanisms during infection of human or plant hosts by members of this bacterial clade². This system is conserved in non-pathogenic as well as pathogenic *E. coli*.

Our previous studies on YehU/YehT in *E. coli* identified *yjiY* as its sole target gene³ (Fig. 1). This gene codes for the putative carbon starvation transporter YjiY, which is homologous (61.1% identity) to CstA⁴ and was found to be expressed in cells that were grown in complex media containing a high content of amino acids, such as LB or CAA (casamino acids), as well as in minimal medium supplemented with certain carbon sources, such as gluconic or glucuronic acid. Studies in *E. coli* revealed that YehT-mediated *yjiY* transcription is also regulated by the cAMP/CRP complex³ (Fig. 1), and down-regulated in the presence of energetically favorable carbon sources like glucose. Furthermore, YjiY is subject to translational control via the Csr regulatory circuit⁵ (Fig. 1), which synchronizes the output of *E. coli* central carbohydrate metabolism (glycolysis versus gluconeogenesis) with YjiY production^{1,6}. Finally, *yjiY* transcription is under positive feedback regulation by a second two-component system, YpdA/YpdB, and its gene product YhjX¹ (Fig. 1).

Here, we performed a comprehensive *in vivo* characterization of *yjiY* expression in order to identify the primary stimulus sensed by the histidine kinase YehU. We found that the YehU/YehT system responds to depletion of nutrients specifically serine and the concomitant presence of extracellular pyruvate. Biochemical studies revealed that pyruvate binds specifically to the extracellular side of the membrane-spanning domain of YehU. We therefore renamed the system BtsS/BtsR, for “**B**renzt**r**aubens**ä**ure”, the original name given by Jöns Jakob

¹Munich Center for Integrated Protein Science (CIPSM) at the Department of Microbiology, Ludwig-Maximilians-Universität München, 82152, Martinsried, Germany. ²Helmholtz Zentrum München, Deutsches Forschungszentrum für Gesundheit und Umwelt (GmbH), Research Unit Analytical BioGeoChemistry, 85764, Neuherberg, Germany.

³Departments of Pharmacology, Vanderbilt University Medical Center, Nashville, TN 37232, USA. ⁴Departments of Pathology, Microbiology & Immunology, Vanderbilt University Medical Center, Nashville, TN 37232, USA.

⁵Departments of Urologic Surgery, Vanderbilt University Medical Center, Nashville, TN 37232, USA. Correspondence and requests for materials should be addressed to K.J. (email: jung@lmu.de)

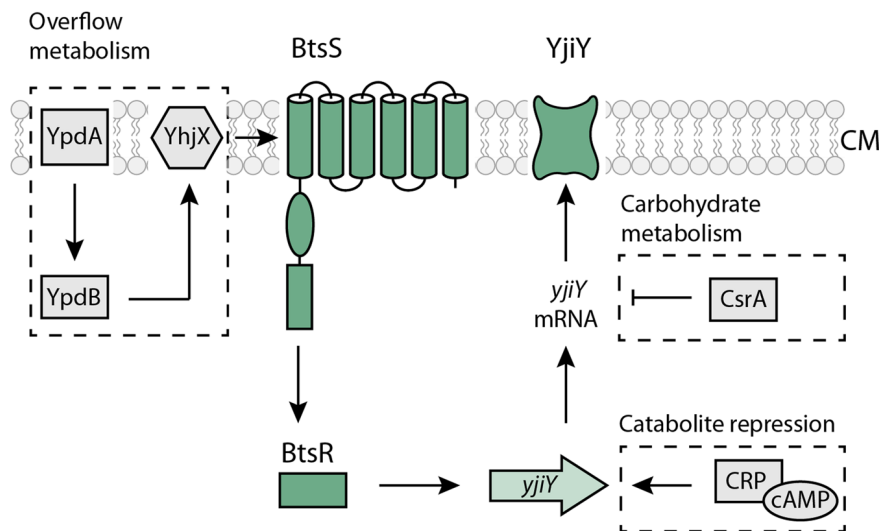


Figure 1. Schematic depiction of the BtsS/BtsR (YehU/YehT) system in *Escherichia coli*. The scheme summarizes the regulatory network associated with signal transduction by the BtsS/BtsR two-component system, the influence of two-component system YpdA/YpdB and the global regulators CsrA and CRP. Membrane proteins are integrated in the cytoplasmic membrane (CM). Activating (↑) and inhibitory (⊥) effects are indicated. See text for details.

Berzelius to the compound when he first synthesized pyruvic acid in 1835⁷. Finally, we found that the BtsS/BtsR system of uropathogenic *E. coli* may contribute to acute urinary tract infection.

Results

Elucidation of the stimulus for BtsS/BtsR (YehU/YehT) by *in vivo* *yjiY* expression analyses. It was previously shown that cultivation of *E. coli* in amino acid-rich media leads to activation of the BtsS/BtsR system and transient expression of the target gene *yjiY* in the late-exponential growth phase³. To identify a potential quorum sensing-like molecule, we used a combination of chemical fractionation of the medium and measurements of reporter strain activity. For this purpose, we cultivated *E. coli* MG1655 $\Delta yjiY$ /pBBR *yjiY-lux* in M9-minimal medium with gluconic acid as sole carbon source³. Shortly before the induction of *yjiY* we removed the cells and fractionated the supernatant by high pressure liquid chromatography. All fractions were analyzed for their potential to induce *yjiY* using reporter strain *E. coli* KX1468 pBBR *yjiY-lux* grown in minimal medium and succinate as C-source. After several rounds of fractionation/freeze-drying we found that the fraction with the highest induction potential contained a high concentration of gluconic acid, the initial carbon source (data not shown). This result ruled out the possibility that *E. coli* produces and senses a quorum sensing-like molecule. Then we quantified *yjiY* expression as a function of nutrient levels. For this purpose, we cultivated the reporter strain *E. coli* MG1655/pBBR *yjiY-lux* in LB medium with decreasing amounts of nutrients (1.0x, 0.5x, 0.4x, 0.3x LB, 0.2x LB and 0.1x LB), keeping the osmolarity of the medium constant. The growth rates (μ) of *E. coli* cells decreased with the dilution of LB medium, and exponential growth ceased at different time points (Table S1). Strikingly, expression of *yjiY* always began shortly before the onset of stationary phase (Fig. S1), and *E. coli* cells grown in 0.1x LB did not express *yjiY*. These results suggested that BtsS/BtsR somehow responds to nutrient limitation. We reasoned that supplying the relevant nutrient(s) in excess should suppress or postpone *yjiY* induction. Therefore, the reporter strain was grown in LB media supplemented with an excess of each individual L-amino acid (Fig. 2A). Particularly, the addition of L-serine delayed the expression of *yjiY* by almost two doubling periods (Fig. 2A). Subsequently, we tested different concentrations of L-serine in the reporter assay and found a concentration-dependent delay in *yjiY* expression, accompanied by a decrease in peak expression levels (Fig. 2B). The addition of serine does not influence the growth of *E. coli* and does not delay the onset of stationary phase (Fig. 2C). Although L-serine is not a preferred carbon source for *E. coli* and high external concentrations are actually toxic to the organism, it is the first amino acid to be consumed when mixtures of amino acids are available⁸. These data suggest that BtsS/BtsR responds to depletion of nutrients, specifically serine.

Changes in extracellular serine and pyruvate concentrations during growth of *E. coli*. When *E. coli* is grown in amino acid-rich media, 50.7% of L-serine is converted directly to pyruvate, whereas 36.3% is used for glycine synthesis, 6.5% for cell biomass, and the remainder for other metabolites⁹. Its central role in pyruvate supply provides one explanation for the importance of L-serine in growing *E. coli*¹⁰. We therefore monitored the changes in extracellular serine and pyruvate concentrations during growth in LB medium, and found that extracellular levels of serine decreased at a constant rate (Fig. 3). The starting concentration of serine in the medium (approximately 200 μ M) was completely exhausted after 120 min of growth at the late-exponential growth phase. At the same time, the abundance of extracellular pyruvate peaked (approx. 500 μ M) and shortly after *yjiY* expression reached its maximum level (Fig. 3). It was previously shown that the external pyruvate derives from overflow

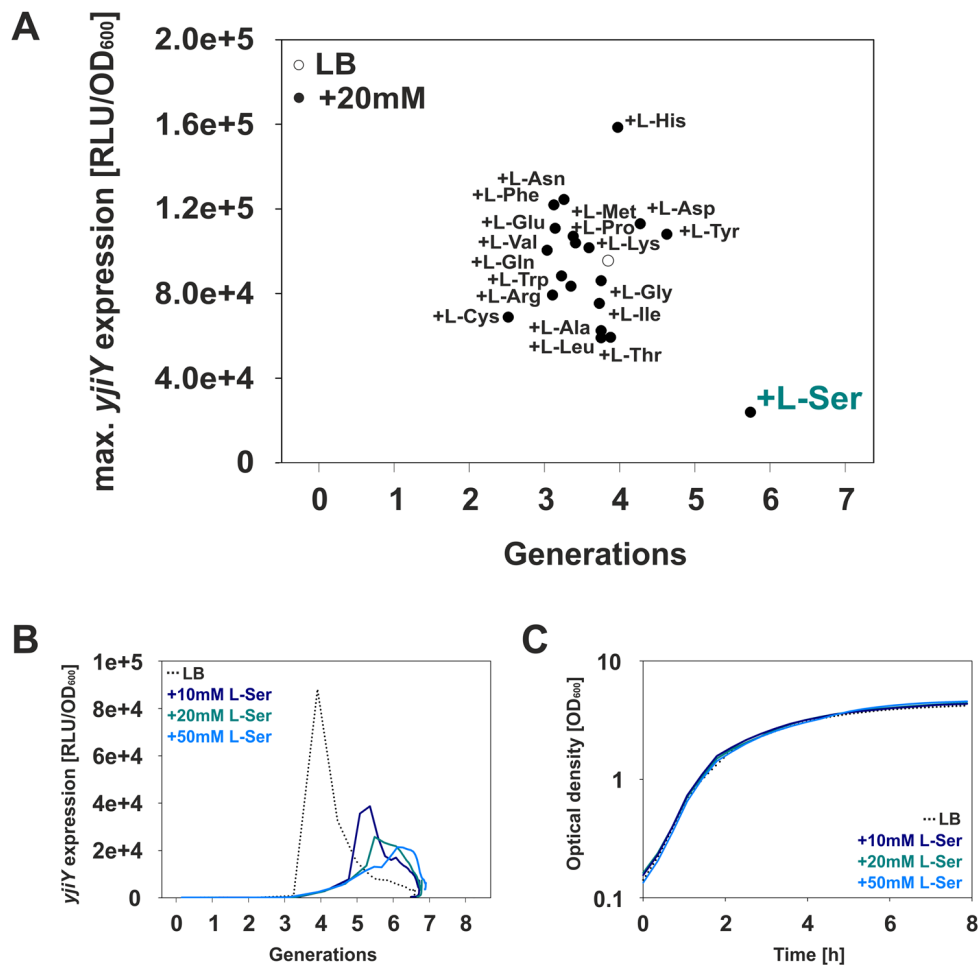


Figure 2. Effects of an excess of individual amino acids on the expression of *yjiY*. (A) *E. coli* MG1655/pBBR *yjiY-lux* was grown in LB medium supplemented with one of the indicated amino acids (at 20 mM), and growth and luminescence were monitored over time. Maximal *yjiY* expression values are depicted. The open circle provides a benchmark and indicates *yjiY* expression in *E. coli* grown in LB medium. (B) Expression of *yjiY* in LB (dotted line) supplemented with increasing L-serine concentrations. (C) Corresponding *E. coli* growth curves in LB media supplemented with increasing L-serine concentrations. Experiments were performed at least three times (standard deviation <10%), and results of a representative experiment are shown.

metabolism in *E. coli* during growth in amino acid-rich media¹¹, which was confirmed by monitoring the intracellular concentrations of serine and pyruvate (Fig. S2).

These data reveal that induction of BtsS-dependent *yjiY* expression coincides with the decline of serine in the medium and an extracellular accumulation of pyruvate (Fig. 3).

Extracellular pyruvate triggers *yjiY* expression under nutrient limitation. In the next experiment we tested the influence of serine, pyruvate and related metabolites on *yjiY* expression in *E. coli* cells growing in low-nutrient environment. Since *E. coli* harbors a second two-component system, YpdA/YpdB, which responds to high concentrations of extracellular pyruvate (the threshold concentration that leads to induction was determined to be 600 μ M) and positively regulates the BtsS/BtsR system¹¹, we modified our reporter strain by deleting *yhjX*, which is sufficient to interrupt the feedback loop¹. The resulting strain was then cultivated in 10-fold diluted (0.1x) LB medium for 1 h. At this time point, cells do not induce expression of *yjiY*, but experience soon carbon limitation (Fig. 4A, Fig. S1). However, expression of *yjiY* was rapidly triggered upon addition of pyruvate, and the induction level increased linearly with increasing pyruvate concentration (Fig. 4A). Addition of L-serine also induced *yjiY* expression, but only after a 20-min delay (Fig. 4B). Under these conditions the growth of *E. coli* did not differ significantly by addition of pyruvate or serine (Fig. S3). Only supplementation of 10 mM serine prolonged the exponential growth phase. Moreover, higher serine concentrations delayed *yjiY* expression for even longer, and decreased the level of induction attained (Fig. 4B). The threshold concentration of pyruvate required for detectable *yjiY* expression was 10 μ M, and that for L-serine 50 μ M. None of the other tested compounds (each of the other 19 amino acids, phosphoenolpyruvate, lactate, oxaloacetate, α -ketoglutarate, valerate, propionate, acetate, malate) were able to induce *yjiY* in this context. These results suggest that extracellular pyruvate acts as a direct stimulus for BtsS/BtsR-mediated *yjiY* expression, whereas delayed *yjiY* induction in response to L-serine

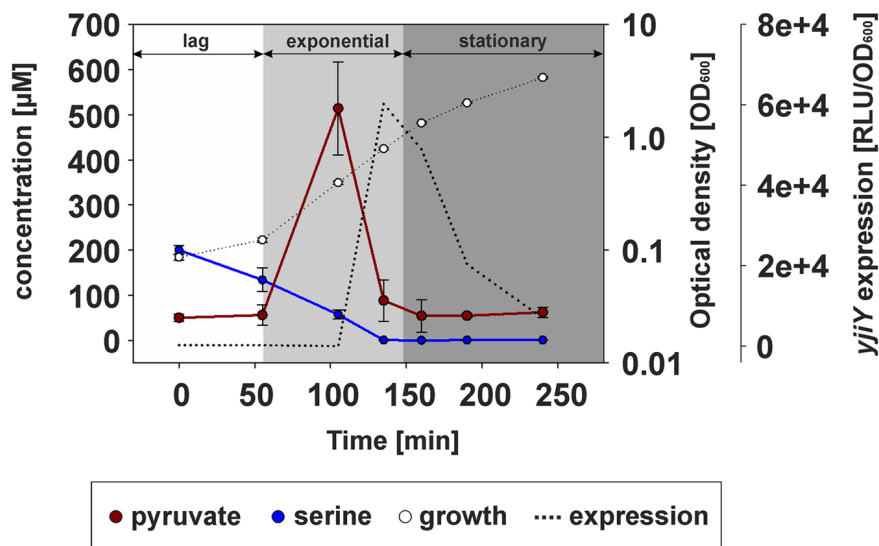


Figure 3. Determination of changes in extracellular concentrations of serine and pyruvate during growth of *E. coli*. *E. coli* MG1655/pBBR *yjiY-lux* was cultivated in LB medium, and growth (OD_{600}) and luminescence were monitored. At the times indicated, cells were harvested, and serine and pyruvate levels were quantified by hydrophilic interaction liquid chromatography. All experiments were performed in triplicate, and the error bars indicate the standard deviation of the means. The growth phases of *E. coli* are marked as following: lag phase (white), exponential growth (light grey) and stationary phase (dark grey).

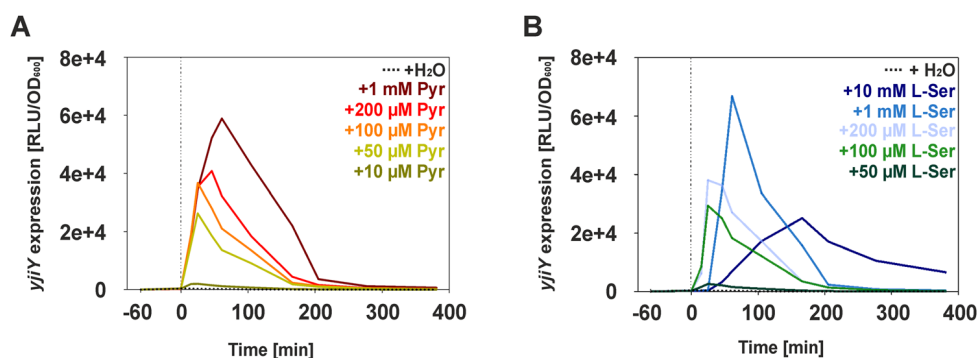


Figure 4. Stimulus-dependent *yjiY* expression under nutrient-limiting conditions. *E. coli* MG1655 mutant $\Delta yhjX$ harboring pBBR *yjiY-lux* was cultivated in 0.1x LB medium to establish low nutrient conditions. After 1 h (time point 0), the indicated concentration of pyruvate (A), or L-serine (B), or the equivalent volume of water was added. Experiments were performed at least three times (standard deviation < 10%), and results of a representative experiment are shown.

may depend on uptake of the amino acid, its conversion to pyruvate and excretion of the pyruvate into the culture medium.

The sensor histidine kinase BtsS binds pyruvate with high affinity. BtsS cannot be autophosphorylated, possibly owing to a defective ATP-binding site within the G1 box³ (data not shown). Therefore, we used the method of differential radial capillary action of ligand assays (DRaCALA)¹² to determine whether BtsS physically interacts with pyruvate as ligand. The technique is based on the ability of proteins that have been immobilized on a nitrocellulose membrane to bind a radiolabeled ligand, whereas unbound ligands undergo radial diffusion. DRaCALA allows rapid detection of both the total ligand and the ligand sequestered by proteins. The fraction of ligand bound to the protein, defined as F_B , is calculated from the signal intensity of the area with protein (inner circle) and the total signal intensity of the area (outer circle)¹². For the DRaCALA we used unsealed membrane vesicles prepared from *E. coli* cells overproducing BtsS (MV BtsS) and calculated an F_B value of >0.15 (Fig. 5A). Control membrane vesicles (MV, lacking overproduced BtsS) were used and the low value of F_B (0.05) reflected only minor, non-specific binding. Therefore this assay was judged to be suitable for membrane vesicles, and it clearly indicated binding of radiolabeled pyruvate to BtsS. We also tested ³H-serine binding to BtsS in membrane vesicles using the DRaCALA technique. However, we only observed unspecific binding (data not shown).

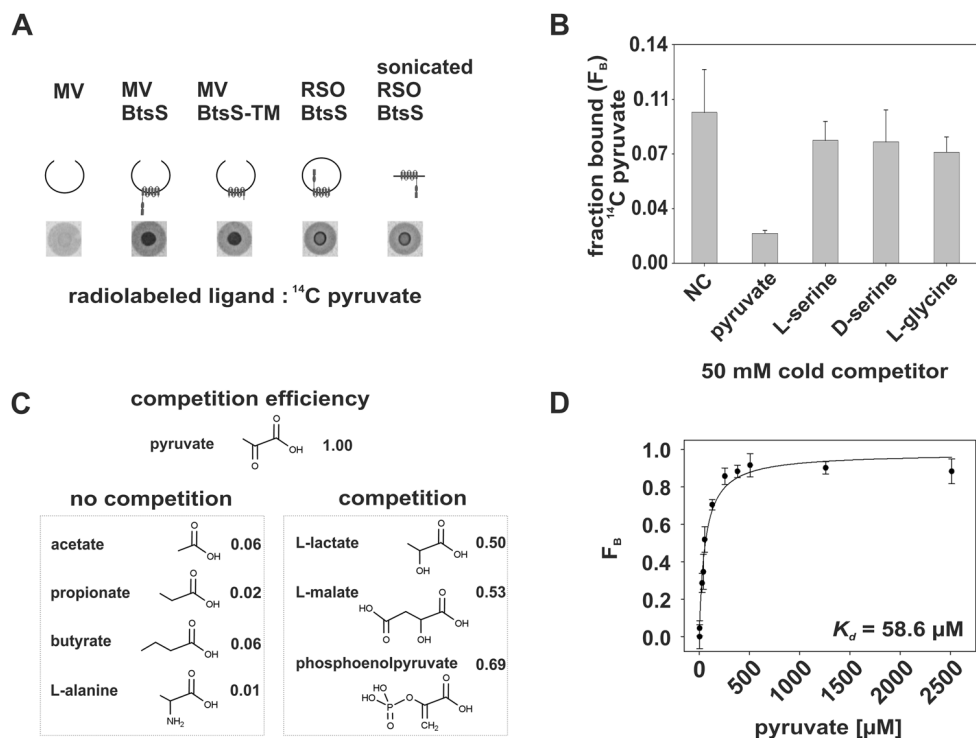


Figure 5. Analysis of the interaction of BtsS with selected ligands by DRaCALA. (A) A mixture of membrane vesicles (MV) or right-side-out vesicles (RSO) enriched with the corresponding proteins (indicated by graphical representations) and radiolabeled ^{14}C pyruvate ($5\ \mu\text{M}$) is dropped onto a nitrocellulose membrane, and ligand migration via capillary action is analyzed. (B) Competition assays. Binding of radiolabeled pyruvate ($5\ \mu\text{M}$) to BtsS in MVs was analyzed in the presence of various unlabeled competitors (each $50\ \text{mM}$). NC, no competitor. (C) Relative efficiency of competition by various carboxylic acids. Binding of radiolabeled pyruvate ($5\ \mu\text{M}$) to BtsS in MVs was analyzed in the presence of various carboxylic acids (each $50\ \text{mM}$). The efficiency of competition by cold pyruvate was set to 1.00, and the effect of the indicated compounds was calculated accordingly. (D) Determination of the dissociation constant (K_d) for pyruvate to BtsS using DRaCALA. For each reaction radiolabeled pyruvate was used at $5\ \mu\text{M}$. Normalized F_B values [$F_B = (F_{B(\text{NC})} - F_{B(\text{pyr})})/F_{B(\text{NC})}$; see Methods for details] were plotted as function of the pyruvate concentration. The best-fit line was determined by nonlinear regression using the equation $y = B_{\text{max}} * x / (K_d + x)$.

In addition, we tested MVs harboring a membrane-integrated truncated variant of BtsS (MV BtsS-TM) lacking its soluble domains, and found that this truncated sensor also binds pyruvate ($F_B > 0.15$). Furthermore, we prepared sealed right-side-out vesicles (RSO BtsS), in which membrane proteins retain their native orientation¹³. BtsS in these vesicles also showed pyruvate binding, and no significant change in binding was observed when these vesicles were fragmented by sonication and had a random orientation (sonicated RSO BtsS) (F_B values of each 0.18) (Fig. 5A). These data reveal that pyruvate binds to the external side of the membrane-spanning domain of BtsS.

The specificity of pyruvate binding to BtsS was then addressed by using a competition assay (Fig. 5B), in which several competitors were added in excess to the reaction mixture. Only unlabeled (“cold”) pyruvate was able to prevent binding of radiolabeled pyruvate. L-serine, D-serine or glycine did not interfere with pyruvate binding to BtsS, suggesting that pyruvate binds specifically to BtsS.

Next we investigated the effects of varying the length and side-chain charge on ligand binding by BtsS. Using competition assays, we found that acetate, propionate and butyrate all failed to compete with pyruvate for binding, indicating the importance of the C- α keto group of pyruvate (Fig. 5C). The influence of polarity at the C- α position was then tested by addition of lactate and malate, which contain C- α hydroxyl groups. These molecules were able to decrease pyruvate binding by about 50% suggesting that a negative charge seems to be recognized. It should be noted that these compounds were tested in a 10^4 -fold excess over pyruvate. Phosphoenolpyruvate, which harbors a phosphoryl group at the C- α position, also competed with pyruvate, reducing binding by approximately 50%. In contrast, a positive charge at the C- α position in the form of the amino group in alanine had no effect, reducing pyruvate binding by 1% (Fig. 5C). Notably, none of these compounds were able to induce *yjiY* expression *in vivo*, which emphasizes the specificity of BtsS for pyruvate. The dissociation constant (K_d) for pyruvate binding to the histidine kinase was found to be $58.6 \pm 8.8\ \mu\text{M}$ (Fig. 5D).

To our knowledge this is the first application of DRaCALA to measure the interaction between a ligand and a membrane-embedded protein. Moreover, these assays unambiguously demonstrated that pyruvate binds specifically and with high affinity to BtsS.

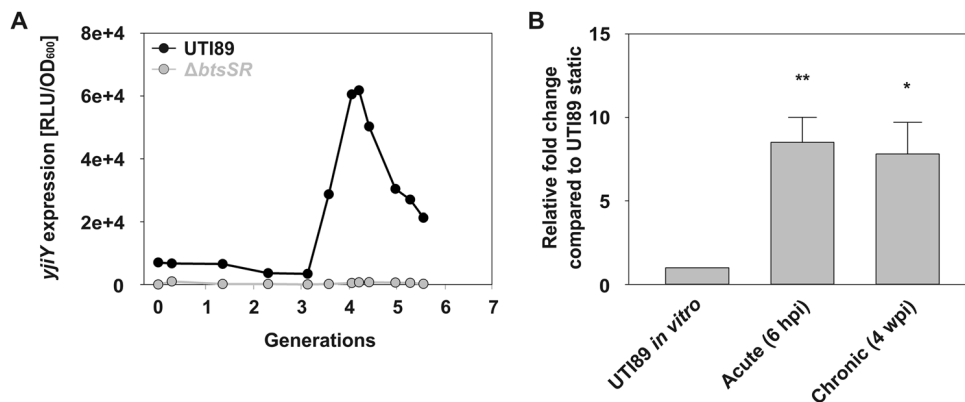


Figure 6. BtsS/BtsR importance during urinary tract infection. **(A)** The plot indicates the activity of the pBBR *yjiY-lux* reporter fusion in WT UTI89 and the isogenic *btsS/btsR* mutant during growth in LB, and depicts a representative of at least 6 biological replicates. **(B)** Change in the level of the *yjiY* transcript during acute and chronic phases of UTI relative to that measured in samples incubated *in vitro* without agitation. Data shown are the mean values of samples extracted from three different mice per time point. RNA was extracted from dissected bladders for each time point and enriched for bacterial RNA by depleting ribosomal and mammalian RNA as described in Materials and Methods. Profiling was performed using an *yjiY*-specific probe. Expression was normalized to that of the housekeeping gene *gyrB* and compared to expression in cDNA samples corresponding to the starting inoculum (static *in vitro* culture, prepared as described in Materials and methods). Relative fold change was measured using the method described by Pfaffl *et al.*⁵⁴ (hpi, hours post infection; wpi, weeks post infection).

BtsS/BtsR importance during urinary tract infection. To understand the potential implications of BtsS/BtsR for pathogenesis, we therefore turned our attention to uropathogenic *E. coli* (UPEC) that colonize a nutritionally demanding environment – the mammalian bladder. However, responses to nutritional stress are of the utmost importance for the survival of both commensal and pathogenic bacteria within a given host.

UPEC strains are the primary causative agent of urinary-tract infections (UTIs) worldwide, accounting for over 85% of all reported episodes¹⁴. In the bladder, bacteria adhere to the apical surface of the epithelium and are internalized, before replicating to form biofilm-like pods within host bladder cells^{15, 16}. Subsequent to this transient intracellular cascade, adverse outcomes such as chronic colonization can ensue as a result of an aberrant host immune response¹⁷. Previous studies have demonstrated that successful UTI requires aerobic respiration and amino acid utilization^{18–20}. To investigate the significance of BtsS/BtsR in bladder infection, we first created a *btsS/btsR* mutant in the UPEC cystitis isolate UTI89. Using the same reporter fusion, we demonstrated that this strain, unlike the wild-type parental UTI strain, failed to induce transient expression of *yjiY* (Fig. 6A). Both pyruvate and L-serine are present in human and murine urine, and levels are elevated in diabetic populations^{21–23}. Given that BtsS/BtsR responds directly to extracellular pyruvate levels and indirectly to L-serine, we asked whether BtsS/BtsR is active in the bladder lumen during acute and chronic UTI.

Mice were infected with the cystitis isolate UTI89 and RNA samples were extracted from bladder homogenates at 6 h post infection (coinciding with the acute stage of UTI), and at 2 weeks post infection from mice that went on to develop chronic cystitis. At this stage, the majority of bacteria are found on the bladder epithelial surface in the form of an extracellular biofilm¹⁷. Subsequent TaqMan-based qPCR analysis compared the expression of *yjiY* in the corresponding cDNA samples to the expression of *yjiY* in the starting bacterial inoculum. Our results demonstrated robust expression of *yjiY* in both the acute and chronic stages of infection from at least three separate mice per time-point (Fig. 6B). Taken together, these data suggest that, in the murine UTI model BtsS/BtsR responds to serine/pyruvate fluctuations and could play a role in promoting the infection process.

Discussion

Although numerous studies continue to demonstrate the importance of histidine kinase-mediated signal transduction in bacterial physiology, the natural ligands have been identified for very few histidine kinases^{24–26}. This study presents compelling evidence demonstrating that the histidine kinase BtsS is a high-affinity receptor for extracellular pyruvate. Induction of the BtsS/BtsR target gene *yjiY*, which codes for a “carbon starvation” CstA-like transporter, correlates with the depletion of serine in complex medium, explaining the observation that BtsS/BtsR senses low serine. At the same time, while serine is being depleted from LB medium, *E. coli* excretes a substantial amount of pyruvate from overflow metabolism into the medium. Shortly afterwards, the concentration of extracellular pyruvate returns to its basal level (Fig. 3 and ref. 11). In previous studies, we demonstrated activation of a different system, YpdA/YpdB in response to high levels of extracellular pyruvate¹¹ and showed that induction of YpdA/YpdB enhances BtsS/BtsR activation¹. The current work provides a comprehensive characterization of how BtsS/BtsR directly responds to extracellular pyruvate levels and fine-tunes the metabolic fitness of *E. coli* under low-nutrient conditions. Sequence comparison between YpdA and YehU did not identify putative amino acids involved in pyruvate binding. In non-pathogenic *E. coli*, each of these signaling systems induces the expression of exactly one gene, which codes for a transporter. One (YhjX) belongs to the major facilitator

superfamily, and is assumed to be a low-affinity carboxylate antiporter²⁷. The other one (YjiY) belongs to the CstA-like transporters, which are characterized by an unusually large number of transmembrane helices (17 in the case of YjiY). Neither transporter has been characterized thus far. It is hypothesized that both are involved in nutrient uptake, but with different affinities. The interconnectivity between the high-affinity pyruvate signaling system BtsS/BtsR with the putative low-affinity pyruvate signaling system YpdA/YpdB by a positive and a negative feedback loop¹ would provide *E. coli* with a network that could tailor pyruvate uptake in each individual cell according to its availability. Switching between low- and high-affinity phosphate transporters based on the needs of the individual cell was recently demonstrated for *S. cerevisiae*²⁸, and seems to be a widely distributed strategy for the maintenance of nutrient homeostasis as stocks of essential nutrients decline²⁹.

Although nutrient sensing is crucial for host-microbe and microbe-microbe interactions, the majority of studies in non-pathogenic *E. coli* strains have focused on metabolic engineering, aiming to understand how processes such as elevated intracellular pyruvate levels affect metabolite distribution^{30,31} or how central mutations trigger/alter metabolic fluxes^{32–34}. In recent years, technological advances have permitted detailed analyses of *in vivo* metabolism³⁵, revealing its complexity and its influence on virulence and pathogenesis³⁶. These studies have shown pyruvate to be one of the major factors connecting cellular metabolism to cell division³⁷. Moreover, pyruvate levels are thought to reflect the quantitative relationship between carbon and nitrogen availability in the cell, and affect amino acid biosynthesis³⁸.

Investigations of how metabolic decisions determine pathogen fitness within host niches are increasingly uncovering opportunities for the development of robust and pathogen-specific drugs. Different *E. coli* pathotypes cause various clinical syndromes, depending on their genetic makeup and expression patterns. They obviously differ extensively from each other and from commensal *E. coli*. For example, uropathogenic and enterohemorrhagic *E. coli* differ significantly in genome content, and employ different strategies to infect their niches - the bladder and the gut, respectively. Very recent work has pointed to the need for aerobic respiration and amino acid utilization for optimal colonization of the urinary tract by UPEC^{18–20}. Pyruvate is a crucial molecule required for fueling the aerobic arm of the tricarboxylic acid cycle, which is used by UPEC during infection^{18,19,39}. Thus, it is reasonable to postulate that UPEC has the capacity to sense and respond to pyruvate fluctuations within the urinary tract. Here we demonstrate that BtsS/BtsR mediates *yjiY* expression during infection by a clinically relevant UPEC isolate, which strongly suggests that BtsS/BtsR constitutes part of the metabolic circuitry engaged during UTI. Thus understanding how UPEC can sense the metabolic signature of the bladder lumen, the kidney and the urothelial cell cytosol (in which they form intracellular bacterial communities) will be vital for a complete understanding of pathogen strategies and the design of more effective therapeutics. However, the study in *Salmonella enterica* Serovar Typhi and Typhimurium showed no detectable effect on the ability of *yehUT* mutant strain to invade cultured epithelial cells or induce colitis in a murine model⁴⁰.

In summary, this study has uncovered a signal transduction network that responds with exquisite sensitivity to extracellular pyruvate levels and fine-tunes carbon utilization in *E. coli* strains. Furthermore we provide direct evidence for receptor-ligand interactions between BtsS and pyruvate, and demonstrate that BtsS/BtsR mediates *yjiY* expression during UTI. Future studies will focus on understanding the contribution of this system to pathogenic *E. coli* intra-host fitness and dissecting molecular determinants that drive the fine-tuning of bacterial fitness in response to external metabolic cues.

Methods

Strains, plasmids, and oligonucleotides. In this study we used the *E. coli* strains MG1655⁴¹, *E. coli* MG1655 $\Delta yhjX^1$, *E. coli* MG1655 $\Delta yjiY^1$, BL21(DE3)⁴², *E. coli* KX1468⁴³ and the cystitis isolate UTI89⁴⁴. Plasmids used in this study include the transcriptional promoter-luciferase fusion construct for P_{yjiY} activity (pBBR *yjiY-lux*)³. For protein production we used the arabinose-inducible expression vectors pBAD24⁴⁵, pBAD24-*yehU*³ and pBAD24-*yehU*-TM (YehU (BtsS) amino acids 1–205). DNA fragments for plasmid construction were amplified from genomic DNA by PCR. Scarless deletion of *btsS/btsR* genes in UTI89 was performed using the method published by Murphy and Campellone⁴⁶, and verified via PCR with oligonucleotides flanking the deleted loci. All oligonucleotide sequences are available on request.

Molecular biological techniques. Plasmid and genomic DNAs were isolated using a HiYield plasmid minikit (Suedlaborbedarf) and a DNeasy blood and tissue kit (Qiagen), respectively. DNA fragments were purified from agarose gels using a HiYield PCR cleanup and gel extraction kit (Suedlaborbedarf). Q5 DNA polymerase (New England BioLabs) was used according to the supplier's instructions. Restriction enzymes and other DNA-modifying enzymes were also purchased from New England BioLabs and used according to the manufacturer's directions.

Growth conditions. All strains were grown overnight in LB medium. After inoculation, bacteria were routinely grown in LB, LB supplemented with the indicated amino acids or diluted LB medium [containing 1% (w/v) NaCl] under agitation (200 rpm) at 37 °C. For solid medium, 1.5% (w/v) agar was added. Where appropriate, media were supplemented with antibiotics (ampicillin sodium salt, 100 µg/ml; kanamycin sulfate, 50 µg/ml; gentamicin sulfate, 50 µg/ml). For infection studies in mice, UTI89 was inoculated into 10 ml of LB medium and grown without shaking at 37 °C for 24 h. This culture was used to seed a fresh flask with 10 ml of a 1:1000 dilution, which was incubated for another 24 h to maximize expression of type 1 pili, as previously described⁴⁷. The growth phases of *E. coli* marked in graphs were according to the definition in ref. 48.

In vivo expression studies. *In vivo* expression of *yjiY* was quantified by means of luciferase-based reporter-gene assays, using bacteria that had been transformed with plasmid pBBR *yjiY-lux*. Cells from an overnight culture were transferred to fresh medium to give a starting optical density at 600 nm (OD₆₀₀) of 0.05, and

incubated under aerobic growth conditions at 37 °C while OD₆₀₀ and luminescence were continuously monitored. The optical density was determined in a microplate reader (Tecan Sunrise) at 600 nm. Luminescence levels were determined in a luminescence reader (Centro LB960; Berthold Technology) for 0.1 s and are reported as relative light units (RLU; counts s⁻¹).

Identification of quorum sensing-like molecule. The cells of *E. coli* MG1655 $\Delta yjiY$ /pBBR *yjiY-lux* were cultivated in M9-minimal medium supplemented with 20 mM gluconic acid and OD₆₀₀ and luminescence were constantly monitored. Cells were harvested shortly before, at and after the induction of *yjiY*. The supernatant was sterile filtrated (Stericup[®], Filter Unit Millipore Express[®] PLUS(PES), 0.22 μ m) and separated by high pressure liquid chromatography (HPLC) using column C18-Hypersil Gold, with the gradient 1–100% (v/v) acetonitrile in 40 min. Fractions were collected, concentrated and used in reporter strain *E. coli* KX1468⁴³/pBBR *yjiY-lux* grown in M9-minimal medium supplemented with 20 mM succinate. The fraction with the highest induction potential was then analyzed via UPLC-UHR-ToF-MS using a Waters XBridge Amide column.

Production of BtsS-6His in membrane vesicles. *E. coli* BL21(DE3) cells were transformed with the vector pBAD24-*yehU*³, which codes for BtsS-6His, and grown in LB medium at 37 °C to an OD₆₀₀ of 0.5. Recombinant gene expression was induced by addition of 0.2% (w/v) arabinose. After 3 h of further incubation, cells were harvested by centrifugation, disrupted and fractionated. At each step, the pellet was resuspended in buffer consisting of MES/NaOH (pH 6), 10% (v/v) glycerol and 10 mM MgCl₂. To produce BtsS-6His in right-side-out vesicles, cells were cultivated as described before. After harvesting the cells by centrifugation, lysozyme (50 μ g/ml) and EDTA (10 mM) were added for 45 min at room temperature to remove the cell wall. After low-speed centrifugation, the spheroplasts were resuspended in buffer consisting of 100 mM MES/NaOH (pH 6), 30% (w/v) sucrose, 20 mM MgSO₄, DNase and RNase, and then diluted 100-fold into pre-warmed buffer (100 mM MES/NaOH (pH 6)) to trigger osmotic lysis. After centrifugation, the pellet was resuspended in 100 mM MES/NaOH (pH 6), 10% (v/v) glycerol and 10 mM MgCl₂. Formation of spheroplasts and right-side-out vesicles was monitored under the microscope. His-tagged BtsS was detected by Western blot analysis with an anti-His antibody (Qiagen) and an alkaline phosphatase-conjugated anti-mouse antibody as the secondary antibody.

Protein-ligand interactions. Protein-ligand interactions were analyzed via DRaCALA, a method established by Roelofs *et al.*¹². Membrane vesicles enriched for overproduced BtsS-6His were mixed with 5 μ M radiolabeled (3-¹⁴C) pyruvic acid sodium salt (55 mCi mmol⁻¹, Biotrend) or radiolabeled (³H) L-serine (11.0 Ci mmol⁻¹, Hartmann Analytics) and incubated for 5 min at room temperature. Triplicate 5- μ l aliquots were transferred to a nitrocellulose membrane, dried and visualized by a PhosphorImager. Quantification of radioactive signal was done with the software ImageQuant. The fraction bound to protein was calculated according to the signal intensities using an equation defined earlier: $F_B = (I_{\text{inner}} - I_{\text{background}})/I_{\text{total}}$ ¹². For the evaluation the corresponding cold ligand (50 mM) was added to the reaction mixture and incubated for further 3 min. To estimate the K_d value, increasing concentrations of cold pyruvate (0 μ M to 2.5 mM) were used. In this case the F_B value was normalized as follows: $F_B = (F_{B(\text{NC})} - F_{B(\text{pyr})})/F_{B(\text{NC})}$. Here, $F_{B(\text{NC})}$ is calculated from the sample with pure ¹⁴C-labeled pyruvate, and $F_{B(\text{pyr})}$ are all values for mixtures containing ¹⁴C-labeled pyruvate together with increasing concentrations of unlabeled pyruvate. The amount of ¹⁴C-pyruvate was kept constant in all assays.

Extraction and determination of extra- and intracellular metabolites. The reporter strain *E. coli* MG1655/pBBR *yjiY-lux* was cultivated in LB medium, and OD₆₀₀ and luminescence were constantly monitored. At selected time points, cells were harvested and the supernatants were saved. Cells were washed with 10% (v/v) glycerol, and subsequently cell pellets and supernatants were analyzed via hydrophilic interaction liquid chromatography (HILIC). Acetonitrile (ACN), methanol (MeOH), ammonium acetate and ammonium hydroxide (all of LC-MS grade) were obtained from Sigma-Aldrich (Sigma-Aldrich GmbH). Water was purified using a Merck Millipore Integral water purification system to a resistance of 18 M Ω and TOC < 5 ppb. Sodium pyruvate and serine were also obtained from Sigma-Aldrich and dissolved in water at a concentration of 100 mM and further diluted with ACN. Cell pellets were extracted with 200 μ l ice-cold water/MeOH (50/50, v/v). Samples were vortexed vigorously and lysed in an ice-cold sonic bath for 15 min. After centrifugation at 20,000 \times g and 4 °C for 10 min, supernatants were transferred to autosampler vials.

Pyruvate and serine were quantified using a modified version of the method published by Yuan *et al.*⁴⁹. Separation was achieved using a Waters XBridge Amide column (3.5 μ m, 100 mm \times 4.6 mm ID) and an ACN/water gradient using a Waters Acquity UPLC system coupled to a Bruker maXis UHR-ToF-MS (Bruker Daltonics). Eluent A consisted of 5% (v/v) ACN, 95% (v/v) water, 20 mM ammonium hydroxide, 20 mM ammonium acetate, pH 9.0 and eluent B was pure ACN.

Metabolites were eluted with the following gradient: After 3 min of 85% B, a linear decrease to 2% B over 9 min, isocratic hold for 3 min and return to initial conditions for 1 min and a 7-min re-equilibration time. Sample (5 μ l) was injected via partial loop injection.

For quantification a calibration curve was generated from different concentrations of standard compounds (0 μ M, 0.5 μ M, 1.0 μ M, 2.5 μ M, 5 μ M, 10 μ M, 25 μ M, 50 μ M, 100 μ M, 250 μ M). If the concentration of a sample was beyond the range of the calibration curve, it was appropriately diluted with water/MeOH. Quantification was performed with Bruker Quant Analysis.

Murine infections. A cohort (15) of 7- to 8-week old female C3H/HeN mice was infected with strain UTI89 via transurethral catheterization as described in Hung *et al.*⁵⁰. Five mice were sacrificed at 6 h after infection, marking the acute stage of UTI in this murine model⁵¹. Bladders were excised for CFU enumeration and RNA extraction. The remaining 10 mice were monitored for chronic infection using longitudinal urinalysis, as previously described⁵². Mice that consistently shed more than 100,000 CFUs/ml of urine were separated from the

rest of the cohort, and flagged as chronically infected. These mice were sacrificed at 4 weeks post infection and bladders were obtained for CFU enumeration and RNA extraction.

To ensure the proper and humane treatment of animals, all animal studies were carried out in strict accordance with the recommendations in the Guide for the Care and Use of Laboratory Animals of the National Institutes of Health, and the Vanderbilt University Medical Center's Institutional Animal Care and Use Committee (IACUC), who approved all protocols. Statistical analyses were performed using two-tailed Mann-Whitney t-test.

RNA extraction, cDNA synthesis and qPCR. RNA extraction and bacterial RNA enrichment were performed as described by Conover *et al.*⁴⁷. DNase treatment, reverse transcription, and real-time quantitative PCR were done as described by Guckes *et al.*⁵³. qPCR analysis was carried out with three concentrations of cDNA (50 ng, 25 ng, 12.5 ng), each in triplicate for each sample, and levels of *gyrB* (DNA gyrase) were used for normalization. The following primers (Integrated DNA Technologies) were used for amplification: *yjiY*_Fwd (5'-GGCAGCAGCCGAAACT-3'), *yjiY*_Rev (5'-GCCGTAGCCGATGAAACG-3'), *gyrB*_L (5'-GATGCGCGTGAAGGCCTGAATG-3'), *gyrB*_R (5'-CACGGGCACGGGCAGCATC-3'). The following probes (Applied Biosystems) were used for quantification; *yjiY* (5'-FAM-TGGCTAATGAAACCGACGC-MGBNFQ-3'); *gyrB* (5'-VIC-ACGAAGTCTG-GCGGA-MGBNFQ-3').

References

- Behr, S., Fried, L. & Jung, K. Identification of a novel nutrient-sensing histidine kinase/response regulator network in *Escherichia coli*. *J. Bacteriol.* **196**, 2023–2029, doi:10.1128/JB.01554-14 (2014).
- Galperin, M. Y. Telling bacteria: do not LytTR. *Structure* **16**, 657–659, doi:10.1016/j.str.2008.04.003 (2008).
- Kraxenberger, T., Fried, L., Behr, S. & Jung, K. First insights into the unexplored two-component system YehU/YehT in *Escherichia coli*. *J. Bacteriol.* **194**, 4272–4284, doi:10.1128/JB.00409-12 (2012).
- Schultz, J. E. & Matin, A. Molecular and functional characterization of a carbon starvation gene of *Escherichia coli*. *J. Mol. Biol.* **218**, 129–140, doi:10.1016/0022-2836(91)90879-B (1991).
- Romeo, T., Vakulskas, C. A. & Babitzke, P. Post-transcriptional regulation on a global scale: form and function of Csr/Rsm systems. *Environ. Microbiol.* **15**, 313–324, doi:10.1111/j.1462-2920.2012.02794.x (2013).
- Sabnis, N. A., Yang, H. & Romeo, T. Pleiotropic regulation of central carbohydrate metabolism in *Escherichia coli* via the gene *csrA*. *J. Biol. Chem.* **270**, 29096–29104, doi:10.1074/jbc.270.49.29096 (1995).
- Berzelius, J. Ueber die Destillationsproducte der Traubensäure. *Ann. Phys.* **112**, 1–29, doi:10.1002/andp.18351120902 (1835).
- Prüss, B., Nelms, J. M., Park, C. & Wolfe, A. J. Mutations in NADH: ubiquinone oxidoreductase of *Escherichia coli* affect growth on mixed amino acids. *J. Bacteriol.* **176**, 2143–2150, doi:10.1002/bit.22119 (1994).
- Selvarasu, S. *et al.* Characterizing *Escherichia coli* DH5 α growth and metabolism in a complex medium using genome-scale flux analysis. *Biotechnol. Bioeng.* **102**, 923–934, doi:10.1002/bit.v102:3 (2009).
- Polzin, S. *et al.* Growth media simulating ileal and colonic environments affect the intracellular proteome and carbon fluxes of enterohemorrhagic *Escherichia coli* O157: H7 strain EDL933. *Appl. Environ. Microbiol.* **79**, 3703–3715, doi:10.1128/AEM.00062-13 (2013).
- Fried, L., Behr, S. & Jung, K. Identification of a target gene and activating stimulus for the YpdA/YpdB histidine kinase/response regulator system in *Escherichia coli*. *J. Bacteriol.* **195**, 807–815, doi:10.1128/JB.02051-12 (2013).
- Roelofs, K. G., Wang, J., Sintim, H. O. & Lee, V. T. Differential radial capillary action of ligand assay for high-throughput detection of protein-metabolite interactions. *Proc. Natl. Acad. Sci. USA* **108**, 15528–15533, doi:10.1073/pnas.1018949108 (2011).
- Kaback, H. Bacterial Membranes. *Methods Enzymol.* **22**, 99–120, doi:10.1016/0076-6879(71)22015-2 (1971).
- Foxman, B. The epidemiology of urinary tract infection. *Nat. Rev. Urol.* **7**, 653–660, doi:10.1038/nrurol.2010.190 (2010).
- Mulvey, M. A. *et al.* Induction and evasion of host defenses by type 1-piliated uropathogenic *Escherichia coli*. *Science* **282**, 1494–1497, doi:10.1126/science.282.5393.1494 (1998).
- Anderson, G. G. *et al.* Intracellular bacterial biofilm-like pods in urinary tract infections. *Science* **301**, 105–107, doi:10.1126/science.1084550 (2003).
- Hannan, T. J. *et al.* Host-pathogen checkpoints and population bottlenecks in persistent and intracellular uropathogenic *Escherichia coli* bladder infection. *FEMS Microbiol. Rev.* **36**, 616–648, doi:10.1111/j.1574-6976.2012.00339.x (2012).
- Alteri, C. J., Smith, S. N. & Mobley, H. L. Fitness of *Escherichia coli* during urinary tract infection requires gluconeogenesis and the TCA cycle. *PLoS Pathog.* **5**, e1000448, doi:10.1371/journal.ppat.1000448 (2009).
- Hadjifrangiskou, M. *et al.* A central metabolic circuit controlled by QseC in pathogenic *Escherichia coli*. *Mol. Microbiol.* **80**, 1516–1529, doi:10.1111/j.1365-2958.2011.07660.x (2011).
- Floyd, K. A. *et al.* Adhesive fiber stratification in uropathogenic *Escherichia coli* biofilms unveils oxygen-mediated control of type 1 pili. *PLoS Pathog.* **11**, e1004697, doi:10.1371/journal.ppat.1004697 (2015).
- Stec, D. F. *et al.* Alterations of urinary metabolite profile in model diabetic nephropathy. *Biochem. Biophys. Res. Com.* **456**, 610–614, doi:10.1016/j.bbrc.2014.12.003 (2015).
- Bouatra, S. *et al.* The human urine metabolome. *PLoS One* **8**, doi:10.1371/journal.pone.0073076 (2013).
- Kaur, P. *et al.* Quantitative metabolomic and lipidomic profiling reveals aberrant amino acid metabolism in type 2 diabetes. *Mol. Biosyst.* **9**, 307–317, doi:10.1039/c2mb25384d (2013).
- Reinelt, S., Hofmann, E., Gerharz, T., Bott, M. & Madden, D. R. The structure of the periplasmic ligand-binding domain of the sensor kinase CitA reveals the first extracellular PAS domain. *J. Biol. Chem.* **278**, 39189–39196, doi:10.1074/jbc.M305864200 (2003).
- Cheung, J. & Hendrickson, W. A. Structural analysis of ligand stimulation of the histidine kinase NarX. *Structure* **17**, 190–201, doi:10.1016/j.str.2008.12.013 (2009).
- Gudipaty, S. A. & McEvoy, M. M. The histidine kinase CusS senses silver ions through direct binding by its sensor domain. *Biochim. Biophys. Acta* **1844**, 1656–1661, doi:10.1016/j.bbapap.2014.06.001 (2014).
- Pao, S. S., Paulsen, I. T. & Saier, M. H. Jr. Major facilitator superfamily. *Microbiol. Mol. Biol. Rev.* **62**, 1–34 (1998).
- Wykoff, D. D., Rizvi, A. H., Raser, J. M., Margolin, B. & O'Shea, E. K. Positive feedback regulates switching of phosphate transporters in *S. cerevisiae*. *Mol. Cell* **27**, 1005–1013, doi:10.1016/j.molcel.2007.07.022 (2007).
- Levy, S., Kafri, M., Carmi, M. & Barkai, N. The competitive advantage of a dual-transporter system. *Science* **334**, 1408–1412, doi:10.1126/science.1207154 (2011).
- Yang, Y.-T., Bennett, G. N. & San, K.-Y. The effects of feed and intracellular pyruvate levels on the redistribution of metabolic fluxes in *Escherichia coli*. *Metab. Eng.* **3**, 115–123, doi:10.1006/mben.2000.0166 (2001).
- Sauer, U. & Eikmanns, B. J. The PEP-pyruvate-oxaloacetate node as the switch point for carbon flux distribution in bacteria. *FEMS Microbiol. Rev.* **29**, 765–794, doi:10.1016/j.femsre.2004.11.002 (2005).
- Fischer, E. & Sauer, U. Metabolic flux profiling of *Escherichia coli* mutants in central carbon metabolism using GC-MS. *Eur. J. Biochem.* **270**, 880–891, doi:10.1046/j.1432-1033.2003.03448.x (2003).

33. Wang, Q., Ou, M. S., Kim, Y., Ingram, L. & Shanmugam, K. Metabolic flux control at the pyruvate node in an anaerobic *Escherichia coli* strain with an active pyruvate dehydrogenase. *Appl. Environ. Microbiol.* **76**, 2107–2114, doi:10.1128/AEM.02545-09 (2010).
34. Murarka, A., Clomburg, J. M. & Gonzalez, R. Metabolic flux analysis of wild-type *Escherichia coli* and mutants deficient in pyruvate-dissimilating enzymes during the fermentative metabolism of glucuronate. *Microbiology* **156**, 1860–1872, doi:10.1099/mic.0.036251-0 (2010).
35. Eylert, E. *et al.* Carbon metabolism of *Listeria monocytogenes* growing inside macrophages. *Mol. Microbiol.* **69**, 1008–1017, doi:10.1111/j.1365-2958.2008.06337.x (2008).
36. Eisenreich, W., Dandekar, T., Heesemann, J. & Goebel, W. Carbon metabolism of intracellular bacterial pathogens and possible links to virulence. *Nat. Rev. Microbiol.* **8**, 401–412, doi:10.1038/nrmicro2351 (2010).
37. Göhler, A.-K. *et al.* More than just a metabolic regulator - elucidation and validation of new targets of PdhR in *Escherichia coli*. *BMC Syst. Biol.* **5**, 197, doi:10.1186/1752-0509-5-197 (2011).
38. Chubukov, V., Gerosa, L., Kochanowski, K. & Sauer, U. Coordination of microbial metabolism. *Nat. Rev. Microbiol.* **12**, 327–340, doi:10.1038/nrmicro3238 (2014).
39. Floyd, K. A. *et al.* The UbiI (VisC) aerobic ubiquinone synthase is required for expression of type 1 pili, biofilm formation, and pathogenesis in uropathogenic *Escherichia coli*. *J. Bacteriol.* **198**, 2662–2672, doi:10.1128/JB.00030-16 (2016).
40. Wong, V. K. *et al.* Characterization of the *yehUT* Two-Component Regulatory System of *Salmonella enterica* Serovar Typhi and Typhimurium. *PLoS One* **8**, doi:10.1371/journal.pone.0084567 (2013).
41. Blattner, F. *et al.* The complete genome sequence of *Escherichia coli* K-12. *Science* **277**, 1453–1474, doi:10.1126/science.277.5331.1453 (1997).
42. Studier, F. W. & Moffatt, B. A. Use of bacteriophage T7 RNA polymerase to direct selective high-level expression of cloned genes. *J. Mol. Biol.* **189**, 113–130, doi:10.1016/0022-2836(86)90385-2 (1986).
43. Xavier, K. B. & Bassler, B. L. Regulation of uptake and processing of the quorum-sensing autoinducer AI-2 in *Escherichia coli*. *J. Bacteriol.* **187**, 238–248, doi:10.1128/JB.187.1.238-248.2005 (2005).
44. Schilling, J. D., Mulvey, M. A., Vincent, C. D., Lorenz, R. G. & Hultgren, S. J. Bacterial invasion augments epithelial cytokine responses to *Escherichia coli* through a lipopolysaccharide-dependent mechanism. *J. Immunol.* **166**, 1148–1155, doi:10.4049/jimmunol.166.2.1148 (2001).
45. Guzman, L., Belin, D., Carson, M. & Beckwith, J. Tight regulation, modulation, and high-level expression by vectors containing the arabinose P_{BAD} promoter. *J. Bacteriol.* **177**, 4121–4130, doi:10.1128/jb.177.14.4121-4130.1995 (1995).
46. Murphy, K. C. & Campellone, K. G. Lambda Red-mediated recombinogenic engineering of enterohemorrhagic and enteropathogenic *Escherichia coli*. *BMC Mol. Biol.* **4**, 1, doi:10.1186/1471-2199-4-11 (2003).
47. Conover, M. S. *et al.* Metabolic Requirements of *Escherichia coli* in Intracellular Bacterial Communities during Urinary Tract Infection Pathogenesis. *mBio* **7**, e00104–00116, doi:10.1128/mBio.00104-16 (2016).
48. Pörtner, R. Grundlagen der Bioverfahrenstechnik. In Antranikian, G. (Ed.) *Angewandte Mikrobiologie* Springer-Verlag, Berlin, Heidelberg p. 240 (2006)
49. Yuan, M., Breitskopf, S. B., Yang, X. & Asara, J. M. A positive/negative ion-switching, targeted mass spectrometry-based metabolomics platform for bodily fluids, cells, and fresh and fixed tissue. *Nat. Protoc.* **7**, 872–881, doi:10.1038/nprot.2012.024 (2012).
50. Hung, C.-S., Dodson, K. W. & Hultgren, S. J. A murine model of urinary tract infection. *Nat. Protoc.* **4**, 1230–1243, doi:10.1038/nprot.2009.116 (2009).
51. Justice, S. S. *et al.* Differentiation and developmental pathways of uropathogenic *Escherichia coli* in urinary tract pathogenesis. *Proc. Natl. Acad. Sci. USA* **101**, 1333–1338, doi:10.1073/pnas.0308125100 (2004).
52. Hannan, T. J., Mysorekar, I. U., Hung, C. S., Isaacson-Schmid, M. L. & Hultgren, S. J. Early severe inflammatory responses to uropathogenic *Escherichia coli* predispose to chronic and recurrent urinary tract infection. *PLoS Pathog.* **6**, doi:10.1371/journal.ppat.1001042 (2010).
53. Guckes, K. R. *et al.* Strong cross-system interactions drive the activation of the QseB response regulator in the absence of its cognate sensor. *Proc. Natl. Acad. Sci. USA* **110**, 16592–16597, doi:10.1073/pnas.1315320110 (2013).
54. Pfaffl, M. W. A new mathematical model for relative quantification in real-time RT-PCR. *Nucleic Acids Res* **29**, e45–e45, doi:10.1093/nar/29.9.e45 (2001).

Acknowledgements

This work was supported by the Deutsche Forschungsgemeinschaft (Exc114/2, SPP1617, JU270/12-2 to K.J.), by Vanderbilt University Medical Center Academic Professional development funds (to M.H.) by the NIDDK Diabetic Complications Consortium (DiaComp, www.diacomp.org), grant DK076169 (to M.H.), and National Science Foundation Graduate Research Fellowship Program under Grant Number 1445197 (to E.J.B.) and T32 GM07628 (to E.J.B.). We thank Lena Stelzer for excellent technical assistance.

Author Contributions

S.B., M.W., P.S.-K., M.H. and K.J. designed the experiments. S.B., I.K., M.W., E.B., A.E., C.S. performed the experiments. S.B., I.K., M.H., and K.J. wrote the manuscript.

Additional Information

Supplementary information accompanies this paper at doi:10.1038/s41598-017-01410-2

Competing Interests: The authors declare that they have no competing interests.

Publisher's note: Springer Nature remains neutral with regard to jurisdictional claims in published maps and institutional affiliations.



Open Access This article is licensed under a Creative Commons Attribution 4.0 International License, which permits use, sharing, adaptation, distribution and reproduction in any medium or format, as long as you give appropriate credit to the original author(s) and the source, provide a link to the Creative Commons license, and indicate if changes were made. The images or other third party material in this article are included in the article's Creative Commons license, unless indicated otherwise in a credit line to the material. If material is not included in the article's Creative Commons license and your intended use is not permitted by statutory regulation or exceeds the permitted use, you will need to obtain permission directly from the copyright holder. To view a copy of this license, visit <http://creativecommons.org/licenses/by/4.0/>.

© The Author(s) 2017

Chapter 3

BtsT - a novel and specific pyruvate/H⁺ symporter in *Escherichia coli*

Kristofcova, I., Vilhena, C., Behr, S., Jung, K.

J Bacteriol, 2017, in press

<http://doi.org/10.1128/JB.00599-17>

1 BtsT - a novel and specific pyruvate/H⁺ symporter in *Escherichia coli*

2 Ivica Kristoficova, Cláudia Vilhena, Stefan Behr^{*}, Kirsten Jung[#]

3

4 Munich Center for Integrated Protein Science (CIPSM) at the Department of Microbiology,

5 Ludwig-Maximilians-Universität München, 82152 Martinsried, Germany

6

7 Running head: Pyruvate transporter BtsT in *Escherichia coli*

8

9 [#]To whom correspondence should be addressed: Dr. Kirsten Jung, Ludwig-Maximilians-

10 Universität München, Department Biologie I, Bereich Mikrobiologie, Großhaderner Str. 2-4,

11 82152 Martinsried, Germany. Phone: +49-89-2180-74500; Fax: +49-89-2180-74520; E-mail:

12 jung@lmu.de

13

14 ^{*}Present address: Stefan Behr, Roche Diagnostics GmbH, Nonnenwald 2, 82377 Penzberg

15 **ABSTRACT**

16 The CstA (the peptide transporter carbon starvation CstA family; TC# 2.A.114) family of
17 peptide transporters belongs to the second largest superfamily of secondary transporters, the
18 amino acid/polyamine/organocation (APC) superfamily. No representative of the CstA family
19 has previously been characterized either biochemically or structurally, but we have now
20 identified the function of one of its members, the transport protein YjiY of *Escherichia coli*.
21 Expression of the *yjiY* gene is regulated by the LytS-like histidine kinase BtsS, a sensor of
22 extracellular pyruvate, together with the LytTR-like response regulator BtsR. YjiY consists of
23 716 amino acids, which form 18 putative transmembrane helices. Transport studies with intact
24 cells provided evidence that YjiY is a specific and high-affinity transporter for pyruvate (K_m
25 16 μ M). Furthermore, reconstitution of the purified YjiY into proteoliposomes revealed that
26 YjiY is a pyruvate/H⁺ symporter. It has long been assumed that *E. coli* possesses
27 transporter(s) for pyruvate, but the present study is the first to definitively identify such a
28 protein. Based on its function, we propose to rename the uncharacterized gene *yjiY* as *btsT*
29 (for “Brenztraubensäure” transporter, from the German word for pyruvate).

30

31 **IMPORTANCE**

32 BtsT (formerly known as YjiY) is found in many commensal and pathogenic representatives
33 of the *Enterobacteriaceae*. This study for the first time characterizes a pyruvate transporter in
34 *Escherichia coli*, BtsT, as a specific pyruvate/H⁺ symporter. When nutrients are limiting, BtsT
35 takes up pyruvate from the medium, thus enabling it to be used as a carbon source for the
36 growth and survival of *E. coli*.

37

38

39 INTRODUCTION

40 YjiY belongs to a small family of transporters, named for the peptide transporter CstA
41 (the peptide transporter carbon starvation CstA family; TC# 2.A.114) (1). The CstA family is
42 part of the amino acid/polyamine/organocation (APC) superfamily of secondary transporters
43 (2). The latter is the second largest superfamily of secondary transporters, and its
44 representatives cover a broad substrate spectrum, ranging from amino acids to metal ions and
45 peptides (2). Within the APC transporters, the CstA family displays the highest diversity in
46 sequence and topology. Some members of the CstA family are already characterized: CstA of
47 *E. coli* (3), CstA of *Campylobacter jejuni* (4), CstA and YjiY of *Salmonella enterica* serovar
48 Typhimurium (5). In both species, *E. coli* and *C. jejuni*, the gene *cstA* is upregulated under
49 carbon starvation, and knockout mutants have a lower growth rate in the presence of peptides
50 as nitrogen source (3, 6). Furthermore, a *cstA* or a *yjiY* mutant of *S. Typhimurium* is impaired
51 in the utilization of several dipeptides (5). However, no representative of CstA family has yet
52 been biochemically analyzed to ascertain the identity of its substrate(s).

53 Our studies focus on YjiY, which displays high sequence similarity (75.4%) and
54 identity (61.1%) to CstA from *E. coli* (7). The corresponding gene *yjiY* is the sole target gene
55 of the histidine kinase/response regulator system BtsS/BtsR, and its expression leads to the
56 synthesis of a 716-amino acid protein (7). In the *E. coli* genome *yjiY* is disconnected from the
57 *yehUT* operon. However, in other bacterial genomes these genes are adjacent to each other (7,
58 8), which suggests that they might be functionally related (7). Expression of *yjiY* is
59 additionally regulated by cAMP-CRP and post-transcriptionally modulated by CsrA (7).

60 It has been hypothesized that YjiY is involved in nutrient uptake, most probably the
61 transport of pyruvate (9). This assumption is supported by proteome studies of *E. coli* under
62 different growth conditions, which demonstrated that levels of YjiY are increased by up to 74-
63 fold when cells are grown in minimal medium with pyruvate as a carbon source compared to

64 cells grown in amino-acid-rich LB medium (10). Additionally, a quantitative fitness screen of
65 bar-coded *E. coli* BW25113 transposon mutants revealed that the *yjiY* mutant displays
66 reduced fitness when grown in minimal media containing pyruvate as sole carbon source (11).
67 Furthermore, pyruvate is vital to most living cells, both as a source of energy and carbon,
68 since it forms the central node of carbon metabolism (together with phosphoenolpyruvate) in
69 *E. coli* (12). Under conditions that require increased consumption of organic compounds
70 during exponential growth, *Escherichia coli* excretes acetate as well as pyruvate via overflow
71 metabolism (13). In later phases of growth, the extracellular pyruvate is then scavenged by the
72 cells (14). It was shown that BtsS/BtsR responds to such external pyruvate by activating the
73 expression of *yjiY* (9). The histidine kinase BtsS is a high-affinity receptor for extracellular
74 pyruvate (9). It is therefore tempting to speculate that YjiY is a pyruvate transporter.

75 To date, little is known about pyruvate transport in *E. coli*. It has been shown that a
76 separate transport system for pyruvate exists in *E. coli* (15), and that cells possess an active
77 uptake system for pyruvate (16). However, pyruvate transport has not been assigned to any
78 specific gene product. A gene located at around 15 centisomes on the *E. coli* gene map has
79 been suggested to encode an inducible pyruvate transport system (17), but has not been further
80 characterized. Uptake of pyruvate has also been shown in *Rhodopseudomonas spheroides*
81 (18) and *Lactobacillus plantarum* (19), but the transport systems responsible have not been
82 defined. MctC in *Corynebacterium glutamicum* (20), MctP in *Rhizobium leguminosarum* (21)
83 and TRAP-T in *Anabaena* sp (22) have all been characterized to function as pyruvate
84 transporters. However, the specificity of these transporters is not restricted to pyruvate. MctC,
85 a transporter that requires the electrochemical proton gradient, prefers acetate and propionate,
86 and has a low affinity for pyruvate ($K_{0.5}$ 250 μ M). MctP, a sodium/solute transporter, has a
87 high affinity for pyruvate (K_m 3.8 μ M), but shows a rather broad substrate specificity (alanine,
88 lactate, pyruvate and probably also propionate, acetate, butyrate and α -hydroxybutyrate). The

89 Trap-T transport system takes up several monocarboxylate 2-oxoacids including pyruvate (K_m
90 67 μM).

91 This study represents the first to be devoted to defining the function of YjiY. Analyses
92 with intact cells demonstrated that YjiY is able to transport pyruvate with a high affinity and
93 specificity. In addition, the reconstitution of purified YjiY in proteoliposomes proved that
94 pyruvate transport requires the proton motive force for energization. To indicate its role as a
95 pyruvate transporter in *E. coli* and highlight its functional relationship with the pyruvate-
96 responsive BtsS/BtsR histidine kinase/response regulator system (9), YjiY has been renamed
97 BtsT (for “Brenztraubensäure” transporter), and is so referred to in what follows.

98

99 RESULTS

100 **CstA-like proteins in *Enterobacteriaceae*.** BtsT belongs to the CstA family, which
101 consists of 10 members in the Transporter Classification Database (www.tcdb.org), all which
102 share a high degree of sequence conservation (1). We were interested in elucidating the
103 relationship between the BtsT homologs found among the *Enterobacteriaceae* by comparative
104 genomics. For this purpose, we performed a local alignment search based on the full-length
105 amino acid sequences using Protein BLAST (23). Based on the alignment of 1,617
106 individually identified sequences, we generated a phylogenetic tree and grouped the
107 corresponding proteins (**Dataset S1**). The tree possesses three distinct branches, which were
108 named BtsT-like, CstA1-like and CstA2-like (**Fig. 1**), taking the two known BtsT and CstA
109 proteins in *E. coli* as branch markers. Within the *Enterobacteriaceae*, 43.5% of all sequences
110 were assigned to the BtsT-like branch of the tree, and 40.8%, including *E. coli* CstA, to the
111 CstA1-like branch. Surprisingly, the remaining 15.8% of the identified sequences formed an
112 additional, distinct branch, named CstA2-like. The genus *Escherichia* contained examples of
113 both BtsT and CstA1, while other genera like *Dickeya* and *Serratia* possess representatives of
114 both the CstA1 and CstA2 branches. No single genus contained representatives of all three
115 branches. Although the amino acid sequences show an extraordinarily high level of identity
116 (e.g. 61.1% between BtsT and CstA in *E. coli*), CstA sequences differ sufficiently to be
117 attributed to separate branches. Furthermore, the frequent presence of more than one CstA
118 representative within the same species suggests that members of different branches might
119 have different functions within the *Enterobacteriaceae*.

120 Since BtsT of *S. enterica* was proposed to function as peptide transporter (5), we
121 compared the sequences of BtsT of *E. coli* and *S. enterica* using a consensus-based approach.
122 A consensus derived from 148 BtsT sequences of *E. coli* was aligned to a consensus of 122
123 BtsT sequences of *S. enterica* (**Fig. S1**). The sequence identity was determined to be 97%.

124 Most of the deviating amino acids are located in the loops of BtsT. Although the difference in
125 sequence identity is rather small, a single amino acid substitution might be sufficient to alter
126 the substrate specificity. It is worth mentioning, that there are differences in the metabolic
127 behavior of these two species. While *E. coli* excretes pyruvate during growth in an amino
128 acid-rich medium as part of an overflow metabolism, *S. enterica* did not excrete pyruvate to
129 the same extent (24). In addition, in *E. coli* the histidine kinase/response regulator system
130 BtsS/BtsR (its target gene is *btsT*) forms together with the histidine kinase/response regulator
131 system YpdA/YpdB a regulatory network (25). The YpdA/YpdB system is not encoded in *S.*
132 *enterica*. Here, we elucidate the function of BtsT, whose expression is controlled by the
133 BtsS/BtsR histidine kinase/response regulator system.

134

135 **Secondary structure model of BtsT.** CstA family members contain 13 to 18
136 transmembrane domains (TMs), which are organized into two central 5-TM repeat units with
137 1 to 4 extra TMs on each side. The first helix of the second repeat unit (helix 10 in **Fig. 2**)
138 contains a conserved motif CG-x(2)-SG of unknown function (2). The structural similarity
139 between BtsT and secondary transporters of the APC superfamily (TMs 4-17) was confirmed
140 by Phyre2, a protein homology/analogy recognition engine (26). Furthermore, hydropathy
141 analyses of BtsT with UniProt predicted that the membrane-integrated portion contains 17
142 putative TMs, while CstA displays 18 TMs (**Fig. S2**) (27).

143 Since the C-terminus of BtsT is located on the cytoplasmic side of the membrane (28),
144 the odd number of domains implied that the N-terminus of BtsT should extend into the
145 periplasm. Because a periplasmically located N-terminus is uncommon among integral
146 membrane proteins, we investigated its location in BtsT by using the MalE fusion strategy
147 (29). Native MalE is a periplasmic maltose-binding protein (MBP), and it contains a leader
148 sequence that enables it to be translocated through the cytoplasmic membrane. MalE without

149 the leader sequence is produced as cytoplasmic protein (30). We fused *malE* with or without a
150 leader sequence to the 5' end of *btsT* to code either for a periplasmically located MBP
151 (MBP_P-BtsT) or a cytoplasmically located MBP (MBP_C-BtsT). We predicted that only a
152 correctly folded hybrid protein would be inserted into the cytoplasmic membrane. We
153 individually overproduced both hybrid proteins in *E. coli* and determined the level and
154 localization of each by Western blot. The MBP_C-BtsT was predominantly found in the
155 membrane fraction (**Fig. S3A**). The level of MBP_P-BtsT was low, and no hybrid protein was
156 detectable in any cellular subfraction (**Fig. S3B**). In addition, we performed complementation
157 studies using the MBP-deficient *E. coli* mutant MM39, which only grows with maltose as a
158 sole carbon source, when it produces a periplasmically located MBP (**Fig. S4**). *E. coli* MM39
159 producing either MBP_P-BtsT or MBP_C-BtsT was unable to grow, corroborating previous
160 results (**Fig. S3**). These results revealed that only BtsT with a cytoplasmically fused MBP is
161 correctly integrated into the cytoplasmic membrane, and therefore suggest that the N-terminus
162 of BtsT is located on the cytoplasmic side of the membrane.

163 Then we compared the predicted secondary structures for BtsT and CstA, and found a
164 long loop between TM11 and TM12 in BtsT (**Fig. S2A**). According to PSIPRED secondary
165 structure prediction (31), amino acids 417-437 in this loop should have a high propensity to
166 form a helix and therefore a TM. Based on the experimental evidence for the location of the
167 N-terminus and the structure prediction for CstA, we propose a secondary structure model of
168 BtsT with an intracellular N-terminus and 18 TMs (**Fig. 2**).

169

170 **BtsT activity in intact cells.** Since pyruvate is an important metabolite of central
171 carbon metabolism, and other pyruvate transport systems in *E. coli* are yet unknown, we
172 started to work with a mutant strain deficient in *btsT* only to analyze BtsT activity in intact
173 cells. It is important to note that there were no growth defects for mutant MG1655 $\Delta btsT$

174 neither in LB medium (**Fig. S5A**) nor in M9 minimal medium supplemented with pyruvate
175 (**Fig. S5B**). Uptake of ^{14}C -pyruvate into intact cells of *E. coli* MG1655 $\Delta btsT$ (25)
176 transformed with either pBAD24-*btsT* (7) or pBAD24 (32) was analyzed by a rapid filtration
177 assay. An initial experiment showed that measurements of ^{14}C -pyruvate are difficult due to
178 extremely fast uptake and/or metabolization (data not shown). Therefore, all subsequent
179 assays were performed at 15°C. At this lower temperature, the rate of uptake of ^{14}C -pyruvate
180 by *E. coli* MG1655 $\Delta btsT$ containing the control plasmid pBAD24 was approximately linear
181 for 60 seconds (**Fig. 3**). Cells transformed with pBAD24-*btsT* displayed a 6-fold higher linear
182 uptake rate for 30 s and reached 4-fold higher steady state (0.5 nmol/mg of protein) at about
183 40 s. Transport rates in intact cells of *E. coli* MG1655 $\Delta btsT$ transformed with pBAD24-*btsT*
184 were also measured at various external pH values (**Fig. S6**). The highest pyruvate uptake rate
185 was found at pH 7.5, the pH-value of the buffer used in all the subsequent experiments. The
186 pyruvate uptake rate decreased at pH 6, no transport was detected at pH of 4.5 and 3.0.

187 In addition, we tested pyruvate uptake by BtsT in intact cells, which have a decreased
188 pyruvate metabolism. For this purpose, we used *E. coli* strain YYC202, which harbors
189 deletions in the pyruvate metabolizing pathways *aceEF*, *pflB*, *poxB* and *pps*, and therefore
190 cannot convert pyruvate into either acetyl-CoA, phosphoenolpyruvate (PEP) or acetate (33).
191 Uptake of ^{14}C -pyruvate into intact cells of *E. coli* YYC202 transformed with either pBAD24-
192 *btsT* or pBAD24 was measured, and we observed a pattern of pyruvate uptake very similar to
193 that in *E. coli* MG1655 $\Delta btsT$ transformed with these plasmids (**Fig. S7**). Therefore,
194 accumulation of pyruvate could not be increased in this mutant, since it is impossible to
195 completely block its metabolization. It is important to state here that expression of
196 chromosomally encoded *btsT* is tightly controlled by the BtsS/BtsR system, and therefore
197 requires specific environmental conditions (9).

198

199 **Characterization of pyruvate transport by BtsT in intact cells.** Previous
200 observations based on the effects of electron transport chain inhibitors on pyruvate transport
201 in *E. coli* K-12 suggested that the process is driven by the proton motive force (16). To test
202 this hypothesis, we used the hydrophobic protonophores 2,4-dinitro-phenol (DNP) and
203 carbonyl cyanide *m*-chlorophenyl hydrazone (CCCP) (**Fig. 4A**). Both reagents abolished
204 substrate accumulation by BtsT, suggesting active transport of pyruvate by BtsT. To
205 determine whether pyruvate transport by BtsT is accompanied by the movement of other ion
206 species, several ionophores were tested. Valinomycin is a highly selective ionophore for K⁺
207 (34), while nonactin forms complexes with K⁺, Na⁺, NH₄⁺ and some other cations with lower
208 affinity (35). Nigericin acts mainly as a potassium-proton antiporter, but can also transport
209 Pb⁺ and H⁺ into the cytosol (36). Pyruvate uptake by BtsT was not affected by any of these
210 ionophores (**Fig. 4A**).

211 Additionally, the specificity of BtsT was tested by assaying several compounds with
212 shared structural similarity for the ability to act as competitive inhibitors for the pyruvate
213 binding site when provided in a 100-fold excess (**Fig. 4B**). Br-pyruvate is a synthetic analogue
214 of pyruvate, and was found to act as a competitive inhibitor of BtsT, which is in agreement
215 with earlier studies in *E. coli* K-12 (16). None of the other compounds used – L-malate and
216 lactate (both configurations) with a C- α hydroxyl group, phosphoenolpyruvate with a C- α
217 phosphoryl group, or L-alanine with a positively charged C- α amino group – reduced the rate
218 of pyruvate uptake. We also tested monocarboxylates (acetate and propionate), a
219 dicarboxylate (succinate) and amino acids (L-serine, L-glycine), but the uptake rate was
220 significantly reduced only in the presence of pyruvate or its synthetic analog Br-pyruvate,
221 indicating the narrow specificity of the transporter. In order to determine the K_m for pyruvate
222 uptake, we quantified the initial rate of pyruvate uptake by BtsT at different concentrations of
223 pyruvate (**Fig. 4C**). Pyruvate can enter the cells by diffusion (**Fig. S8**). Therefore, the uptake

224 rates were corrected by the values determined for pure diffusion. The K_m of the transporter
225 BtsT for pyruvate measured in intact cells was $16.5 \pm 6.4 \mu\text{M}$.

226

227 **Effects of $\Delta\tilde{\mu}_{\text{H}^+}$, $\Delta\Psi$ and ΔpH on BtsT-mediated pyruvate transport.** Energization of
228 pyruvate transport by BtsT was studied in detail in *E. coli* proteoliposomes by determining the
229 consequences for pyruvate transport of an imposed electrical potential ($\Delta\Psi$) across the
230 liposome membrane or a difference in proton concentration (ΔpH) between the interior of the
231 liposomes and the external medium, or a combination of both, thus generating a
232 transmembrane electrochemical proton gradient ($\Delta\tilde{\mu}_{\text{H}^+}$). To this end, BtsT was first expressed
233 at high levels under the control of the pBAD promoter, affinity-purified and integrated into
234 proteoliposomes preloaded with potassium phosphate buffer, pH 7.6 (37) (**Fig. S9**). The
235 proteoliposomes were then diluted 200-fold, in the presence of valinomycin, with either
236 potassium phosphate buffer pH 5.8 (ΔpH), potassium-free buffer pH 7.6 ($\Delta\Psi$), potassium-free
237 buffer pH 5.8 ($\Delta\tilde{\mu}_{\text{H}^+}$) or sodium phosphate buffer pH 7.6 ($\Delta\tilde{\mu}_{\text{Na}^+}$), and the rates of ^{14}C -
238 pyruvate transport were measured.

239 From the results, it is clear that the presence of an electrochemical H^+ gradient ($\Delta\tilde{\mu}_{\text{H}^+}$)
240 is associated with the accumulation of ^{14}C -pyruvate in proteoliposomes, and that uptake is
241 markedly reduced in the absence of such a gradient (dilution in potassium phosphate buffer
242 pH 7.6; **Fig. 5A**). Thus, the initial rate of uptake of pyruvate by BtsT in the presence of $\Delta\tilde{\mu}_{\text{H}^+}$
243 is 27.7 nmol per mg of protein, and the steady state is achieved after about 1 min (**Fig. 5B**).
244 Imposition of ΔpH decreased the initial rate by two-fold and a lower steady state (relative to
245 $\Delta\tilde{\mu}_{\text{H}^+}$) was reached after 1 min. In the presence of a $\Delta\Psi$, we observed a similar initial rate of
246 pyruvate accumulation as in the presence of ΔpH , but it continued to rise for the (10-min)
247 duration of the experiment. ^{14}C -Pyruvate was also accumulated upon the application of $\Delta\tilde{\mu}_{\text{Na}^+}$,

248 although the Na⁺ ions did not stimulate uptake beyond the level seen with ΔpH alone (**Fig.**
249 **5A**).

250 Pyruvate could potentially cross the *E. coli* plasma membrane in its protonated form
251 by simple diffusion (38). In the experiments where a pH gradient is generated (ΔpH, interior
252 alkaline, exterior acidic), the ¹⁴C-pyruvate is added to an extracellular environment with a low
253 pH. Therefore, ¹⁴C-pyruvate might be protonated and transported by diffusion. To rule out
254 this possibility, liposomes without BtsT were prepared as a control (**Fig. S10**). Using these
255 liposomes, we observed only a slight pyruvate accumulation. Therefore, the protonation of
256 pyruvate at low pH does not significantly affect the outcome of these experiments (**Fig. S10**).

257 Lastly, we confirmed the functionality of the transporter BtsT in proteoliposomes in a
258 counterflow assay. In this case, we preloaded the proteoliposomes with a high internal
259 concentration (10 mM) of unlabeled (“cold”) pyruvate and subsequently diluted them 200-
260 fold in the same buffer containing a low concentration of ¹⁴C-pyruvate (4.7 μM). If pyruvate
261 was indeed transported, exchange of the internal (unlabeled) substrate and external (labeled)
262 pyruvate should lead to the accumulation of ¹⁴C-pyruvate in the vesicles due to the
263 concentration gradient across the membrane. We observed such an accumulation of ¹⁴C-
264 pyruvate via BtsT in proteoliposomes, which was low (0.28 nmol x mg⁻¹ x min⁻¹), but
265 significant in light of the competitive inhibition by unlabeled pyruvate (**Fig. 5C**). In the
266 control experiment, proteoliposomes preloaded with 10 mM unlabeled lactate exhibited no
267 ¹⁴C-pyruvate accumulation. These experiments thus demonstrate that BtsT-mediated uptake
268 of pyruvate can occur against a concentration gradient.

269 **DISCUSSION**

270 Pyruvate plays a central role in carbon metabolism. Nevertheless, little is known about
271 how intracellular levels of the compound are regulated in *E. coli*. It has been suggested that
272 pyruvate uptake is driven via specific active transporters (16, 17), but until now their
273 molecular identities have remained unknown.

274 However, interest in pyruvate transporters is growing, primarily as a result of increasing
275 evidence for their roles in biological fitness and virulence of *Enterobacteriaceae*. The
276 pyruvate-tricarboxylic acid cycle node was identified as a focal point for controlling the host
277 colonization and virulence of *Yersinia pseudotuberculosis* (39). *Y. pseudotuberculosis*
278 secretes high amounts of pyruvate when grown in minimal medium with glucose as carbon
279 source. However the pyruvate exporter or importer in *Y. pseudotuberculosis* has not yet been
280 characterized.

281 Metabolic engineering is also focusing its attention on pyruvate in efforts to achieve
282 optimized metabolite production in *E. coli*, *Corynebacterium glutamicum* or *Bacillus subtilis*
283 (40). However, to control the carbon flux between glycolysis and the TCA cycle, further
284 insights into the regulation and characterization of the enzymes and other proteins relevant to
285 the PEP-pyruvate-oxaloacetate node are still required.

286 Here, we were principally interested in elucidating the role of the pyruvate transporter
287 in *E. coli*. It is known that pyruvate overflow occurs under conditions of carbon excess during
288 exponential growth. At the end of the exponential phase, cells experience nutrient limitation
289 and initiate the rapid re-uptake of previously excreted metabolic intermediates, including
290 pyruvate (13). This extracellular pyruvate is sensed by the two-component system BtsS/BtsR,
291 which consequently activates the expression of *btsT* encoding the putative pyruvate
292 transporter BtsT (7, 9). BtsT belongs to the APC superfamily of secondary transporters (2,
293 41). Comparative genomic studies clearly separate BtsT from CstA, and it has been proposed

294 that the two have different functions (**Fig. 1**). Since the histidine kinase BtsS responds to
295 extracellular pyruvate (9), we hypothesized that BtsS/BtsR triggers the production of BtsT
296 transporter to enable cells to take up pyruvate as a scavenging strategy to cope with carbon
297 limitation. Here, we have shown that BtsT indeed serves as a pyruvate transporter in *E. coli*
298 and thus assigned a function to a representative of the CstA family for the first time.

299 First we studied the function of BtsT in intact cells and characterized the protein as a
300 highly specific pyruvate transporter with a K_m of 16 μM (**Fig. 4**). Furthermore, we showed
301 that the pronophores CCCP and DNP had a significant inhibitory effect on pyruvate transport
302 rates, indicating involvement of a $\Delta\Psi$ and/or ΔpH . In comparison, both valinomycin and
303 nigericin did not cause inhibition of pyruvate uptake by BtsT even though these compounds
304 dissipate either $\Delta\Psi$ or ΔpH , respectively. Likewise, valinomycin had no effect on pyruvate
305 transport by *L. plantarum* cells (19). The lack of an inhibitory effect of valinomycin suggests
306 that intact cells somehow circumvent inhibition by a thus far unknown mechanism.
307 Elimination of all the influences from intact cells is therefore required to obtain reliable
308 insights into the energization of pyruvate transport.

309 It is worth mentioning that *E. coli* probably harbors at least one additional pyruvate
310 transporter, based on the observed background pyruvate accumulation by intact cells of an *E.*
311 *coli* ΔbtsT strain (**Fig. 3**), which cannot be solely attributed to diffusion (**Figs. S6 and S8**). It
312 was previously suggested that *E. coli* uses one export and two uptake transporters to modulate
313 the level of intracellular pyruvate (17). Unfortunately, we were unable to identify other
314 pyruvate transporters based on the BtsT sequence, and contrary to a previous suggestion (17),
315 we could find no BtsT-like coding sequence near the 15 centisome position in the *E. coli*
316 genome.

317 Further insights into the mode of action of BtsT were obtained by incorporating the
318 protein into *E. coli* proteoliposomes. In these experiments, a suspension of proteliposomes

319 harboring BtsT was assayed for ^{14}C -pyruvate transport under conditions known to generate
320 either $\Delta\tilde{\mu}_{\text{H}^+}$, $\Delta\Psi$ or ΔpH (**Fig. 5**). From the results, it is obvious that simultaneous imposition
321 of a membrane potential and a proton gradient ($\Delta\tilde{\mu}_{\text{H}^+}$, interior negative and alkaline) is
322 required to drive pyruvate uptake into *E. coli* proteoliposomes. In the presence of either $\Delta\Psi$
323 (interior negative) or ΔpH (interior alkaline), the rate of transport was halved in comparison to
324 that observed in the presence of $\Delta\tilde{\mu}_{\text{H}^+}$. The two gradients most likely contribute with their
325 actual extent to the energization of uptake (**Fig. 5**). Therefore, it seems that the secondary
326 transport of pyruvate by BtsT is coupled to both the influx of protons and the movement of
327 electric charges. Hence, BtsT acts as a pyruvate/ H^+ symporter. Although the exact
328 pyruvate/ H^+ coupling stoichiometry is still unknown, the results suggest a ratio of more than
329 one proton per transported pyruvate.

330 In summary, BtsT is the first identified pyruvate transporter in *E. coli* and the first
331 characterized representative of the CstA family. This study opens the possibility to search for
332 the pyruvate-binding site in BtsT as well as to elucidate the 3D structure of this transporter. It
333 will be interesting to determine which of the 18 putative TMs in BtsT are essential for the
334 recognition and transport of pyruvate. Currently, we can only speculate that the two conserved
335 5-TM repeat units found in members of the CstA family (2) are crucial for this function. BtsT
336 contains 8 additional TMs (4 TMs each before and after the repeat unit) which might perhaps
337 interact with the histidine kinase BtsS (25) or have other regulatory or structural functions.

338

339

340 **MATERIALS AND METHODS**

341 **Bacterial strains and plasmids.** In this study we used the previously described *E. coli* strains
342 LMG194 [*F*⁻ Δ *lacX74 galE galK thi rpsL Δ phoA Δ ara714 leu::Tn10] (32), MG16555 Δ *btsT*
343 (previously termed MG1655 Δ *yjiY*) (25), MM39 (*araD, lacI, Δ UI269 and malE444*) (29) and
344 YYC202 (*Δ aceEF, Δ pflB, Δ poxB, and Δ pps*) (33), and constructed two new plasmids:
345 pMAL_P-*btsT* and pMAL_C-*btsT*. The corresponding *btsT*-6His gene was isolated from plasmid
346 pBAD24-*btsT* (previously known as pBAD24-*yjiY* (7)) by cleavage with EcoRI and XbaI, and
347 ligated into the cognate sites in vectors pMAL-p2X and pMAL-c2X (New England Biolabs).
348 For transport studies we used the arabinose-inducible vector pBAD24-*btsT* (7), which codes
349 for BtsT-6His, and pBAD24 (32) as control.*

350

351 **Growth conditions.** All strains were grown overnight in LB medium (10 g/l tryptone, 5 g/l
352 yeast extract, 10 g/l NaCl) or M9 minimal medium containing 0.5% [wt/vol] maltose or 20
353 mM pyruvate. Cells from the overnight culture were then transferred to corresponding fresh
354 medium. When appropriate, media were supplemented with ampicillin (sodium salt, 100
355 μ g/ml) and/or streptomycin (50 μ g/ml). After inoculation, bacteria were grown under
356 agitation (200 rpm) at 37°C and growth was monitored over time by measuring the optical
357 density at 600 nm (OD₆₀₀).

358

359 **Production of MBP hybrid proteins.** Cells were grown to an OD₆₀₀ of 0.5 as described
360 above. Recombinant gene expression was induced by addition of 0.2% (w/v) arabinose. After
361 3 h of further incubation, cells were harvested by centrifugation, disrupted [using a high
362 pressure cell disrupter (Constant Systems)] and fractionated. At each step, the pellet was
363 resuspended in a buffer consisting of 50 mM Tris/HCl buffer (pH 7.5), 10% (v/v) glycerol, 1
364 mM DTT, 1 mM PMSF and DNase. His-tagged BtsT was detected by Western blot analysis

365 with an anti-His antibody (Abcam) and an alkaline phosphatase-conjugated anti-rabbit
366 antibody (Rockland) as the secondary antibody.

367

368 **Comparative genomic studies.** BtsT-like proteins were identified by Protein BLAST search
369 within the *Enterobacteriaceae* (taxid: 543) using the full-length amino acid sequence of
370 *E. coli* BtsT to query the RefSeq protein database (23). In order to cover a huge amount of
371 highly diverse proteins an Expect (E) value was kept at < 10. An amino acid length tolerance
372 was set to 10% as default parameter resulting in 1,617 sequences. To elucidate the
373 relationship between the BtsT homologs, all sequences were aligned and a phylogenetic tree
374 was generated using CLC Main Workbench 7 (CLC Bio Qiagen). BtsT and CstA of *E. coli*
375 were used as branch markers. Comparison of BtsT conserved in different species, *E. coli* and
376 *S. enterica*, was done via a consensus alignment. For this purpose, a total of 148 sequences of
377 BtsT in *E. coli* (or 122 in *S. enterica*) was retrieved from the branch BtsT of the phylogenetic
378 tree. The consensus sequence was derived from their alignment using CLC Main Workbench
379 7 software.

380

381 **Transport measurements with intact cells.** *E. coli* strain MG1655 $\Delta btsT$ (25) was
382 transformed with pBAD24 (32) or pBAD24-*btsT* (7). Cells grown in LB medium in the
383 absence of arabinose (the leaky expression of *btsT* was suitable for complementation) were
384 harvested in the mid-log phase. Cells were washed twice and resuspended in 100 mM
385 Tris/MES buffer (pH 7.5) containing 5 mM MgCl₂, thereby adjusting the total protein
386 concentration to 0.35 mg/ml. In the experiments performed at different external pH values,
387 the cells were washed and resuspended in buffers: Tris/MES buffer (pH 6), 5 mM MgCl₂ or
388 100 mM citrate buffer (pH 3 / pH 4.5), 5 mM MgCl₂. Uptake of ¹⁴C-pyruvate (50-60 mCi
389 mmol⁻¹, Biotrend) was measured at a total substrate concentration of 10 μ M at 15°C. At

390 various time intervals, transport was terminated by the addition of 100 mM potassium
391 phosphate buffer (pH 6.0) and 100 mM LiCl (stop buffer) followed by rapid filtration through
392 membrane filters (MN GF-5 0.4 μm , Macherey-Nagel). The filters were dissolved in 5 ml of
393 scintillation fluid (MP Biomedicals) and radioactivity was determined in a Liquid Scintillation
394 Analyzer (Perkin-Elmer). Effects of the cold substrates on pyruvate uptake by BtsT were
395 tested by simultaneous addition of cold compound (1 mM) and ^{14}C -pyruvate (10 μM). The
396 effects of protonophores and ionophores were tested after pre-incubation of cells in Tris/MES
397 buffer (pH 7.5) supplemented with 2 mM DNP or 20 μM CCCP, 6 μM nigericin, 10 μM
398 nonactin or DMSO (as control) at 25°C for 30 min. An ionophore valinomycin was pre-
399 incubated in 100 mM potassium phosphate buffer, pH 7.5 at 25°C for 30 min. In experiments
400 where the pyruvate concentration was varied, the amount of ^{14}C -pyruvate was kept constant
401 (9 nmol).

402

403 **Transport measurements with proteoliposomes.** *E. coli* LMG194 cells were transformed
404 with pBAD24-*btsT* (7), and BtsT-6His was produced as described above. At each step, the
405 pellet was resuspended in 100 mM potassium phosphate buffer (pH 7.6) containing 5 mM
406 MgCl_2 , 5% (v/v) glycerol, 1 mM DTT, 1 mM PMSF and DNase. For BtsT solubilization,
407 1.5% (w/v) *n*-dodecyl β -D-maltoside (Glycon Biochemicals) was added while stirring on ice
408 for 30 min, and the sample was centrifuged at 244,000 x *g* for 45 min at 4°C. Ni^{2+} -NTA resin,
409 which had been pre-incubated with buffer W [100 mM potassium phosphate buffer (pH 7.6),
410 5 mM MgCl_2 , 5% (v/v) glycerol and 1 mM DTT], was then added to the supernatant and the
411 mixture was incubated for 1 h with gentle shaking at 4°C. Unbound protein was removed by
412 washing with buffer W containing 30 mM imidazole. Subsequently, BtsT was eluted with
413 buffer W containing 300 mM imidazole. Purified BtsT was reconstituted into preformed
414 liposomes prepared from an acetone-ether-washed *E. coli* polar lipid extract as described

415 before (42). Prior to reconstitution, the liposomes were destabilized by the addition of 0.12%
416 (w/v) Triton X-100, and then mixed with purified protein at a ratio 100:1. Detergents were
417 removed by adding Bio-Beads SM-2 (Bio-Rad) at a bead/detergent ratio of 5:1. Fresh Bio-
418 Beads were added after 1 h and 2 h, and the mixture was gently stirred at 4°C overnight. Bio-
419 Beads were removed by filtration through glass wool, and the proteoliposome suspension was
420 dialyzed twice against buffer A [100 mM potassium phosphate buffer (pH 7.6), 5 mM MgCl₂
421 and 5% (v/v) glycerol], and centrifuged at 160,000 x g for 1 h. The pellet was resuspended in
422 buffer A and stored in liquid N₂. Proteins were visualized by silver-staining and His-tagged
423 BtsT was detected by Western blot analysis as described before. After thawing, samples were
424 extruded through a 400-nm filter (Avestin) to obtain unilamellar proteoliposomes of
425 homogeneous size, and adjusted to 4 mg/ml of protein in buffer A. Aliquots of
426 proteoliposomes were diluted (1:200) into buffers A-E containing 80 μM valinomycin and 40
427 μM ¹⁴C-pyruvate to initiate pyruvate transport, and at defined times (25°C) the entire sample
428 was filtered through 0.2-μm Millipore filters [buffer B (ΔpH): 100 mM potassium phosphate
429 buffer (pH 5.8) and 5 mM MgCl₂, buffer C (ΔΨ): 100 mM Tris/MES buffer (pH 7.6) and 5
430 mM MgCl₂, buffer D (Δ $\tilde{\mu}_{H^+}$): 100 mM Tris/MES buffer (pH 5.8) and 5 mM MgCl₂, buffer E
431 (Δ $\tilde{\mu}_{Na^+}$): 100 mM Tris/MES (pH 5.8), 5 mM MgCl₂ and 50 mM NaCl]. For the counterflow
432 assay, proteoliposomes were preloaded with 10 mM pyruvate or lactate at 4°C overnight. The
433 resulting suspension was diluted 200-fold into buffer A containing ¹⁴C-pyruvate at a
434 concentration of 4.7 μM (final external pyruvate concentration of 54.7 μM). At defined times
435 (25°C) the entire sample was filtered, and the radioactivity of the sample was analyzed as
436 described above.

437

438 **Statistical analysis.** All experiments were repeated at least three times with independently
439 prepared samples. Statistical analysis was carried out using GraphPad Prism (version 5.03 for

440 Windows). Data was assessed for significance between tested groups by using one-way
441 analysis of variance (ANOVA) followed by Tukey's multiple comparison post-hoc test. Error
442 bars represent standard errors of the mean.
443

444 **ACKNOWLEDGEMENTS**

445 We thank Prof. Dr. Heinrich Jung for insightful comments on the methodology applied
446 (Ludwig-Maximilians-Universität München, Germany). This work was supported by the
447 Deutsche Forschungsgemeinschaft (Exc114/2, SPP1617, JU270/13-2 to K.J.)

448

449 **REFERENCES**

- 450 1. Saier MH, Reddy VS, Tamang DG, Vastermark A. 2014. The transporter classification
451 database. *Nucleic Acids Res* 42:251–258.
- 452 2. Vastermark A, Wollwage S, Houle ME, Rio R, Saier MH. 2014. Expansion of the APC
453 superfamily of secondary carriers. *Proteins* 82:2797–2811.
- 454 3. Schultz JE, Matin A. 1991. Molecular and functional characterization of a carbon
455 starvation gene of *Escherichia coli*. *J Mol Biol* 218:129–140.
- 456 4. Cordwell SJ, Len ACL, Touma RG, Scott NE, Falconer L, Jones D, Connolly A,
457 Crossett B, Djordjevic SP. 2008. Identification of membrane-associated proteins from
458 *Campylobacter jejuni* strains using complementary proteomics technologies.
459 *Proteomics* 8:122–139.
- 460 5. Garai P, Lahiri A, Ghosh D, Chatterjee J, Chakravorty D. 2016. Peptide-utilizing
461 carbon starvation gene *yjiY* is required for flagella-mediated infection caused by
462 *Salmonella*. *Microbiology* 16:100–116.
- 463 6. Rasmussen JJ, Vegge CS, Frøkiær H, Howlett RM, Krogfelt KA, Kelly DJ, Ingmer H.
464 2013. *Campylobacter jejuni* carbon starvation protein A (CstA) is involved in peptide
465 utilization, motility and agglutination, and has a role in stimulation of dendritic cells. *J*
466 *Med Microbiol* 62:1135–1143.
- 467 7. Kraxenberger T, Fried L, Behr S, Jung K. 2012. First insights into the unexplored two-
468 component system YehU/YehT in *Escherichia coli*. *J Bacteriol* 194:4272–4284.
- 469 8. Szklarczyk D, Franceschini A, Kuhn M, Simonovic M, Roth A, Minguéz P, Doerks T,
470 Stark M, Müller J, Bork P, Jensen LJ, von Mering C. 2011. The STRING database in
471 2011: functional interaction networks of proteins, globally integrated and scored.
472 *Nucleic Acids Res* 39:561–568.

- 473 9. Behr S, Kristoficova I, Witting M, Breland EJ, Eberly AR, Schmitt-Kopplin P,
474 Hadjifrangiskou M, Jung K. 2017. Identification of a high-affinity pyruvate receptor in
475 *Escherichia coli*. *Sci Rep* 7:1388.
- 476 10. Schmidt A, Kochanowski K, Vedelaar S, Ahrné E, Volkmer B, Callipo L, Knoops K,
477 Bauer M, Aebersold R, Heinemann M. 2016. The quantitative and condition-dependent
478 *Escherichia coli* proteome. *Nat Biotechnol* 34:104–110.
- 479 11. Wetmore KM, Price MN, Waters RJ, Lamson JS, He J, Hoover CA, Blow MJ, Bristow
480 J, Butland G, Arkin AP, Deutschbauer A. 2015. Rapid quantification of mutant fitness
481 in diverse bacteria by sequencing randomly bar-coded transposons. *Mbio* 6:e00306-15.
- 482 12. Postma PW, Lengeler JW, Jacobson GR. 1993. Phosphoenolpyruvate: carbohydrate
483 phosphotransferase systems of bacteria. *Microbial Rev* 57:543–594.
- 484 13. Paczia N, Nilgen A, Lehmann T, Gätgens J, Wiechert W, Noack S. 2012. Extensive
485 exometabolome analysis reveals extended overflow metabolism in various
486 microorganisms. *Microb Cell Fact* 11:122.
- 487 14. Fried L, Behr S, Jung K. 2013. Identification of a target gene and activating stimulus
488 for the YpdA/YpdB histidine kinase/response regulator system in *Escherichia coli*. *J*
489 *Bacteriol* 195:807–15.
- 490 15. Kornberg HL, Smith J. 1967. Genetic control of the uptake of pyruvate by *Escherichia*
491 *coli*. *Biochim Biophys Acta* 148:591–592.
- 492 16. Lang VJ, Leystra-Lantz C, Cook RA. 1987. Characterization of the specific pyruvate
493 transport system in *Escherichia coli* K-12. *J Bacteriol* 169:380–385.
- 494 17. Kreth J, Lengeler JW, Jahreis K. 2013. Characterization of pyruvate uptake in
495 *Escherichia coli* K-12. *PLoS ONE* 8:e67125.
- 496 18. Gibson J. 1975. Uptake of C4 dicarboxylates and pyruvate by *Rhodopseudomonas*

- 497 *spheroides*. J Bacteriol 123:471–480.
- 498 19. Tsau J, Guffanti A a., Montville TJ. 1992. Pyruvate is transported by a proton symport
499 in *Lactobacillus plantarum* 8014. Curr Microbiol 25:47–50.
- 500 20. Jolkver E, Emer D, Ballan S, Krämer R, Eikmanns BJ, Marin K. 2009. Identification
501 and characterization of a bacterial transport system for the uptake of pyruvate,
502 propionate, and acetate in *Corynebacterium glutamicum*. J Bacteriol 191:940–948.
- 503 21. Hosie AHF, Allaway D, Poole PS. 2002. A monocarboxylate permease of *Rhizobium*
504 *leguminosarum* is the first member of a new subfamily of transporters. J Bacteriol
505 184:5436–5448.
- 506 22. Pernil R, Herrero A, Flores E. 2010. A TRAP transporter for pyruvate and other
507 monocarboxylate 2-oxoacids in the cyanobacterium *Anabaena* sp. strain PCC 7120. J
508 Bacteriol 192:6089–6092.
- 509 23. Altschul SF, Madden TL, Schäffer AA, Zhang J, Zhang Z, Miller W, Lipman DJ. 1997.
510 Gapped BLAST and PSI-BLAST: a new generation of protein database search
511 programs. Nucleic Acids Res 25:3389–3402.
- 512 24. Behr S, Brameyer S, Witting M, Schmitt-Kopplin P, Jung K. 2017. Comparative
513 analysis of LytS/LytTR-type histidine kinase/response regulator systems in γ -
514 proteobacteria. PLoS One 12:e0182993.
- 515 25. Behr S, Fried L, Jung K. 2014. Identification of a novel nutrient-sensing histidine
516 kinase/response regulator network in *Escherichia coli*. J Bacteriol 196:2023–9.
- 517 26. Kelley LA, Mezulis S, Yates CM, Wass MN, Sternberg MJE. 2015. The Phyre2 web
518 portal for protein modeling, prediction and analysis. Nat Protoc 10:845–858.
- 519 27. The UniProt Consortium. 2017. UniProt: the universal protein knowledgebase. Nucleic
520 Acids Res 45:158–169.

- 521 28. Daley DO, Rapp M, Granseth E, Melen K, Drew D, Heijne G Von. 2005. Global
522 topology analysis of the *Escherichia coli* inner membrane proteome. *Science*
523 308:1321–3.
- 524 29. Jung K, Odenbach T, Timmen M. 2007. The quorum-sensing hybrid histidine kinase
525 LuxN of *Vibrio harveyi* contains a periplasmically located N terminus. *J Bacteriol*
526 189:2945–2948.
- 527 30. Ueguchi C, Ito K. 1990. *Escherichia coli* sec mutants accumulate a processed immature
528 form of maltose-binding protein (MBP), a late-phase intermediate in MBP export. *J*
529 *Bacteriol* 172:5643–5649.
- 530 31. Jones DT. 1999. Protein secondary structure prediction based on position-specific
531 scoring matrices. *J Mol Biol* 292:195–202.
- 532 32. Guzman L, Belin D, Carson MJ, Beckwith J. 1995. Tight regulation, modulation, and
533 high-level expression by vectors containing the arabinose P_{BAD} promoter. *J Bacteriol*
534 177:4121–4130.
- 535 33. Zelić B, Gerharz T, Vasić-Racki D, Bott M, Wandrey C, Takors R. 2003. Fed-batch
536 process for pyruvate production by recombinant *Escherichia coli* YYC202 Strain. *Eng*
537 *Life Sci* 3:299–305.
- 538 34. Rose L, Jenkins ATA. 2007. The effect of the ionophore valinomycin on biomimetic
539 solid supported lipid DPPTE/EPC membranes. *Bioelectrochemistry* 70:387–393.
- 540 35. Kusche BR, Smith AE, McGuirl MA, Priestley ND. 2009. The alternating pattern of
541 stereochemistry in the nonactin macrocycle is required for antibacterial activity and
542 efficient ion binding. *J Am Chem Soc* 131:17155–17165.
- 543 36. Hamidinia SA, Tan B, Erdahl WL, Chapman CJ, Taylor RW, Pfeiffer DR. 2004. The
544 ionophore nigericin transports Pb²⁺ with high activity and selectivity: a comparison to

- 545 monensin and ionomycin. *Biochemistry* 43:15956–15965.
- 546 37. Jung H, Buchholz M, Clausen J, Nietschke M, Revermann A, Schmid R, Jung K. 2002.
547 CaiT of *Escherichia coli*, a new transporter catalyzing L-carnitine/ γ -butyrobetaine
548 exchange. *J Biol Chem* 277:39251–39258.
- 549 38. Benning C. 1986. Evidence supporting a model of voltage-dependent uptake of auxin
550 into *Cucurbita* vesicles. *Planta* 169:228–237.
- 551 39. Bückner R, Heroven AK, Becker J, Dersch P, Wittmann C. 2014. The pyruvate-
552 tricarboxylic acid cycle node: a focal point of virulence control in the enteric pathogen
553 *Yersinia pseudotuberculosis*. *J Biol Chem* 289:30114–30132.
- 554 40. Sauer U, Eikmanns BJ. 2005. The PEP-pyruvate-oxaloacetate node as the switch point
555 for carbon flux distribution in bacteria. *FEMS Microbiol Rev* 29:765–794.
- 556 41. Wong FH, Chen JS, Reddy V, Day JL, Shlykov MA, Wakabayashi ST, Saier Jr MH.
557 2012. The amino acid-polyamine-organocation superfamily. *J Mol Microbiol*
558 *Biotechnol* 22:105–113.
- 559 42. Jung H, Tebbe S, Schmid R, Jung K. 1998. Unidirectional reconstitution and
560 characterization of purified Na⁺/proline transporter of *Escherichia coli*. *Biochemistry*
561 37:11083–11088.
- 562 43. Omasits U, Ahrens CH, Muller S, Wollscheid B. 2014. Protter: interactive protein
563 feature visualization and integration with experimental proteomic data. *Bioinformatics*
564 30:884–886.
- 565
- 566

567 **FIGURE LEGENDS**

568 **Figure 1. Phylogenetic tree of BtsT-like proteins in *Enterobacteriaceae*.** The tree was
569 constructed based on the alignment of 1,617 individual BtsT-like sequences, and visualized
570 with CLC Main Workbench 7. The lengths of the branches represent the relative amount of
571 evolutionary divergence between any two sequences in the tree.

572

573 **Figure 2. Schematic model of the secondary structure of *E. coli* BtsT.** The model is based
574 on the results of an analysis carried out by the Uniprot program (27), coupled with the
575 experimental evidence for the cytoplasmic location of the N-terminus and the alignment with
576 CstA. The secondary structure of BtsT was visualized using the Protter tool (43).
577 Transmembrane domains (TMs) are numbered. The conserved motif CG-x(2)-SG within CstA
578 homologs is marked in yellow (2). PP, periplasm; CM, cytoplasmic membrane; CP,
579 cytoplasm.

580

581 **Figure 3. Time course of pyruvate uptake by *E. coli* MG1655 $\Delta btsT$.** Rates of ^{14}C -pyruvate
582 uptake by the BtsT-producing strain *E. coli* MG1655 $\Delta btsT$ pBAD24-*btsT* (green) and the
583 control strain *E. coli* MG1655 $\Delta btsT$ pBAD24 (gray) were measured at a final pyruvate
584 concentration of 10 μM at 15°C. Standard deviations are estimated from three biological
585 replicates.

586

587 **Figure 4. Characterization of BtsT-mediated pyruvate uptake by intact *E. coli* cells.** ^{14}C -
588 pyruvate uptake was analyzed in freshly grown cells expressing *btsT* from pBAD24-*btsT*.
589 Initial uptake rates were measured at a pyruvate concentration of 10 μM . (A) Effects of the
590 indicated protonophores and ionophores on pyruvate uptake by BtsT. Cells were pre-

591 incubated at room temperature with the inhibitors for 30 min. (B) Effects of the indicated
592 substrates on pyruvate uptake by BtsT. Each individual compound (1 mM) was added
593 simultaneously with ^{14}C -pyruvate. ANOVA was used to calculate the statistical significance
594 in panels A and B (P values are denoted as * $P \leq 0.05$, ** $P \leq 0.01$). Standard deviations (A
595 and B) are estimated from three biological replicates with no background correction. (C) The
596 K_m value was determined by quantification of the initial rate of pyruvate uptake by BtsT in the
597 presence of various concentrations of the substrate. The values were corrected by the
598 determined diffusion rates (Fig. S8). The best-fit line was determined by nonlinear regression
599 using the equation $y = B_{\text{max}} * x / (K_d + x)$. Error bars represent standard error of the mean.

600

601 **Figure 5. Influence of $\Delta\tilde{\mu}_{\text{H}^+}$, $\Delta\Psi$, ΔpH and $\Delta\tilde{\mu}_{\text{Na}^+}$ on BtsT-mediated pyruvate uptake into**
602 **proteoliposomes of *E. coli*.** Uptake of ^{14}C pyruvate was analyzed using proteoliposomes
603 reconstituted with purified BtsT. Uptake rates were measured at a pyruvate concentration of
604 40 μM . (A) Time course of pyruvate uptake in the presence of artificially imposed $\Delta\tilde{\mu}_{\text{H}^+}$
605 (green), $\Delta\Psi$ (orange), ΔpH (red) or $\Delta\tilde{\mu}_{\text{Na}^+}$ (brown), or in the absence of any gradient (gray).
606 (B) Initial rates of pyruvate uptake by BtsT calculated using linear regression during the linear
607 uptake phase. (C) Counterflow experiment. Uptake of ^{14}C -pyruvate into proteoliposomes
608 preloaded with pyruvate (green). In the control experiment proteoliposomes were preloaded
609 with lactate (gray). ANOVA was used to calculate the statistical significance (P values in B
610 are denoted as * $P \leq 0.05$, ** $P \leq 0.01$, *** $P \leq 0.001$). Standard deviations are estimated
611 from three technical replicates.

612

FIG1

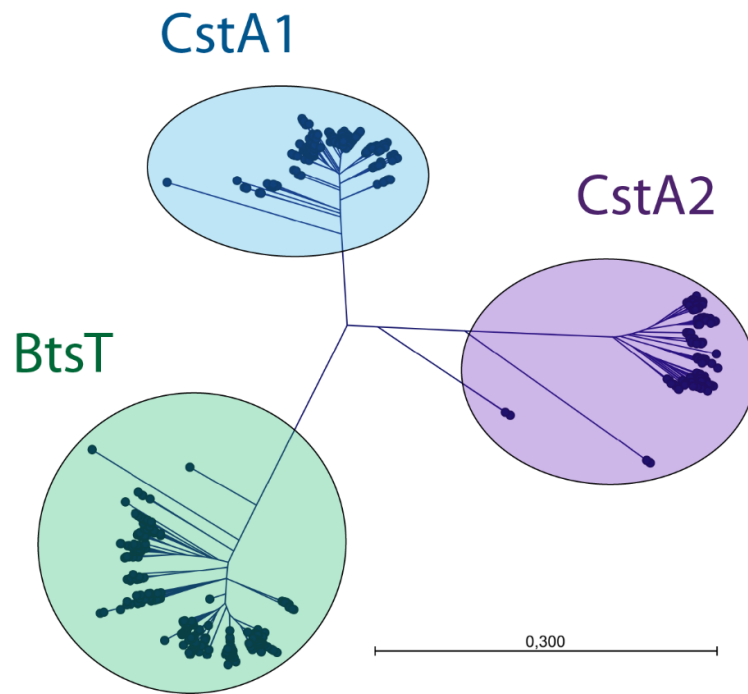


FIG 2

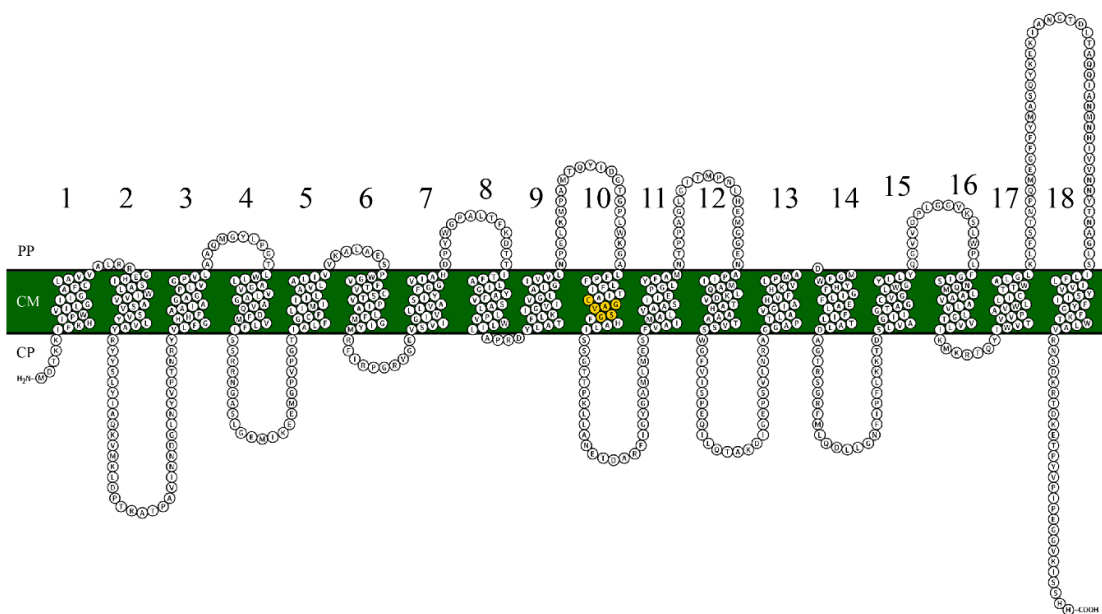


FIG 3

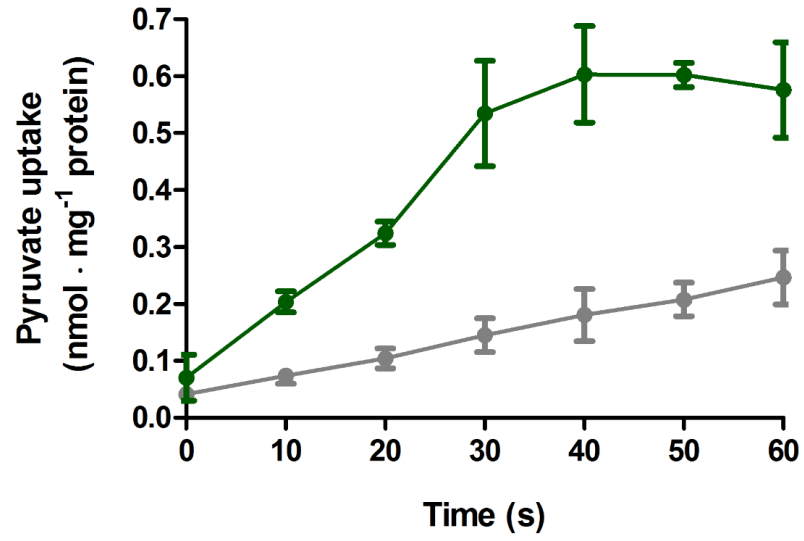


FIG 4

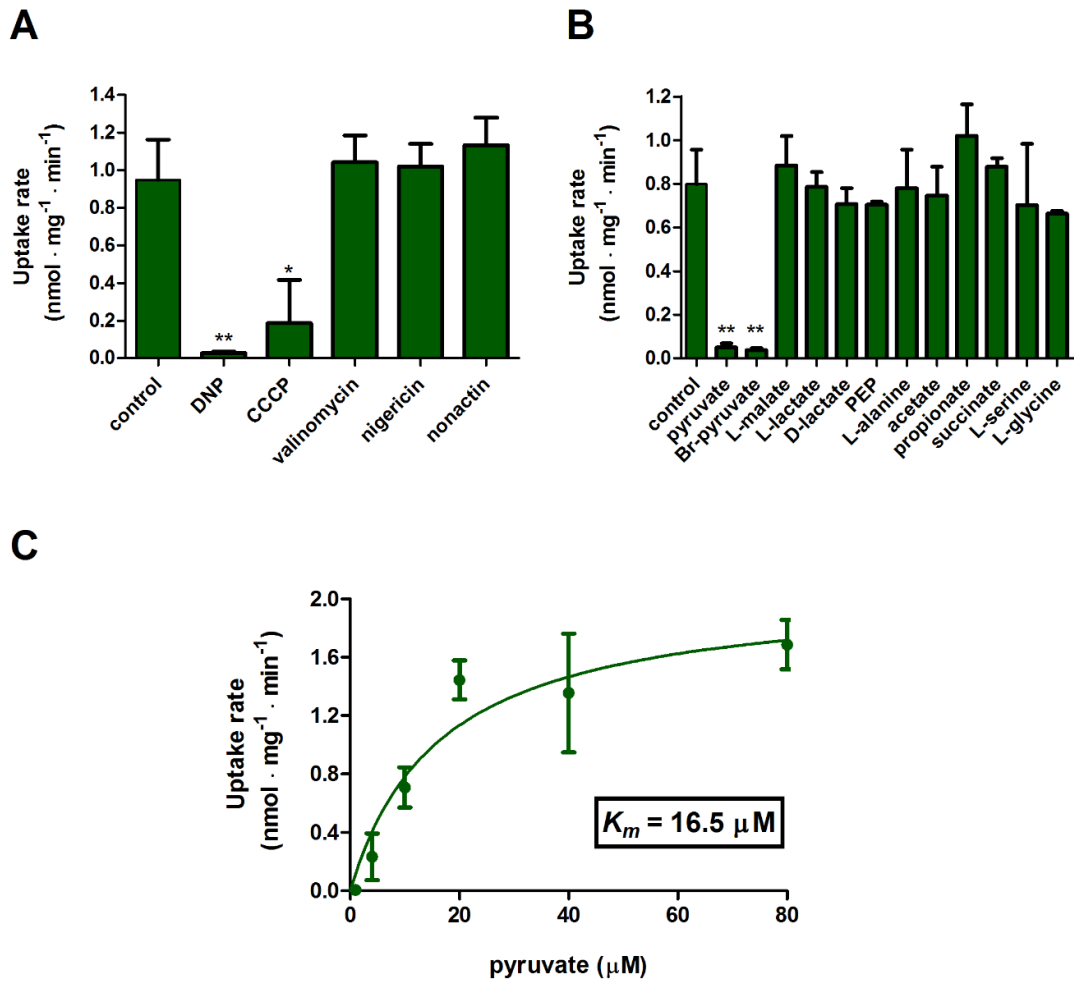
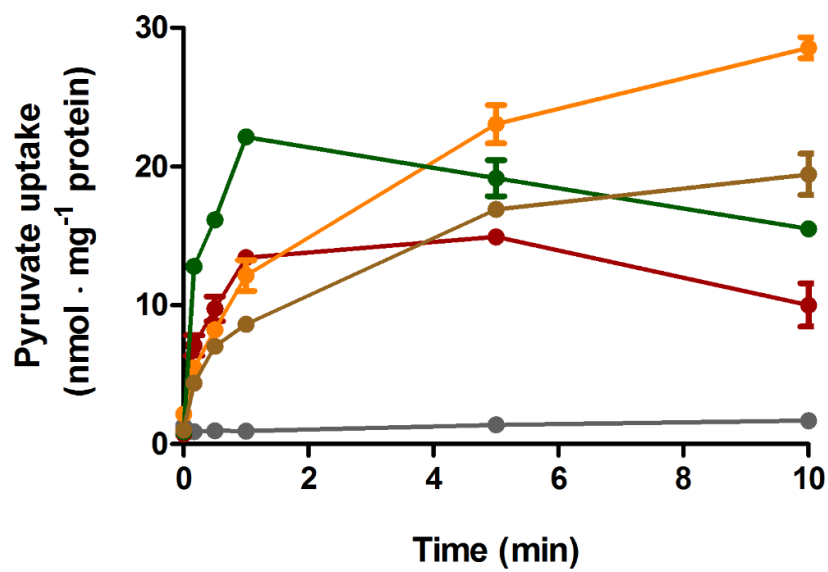
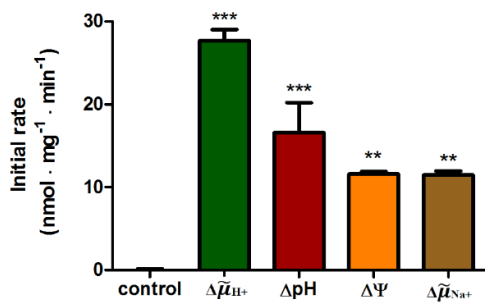


FIG 5

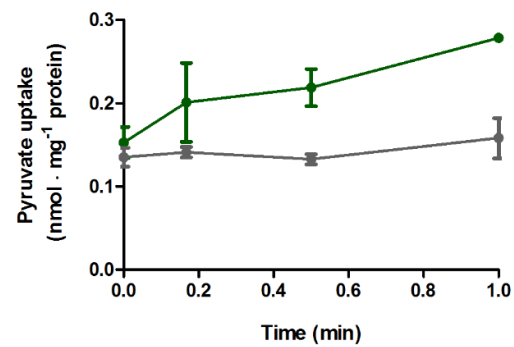
A



B



C



Chapter 4

A single-cell view of the BtsSR/YpdAB pyruvate sensing network in *Escherichia coli* and its biological relevance

Vilhena, C., Kaganovitch, E., Shin, JY., Grünberger, A., Behr, S., **Kristoficova, I.**, Brameyer, S., Kohlheyer, D., Jung, K. (2017).

J Bacteriol, 2017, in press

<http://doi.org/10.1128/JB.00536-17>



A Single-Cell View of the BtsSR/YpdAB Pyruvate Sensing Network in *Escherichia coli* and Its Biological Relevance

Cláudia Vilhena,^a Eugen Kaganovitch,^b Jae Yen Shin,^{a*} Alexander Grünberger,^{b*} Stefan Behr,^{a*} Ivica Kristofcova,^a Sophie Brameyer,^{a*} Dietrich Kohlheyer,^{b,c} Kirsten Jung^a

^aMunich Center for Integrated Protein Science, Department of Microbiology, Ludwig-Maximilians-Universität München, Martinsried, Germany

^bInstitute for Bio- and Geosciences (IBG-1), Department of Biotechnology, Forschungszentrum Jülich GmbH, Jülich, Germany

^cRWTH Aachen University-Microscale Bioengineering (AVT.MSB), Aachen, Germany

ABSTRACT Fluctuating environments and individual physiological diversity force bacteria to constantly adapt and optimize the uptake of substrates. We focus here on two very similar two-component systems (TCSs) of *Escherichia coli* belonging to the LytS/LytTR family: BtsS/BtsR (formerly YehU/YehT) and YpdA/YpdB. Both TCSs respond to extracellular pyruvate, albeit with different affinities, typically during post-exponential growth, and each system regulates expression of a single transporter gene, *yjiY* and *yhjX*, respectively. To obtain insights into the biological significance of these TCSs, we analyzed the activation of the target promoters at the single-cell level. We found unimodal cell-to-cell variability; however, the degree of variance was strongly influenced by the available nutrients and differed between the two TCSs. We hypothesized that activation of either of the TCSs helps individual cells to replenish carbon resources. To test this hypothesis, we compared wild-type cells with the *btsSR ypdAB* mutant under two metabolically modulated conditions: protein overproduction and persister formation. Although all wild-type cells were able to overproduce green fluorescent protein (GFP), about half of the *btsSR ypdAB* population was unable to overexpress GFP. Moreover, the percentage of persister cells, which tolerate antibiotic stress, was significantly lower in the wild-type cells than in the *btsSR ypdAB* population. Hence, we suggest that the BtsS/BtsR and YpdA/YpdB network contributes to a balancing of the physiological state of all cells within a population.

IMPORTANCE Histidine kinase/response regulator (HK/RR) systems enable bacteria to respond to environmental and physiological fluctuations. *Escherichia coli* and other members of the *Enterobacteriaceae* possess two similar LytS/LytTR-type HK/RRs, BtsS/BtsR (formerly YehU/YehT) and YpdA/YpdB, which form a functional network. Both systems are activated in response to external pyruvate, typically when cells face overflow metabolism during post-exponential growth. Single-cell analysis of the activation of their respective target genes *yjiY* and *yhjX* revealed cell-to-cell variability, and the range of variation was strongly influenced by externally available nutrients. Based on the phenotypic characterization of a *btsSR ypdAB* mutant compared to the parental strain, we suggest that this TCS network supports an optimization of the physiological state of the individuals within the population.

KEYWORDS histidine kinase, nutrient limitation, overflow metabolism, persister cells

Typical two-component systems (TCSs) consist of a membrane-bound histidine kinase (HK), which perceives a stimulus, and a cytoplasmic response regulator (RR), which triggers an appropriate response (1, 2). *Escherichia coli* contains 30 TCSs in all.

Received 5 September 2017 Accepted 9 October 2017

Accepted manuscript posted online 16 October 2017

Citation Vilhena C, Kaganovitch E, Shin JY, Grünberger A, Behr S, Kristofcova I, Brameyer S, Kohlheyer D, Jung K. 2018. A single-cell view of the BtsSR/YpdAB pyruvate sensing network in *Escherichia coli* and its biological relevance. *J Bacteriol* 200:e00536-17. <https://doi.org/10.1128/JB.00536-17>.

Editor Thomas J. Silhavy, Princeton University

Copyright © 2017 American Society for Microbiology. All Rights Reserved.

Address correspondence to Kirsten Jung, jung@lmu.de.

* Present address: Jae Yen Shin, Max Planck Institute of Biochemistry, Martinsried, Germany; Alexander Grünberger, Multiscale Bioengineering, Bielefeld University, Bielefeld, Germany; Stefan Behr, Roche Diagnostics GmbH, Penzberg, Germany; Sophie Brameyer, University College London, London, United Kingdom.

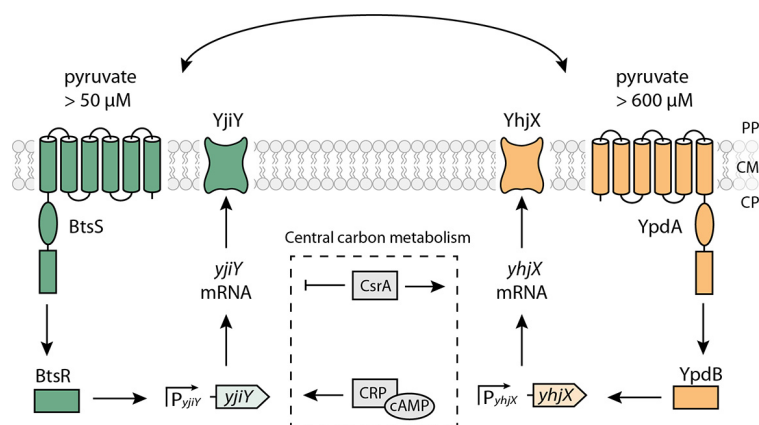


FIG 1 Model of the nutrient-sensing BtsS/BtsR and YpdA/YpdB network in *E. coli*. The scheme summarizes the signal transduction cascades triggered by the BtsS/BtsR and YpdA/YpdB systems and the influence of other regulatory elements. Activating (→) and inhibitory (−) effects are indicated. PP, periplasm; CM, cytoplasmic membrane; CP, cytoplasm. See the text for details.

Members of the LytS/LytTR family make up one prominent class of TCSs, representatives of which are found in many microorganisms. Examples include AgrC/AgrA from *Staphylococcus aureus*, which is involved in the transition from the persistent, avirulent state to the virulent phenotype (3), while FsrC/FsrA from *Enterococcus faecalis* is responsible for the production of virulence-related proteases (4), and VirS/VirR from *Clostridium perfringens* induces the synthesis of exotoxins and collagenase (5, 6). In our laboratory, we are studying the only two known members of the LytS/LytTR family in *E. coli*: BtsS/BtsR (previously YehU/YehT) and YpdA/YpdB (7–10). These two TCSs not only share the same domain structure, they also display over 30% identity at the amino acid sequence level (9). BtsS/BtsR activation leads to the expression of *yjiY*, YpdA/YpdB activation results in *yhjX* expression (Fig. 1). Both target genes code for transporters, which belong to different transporter families: YjiY is a member of the CstA family, and YhjX has been assigned to the oxalate/formate antiporter (OFA) family (7, 8, 11). In addition, the cyclic AMP (cAMP) receptor protein (CRP) complex (CRP-cAMP) upregulates *yjiY* at the transcriptional level (7), whereas the carbon storage regulator A (CsrA) upregulates *yhjX* and downregulates *yjiY* at the posttranscriptional level.

In previous studies we found functional interconnectivity of the two TCSs (9). Deletion of either component of the TCS or its target gene influences the level of expression of the target gene regulated by the other TCS and vice versa (9). In addition, *in vivo* protein-protein interaction assays suggested that the two systems form a single, large signaling unit (Fig. 1). Moreover, when *E. coli* was grown in tryptone-based (LB) medium, both systems are activated at the onset of the post-exponential growth phase (9). A more refined study revealed that the BtsS/BtsR system is activated in the presence of extracellular pyruvate (at a threshold concentration of 50 μM) under nutrient-depleted conditions (10). Biochemical studies confirmed that BtsS is a high-affinity pyruvate receptor ($K_d = 58.6 \mu\text{M}$) (10). Recently, the corresponding YjiY transporter was characterized as a high-affinity pyruvate/ H^+ symporter (12). The YpdA/YpdB system also responds to extracellular pyruvate, albeit at a higher threshold concentration of 600 μM (8).

The biological significance of the BtsS/BtsR and YpdA/YpdB network is still unclear. To explore this issue, we determined the activation states of the two systems at the single-cell level in *E. coli* populations. Using separate fluorescence reporter strains for each system, we found a correlation between the available nutrient resources and the degree of heterogeneity in the transcriptional responses of the target gene promoters in individual cells. Based on this finding and further phenotypic analyses, we suggest that the BtsS/BtsR and YpdA/YpdB systems play a role in optimization of the physiological status of the individual cells within the population.

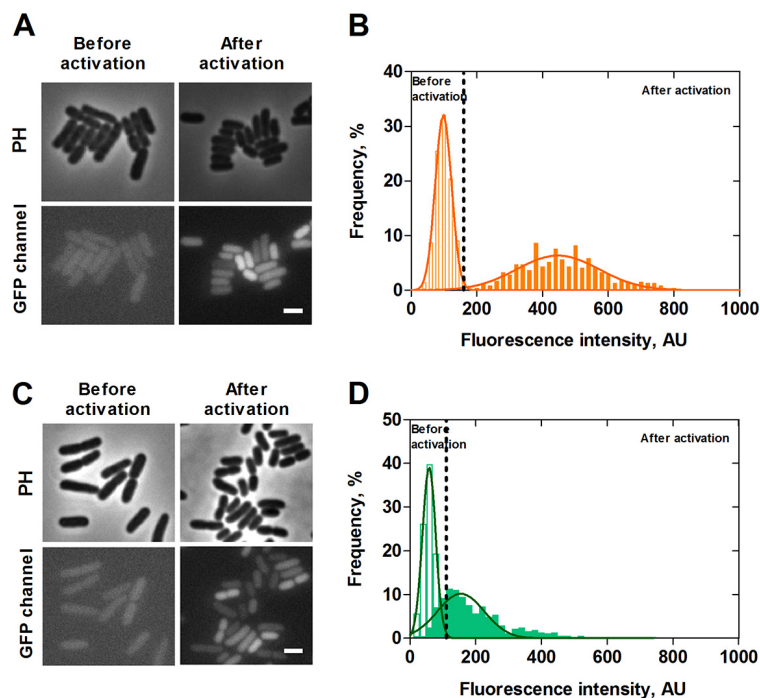


FIG 2 Single-cell analysis of P_{yhjX} and P_{yjiY} activation during growth in LB medium. *E. coli* cells expressing *gfp* under the control of the *yhjX* or *yjiY* promoter, respectively, were grown in LB medium, and fluorescence micrographs were taken before (exponential growth phase) and after activation (post-exponential growth phase) of the two TCSs. Representative fluorescence and phase-contrast images of P_{yhjX} -*gfp* and P_{yjiY} -*gfp* reporter strains are shown in panels A and C, respectively. The corresponding distributions of the fluorescence intensity of the P_{yhjX} -*gfp* and P_{yjiY} -*gfp* reporter strains are depicted in panels B and D. Unfilled bars refer to values prior to activation, and filled bars refer to values observed after activation. Dashed lines represent the threshold of activation for each of the reporter strains. A total of 200 cells were analyzed in each experiment, and frequency refers to the percentage of cells with the indicated intensity (see Materials and Methods for details). The continuous curves represent Gaussian fits based on the histograms of the fluorescence intensity. PH, phase contrast; AU, arbitrary units. Scale bar, 2 μm . Experiments were performed independently three times.

RESULTS

Heterogeneous activation of P_{yhjX} -*gfp* and P_{yjiY} -*gfp*. For the BtsS/BtsR and YpdA/YpdB systems, population-based studies have shown that the promoters of their respective target genes, *yjiY* and *yhjX*, are activated in cells which face nutrient limitation and sense the presence of external pyruvate (9, 10). Since both systems are linked to form a network, we analyzed the activation of these two promoters at the single-cell level. We constructed fluorescent reporter strains by fusing the promoter regions of *yhjX* and *yjiY* to *gfp* and introduced each fusion separately into the genome of *E. coli* MG1655 via single homologous recombination at the native locus. Using this strategy, the regulatory inputs to the native promoters of *yjiY* and *yhjX* were maintained (9), as the promoter fused to *gfp* is inserted upstream of the original one (13). The fluorescence intensity of green fluorescent protein (GFP) was used to quantify the activity of the two promoters, thus allowing us to study the transcriptional activation of *yjiY* and *yhjX* in single cells. The growth rates in LB medium of strains containing a chromosomal copy of either promoter fusion (from now on referred to as P_{yhjX} -*gfp* and P_{yjiY} -*gfp*) were similar to that of the MG1655 wild-type strain (see Fig. S1 in the supplemental material).

From population studies it is known that in cells grown in LB medium, which is rich in amino acids and leads to the overflow of pyruvate, both promoters are activated at the onset of the post-exponential growth phase (9). Hence, as expected, at the single-cell level neither P_{yhjX} -*gfp* nor P_{yjiY} -*gfp* showed any activity during the exponential growth phase (Fig. 2A and C, before activation) in LB medium. However, when cells reached the end of the exponential growth phase, we observed activation of the *yhjX*

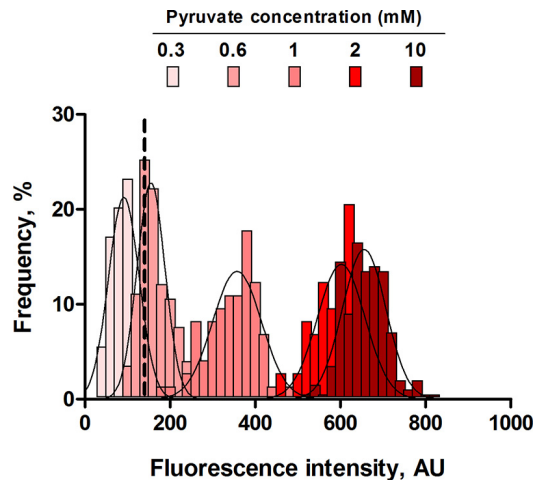


FIG 3 Effects of different external pyruvate concentrations on P_{yhjX} -*gfp* activation at the single-cell level. *E. coli* cells expressing *gfp* under the control of the P_{yhjX} promoter were grown in M9 minimal medium containing increasing concentrations of pyruvate (supplemented with succinate; final carbon concentration, 20 mM) and analyzed by fluorescence microscopy. A total of 200 cells was analyzed in each experiment at the time point of maximal expression, and frequency refers to the percentage of cells with the indicated intensity (see Materials and Methods). Histograms of the fluorescence intensities of cells were fitted using a Gaussian distribution (solid line). The dashed line represents the threshold of activation for the reporter strain. AU, arbitrary units. Experiments were performed independently three times.

promoter, as indicated by a shift of the distribution of fluorescence intensities to higher levels (Fig. 2A and B, after activation) in the majority of the population, albeit with a high degree of cell-to-cell variability as seen in the width of the Gaussian distribution (noise value [standard deviation divided by the mean] = 0.27). Less than 4% of the population was found to be nonfluorescent and therefore did not respond (the threshold of activation is marked by the dashed line in Fig. 2B). To differentiate these cells from dead cells, we stained cells with propidium iodide and found that dead cells made up only 0.4% of the population (data not shown).

Cells of the P_{yjiV} -*gfp* strain cultivated in LB medium also showed heterogeneous activation upon entry into the post-exponential growth phase. These strains exhibited an even higher noise value of 0.52 and a higher percentage of nonresponding cells (9%) (Fig. 2D) (the percentage of dead cells was determined to be 0.6%).

To determine the basal noise level of a promoter in cells at this growth phase, we performed a control experiment, in which *gfp* expression is controlled by a synthetic vegetative promoter (pXGSF). Cells harboring the vector pXGSF activate this promoter at the post-exponential growth phase (R. Hengge, unpublished data). In this experiment the promoter was activated in all the cells, and the variability was lower (i.e., 0.13) than that observed for either P_{yjiV} -*gfp* or P_{yhjX} -*gfp*. Taken together, these results indicate a heterogeneous, almost unimodal pattern of transcriptional activation for each of the two target genes of the BtsS/BtsR and YpdA/YpdB systems at the end of the exponential phase, when cells are grown in LB medium.

The degree of heterogeneity of P_{yhjX} -*gfp* activation depends on the external pyruvate concentration. Although the exact nature of the primary stimulus for the YpdA/YpdB system remains elusive, we know from previous studies that P_{yhjX} is activated in cells which are exposed to extracellular pyruvate concentrations greater than 0.6 mM (9). Aiming to further explore the single-cell behavior of this promoter activity, we analyzed the pyruvate dependence of the activation of YpdA/YpdB by determining the fluorescence intensities of P_{yhjX} -*gfp* reporter cells cultivated in M9 minimal medium supplemented with increasing concentrations of pyruvate (succinate was added to keep the total carbon concentration constant at 20 mM) (Fig. 3). As expected, a pyruvate concentration below the threshold (0.3 mM) failed to activate the YpdA/YpdB system in single cells. At pyruvate concentrations above the threshold, all

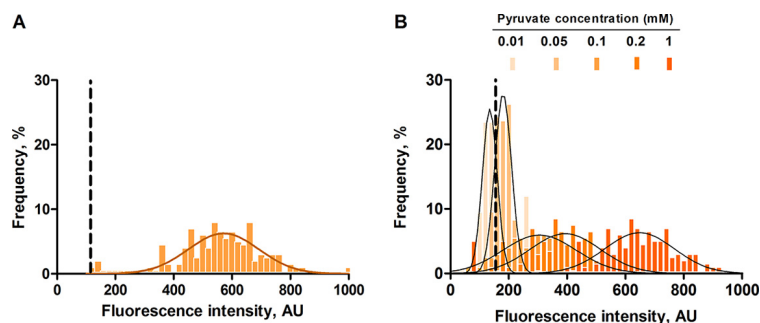


FIG 4 Effects of different external pyruvate concentrations on P_{yjiY} -*gfp* activation at the single-cell level. *E. coli* cells expressing *gfp* under the control of the P_{yjiY} promoter were grown in a nutrient-poor environment ($0.1 \times$ LB medium) for 1 h. The medium was then supplemented with 20 mM pyruvate (A) or with increasing pyruvate concentrations (B), and the cells were subsequently analyzed by fluorescence microscopy. A total of 200 cells were analyzed for each experiment, and frequency is represented as a percentage of the cells (refer to Materials and Methods for a detailed explanation). Histograms of the fluorescence intensities of cells were fitted using a Gaussian distribution (solid line). Dashed lines represent the threshold of activation for the reporter strain. AU, arbitrary units. Experiments were performed three independent times. For further details, see the legends to Fig. 2 and 3.

cells in the population homogeneously activate the *yhjX* promoter. The presence of 0.6 mM pyruvate in the medium generated a low, but detectable P_{yhjX} -*gfp* signal in the cells and the presence of 1 mM pyruvate shifted the expression level toward higher values. Interestingly, the response was markedly less heterogeneous (noise value of 0.18) in cells grown under these conditions than in the cells grown in LB medium (noise value of 0.27). Further increases in the external pyruvate concentration (2 and 10 mM) boosted the signal intensities, while the variability further decreased (to 0.09 and 0.07, respectively) (Fig. 3). These results reveal a correlation between external pyruvate availability and P_{yhjX} -*gfp* activation.

The degree of heterogeneity of P_{yjiY} -*gfp* activation is influenced both by the external pyruvate level and the metabolic state of the cells. As previously described, growth of cells in M9 minimal medium with pyruvate as sole carbon source (20 mM) is not sufficient to activate the P_{yjiY} promoter, because both extracellular pyruvate and nutrient limitation are needed to trigger BtsS/BtsR activation (10). Therefore, our reporter strain had first to be exposed to nutrient limitation (growth in $0.1 \times$ LB medium for 1 h) before pyruvate was added. Under these conditions, no activation of P_{yjiY} -*gfp* was detected (data not shown), in accordance with our previous studies (10). Pyruvate was then added to the cell culture at a final concentration of 20 mM, and cells were analyzed by fluorescence microscopy at various time points. Cells responded within 70 min and exhibited a higher average *gfp* intensity than cells grown in LB medium, which confirmed the strong response of the BtsS/BtsR system to pyruvate after exposure of cells to nutrient limitation (Fig. 4A). Remarkably, in this case activation of P_{yjiY} -*gfp* remained heterogeneous (noise value of 0.27) in spite of the abundance of pyruvate. Subsequently, we tested five different pyruvate concentrations to assess the pyruvate concentration dependence of BtsS/BtsR activation (Fig. 4B). Below the threshold of 50 μ M (0.01 mM) to which BtsS/BtsR responds, there was no detectable P_{yjiY} -*gfp* signal. As expected, only a few cells produced a weak GFP signal in an environment containing 0.05 mM pyruvate. Starting at a concentration of 0.1 mM pyruvate, P_{yjiY} activation was found in all cells, but with a high degree of cell-to-cell variability (noise value of 0.27). At higher pyruvate concentrations, the signal intensity increased, but the noise values were unchanged. The broad Gaussian distribution found at 1 mM pyruvate resembled the profile found for cells at 20 mM pyruvate (Fig. 4A). A *t* test was performed on the mean values of the two distributions, and the *P* value was determined to be 0.88. This value revealed that there is no significant difference between the cellular responses at 1 and 20 mM pyruvate. These results confirmed at the single-cell level that BtsS/BtsR-mediated activation of P_{yjiY} -*gfp* is not only dependent on the pyruvate concentration but is also influenced by internal nutrient limitation.

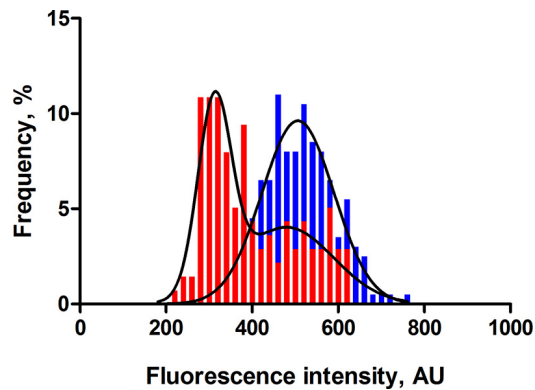


FIG 5 In the absence of the BtsSR/YpdAB network, *rrnB* P1 promoter activity is low and bistable. Wild-type *E. coli* MG1655 (blue) or mutant *btsSR ypdAB* (red) cells harboring a chromosomally encoded *rrnB* P1-*gfp* fusion were grown in LB medium and examined by fluorescence microscopy. For further details, see the legends to Fig. 2 and 3. A total of 200 cells were analyzed for each experiment at the post-exponential growth phase, and frequency is represented as a percentage of the cells (refer to Materials and Methods for detailed explanation). Histograms of the fluorescence intensities of cells were fitted using a Gaussian distribution (solid line). AU, arbitrary units. Experiments were performed three independent times.

Cellular physiology in the post-exponential growth phase. We have shown thus far that transcriptional activation of both target genes of the BtsS/BtsR and YpdA/YpdB network occurs heterogeneously. Furthermore, their activation is influenced by the availability of external pyruvate, albeit with different thresholds.

Since the two systems are activated in the post-exponential growth phase in LB medium, we decided to explore the impact of the BtsS/BtsR and YpdA/YpdB systems on the overall physiological state of *E. coli* during this growth phase. In order to do so, we investigated individual cells of both *E. coli* MG1655 (the wild-type [WT] strain) compared to a strain lacking both systems: MG1655 $\Delta btsSR \Delta ypdAB$ (abbreviated as the *btsSR ypdAB* mutant).

Fast-growing cells express high levels of 16S RNA from the *rrnB* P1 promoter (14). Cells with an inactive *rrnB* P1 promoter are likely to be dormant, antibiotic-tolerant persisters (14, 15). Recently, the strength of *rrnB* P1 promoter activation was shown to correlate with intracellular ATP levels (16). We therefore fused the ribosomal *rrnB* P1 promoter to *gfp* as previously described (14) and integrated this construct into the genomes of the two strains as a marker for their physiological states.

As expected, *E. coli* MG1655 WT *rrnB* P1-*gfp* showed a Gaussian distribution of GFP signal intensities, with a mean fluorescence value of 510 arbitrary units (AU) and noise level of 0.16 (Fig. 5). In contrast, the *btsSR ypdAB rrnB* P1-*gfp* mutant had a lower overall *rrnB* P1-*gfp* activity (average fluorescence intensity of 398 AU), which indicates a lower rate of ribosome synthesis within the population. Most strikingly, a bistable distribution of the signal was observed. These results suggest that, in the absence of both systems, the population differentiates into two subpopulations, one with a normal and another with a reduced ribosome synthesis rate.

The BtsSR/YpdAB network promotes protein overproduction. To test the idea that BtsS/BtsR and YpdA/YpdB systems together act to optimize the physiological state of cells within the population, we set out to metabolically challenge the *btsSR ypdAB* mutant and compare its response to that of the parental *E. coli* MG1655 WT strain. Interestingly, *E. coli* C41 (DE3), also known as the Walker strain, has been optimized for maximal overproduction of membrane and globular proteins (17). Subsequently, the genome of this strain was sequenced and, among other mutations, a point mutation in *btsS* was found that led to constitutive expression of *yjiY* (18). Based on these data, we hypothesized that the BtsS/BtsR and YpdA/YpdB systems might help cells to cope with the metabolic burden of protein overproduction.

In order to test this hypothesis, both strains (WT and the *btsSR ypdAB* mutant) were transformed with the overexpression vector pBAD24-*gfp*, which carries *gfp* under the

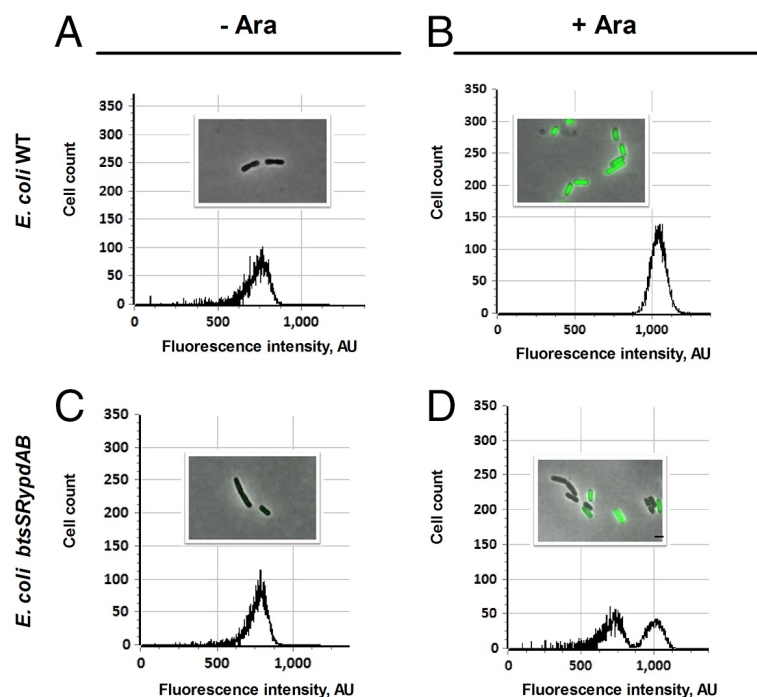


FIG 6 The BtsSR/YpdAB network promotes homogeneous protein overproduction in all cells. Wild-type (WT) or *btsSR ypdAB* mutant cells harboring the overproduction vector pBAD24-*gfp* were grown in LB medium. Samples were taken before and after the addition of the inducer arabinose (Ara) (0.2% [wt/vol]). The cells were analyzed by fluorescence microscopy and flow cytometry. Distributions of fluorescent cell counts and representative views of WT cells before and after addition of arabinose are shown in panels A and B, while the corresponding data for the *btsSR ypdAB* mutant are depicted in panels C and D. About 2,000 events were recorded for each plot. Cell counts represent the numbers of cells, and fluorescence intensity is expressed in arbitrary units (AU). Scale bar, 2 μ m. Experiments were performed independently three times.

control of an arabinose-inducible promoter. Before induction with arabinose, fluorescence microscopy of single WT and *btsSR ypdAB* mutant cells showed no apparent GFP signals, and flow cytometry confirmed that the maximal fluorescence intensity of green cells (\sim 750 AU) was low (Fig. 6A and C), indicating little or no GFP expression. One hour after induction with 0.2% (wt/vol) arabinose, cells of the WT population were producing GFP, which was clearly detected as an increase in the maximum fluorescence observed by flow cytometry (to \sim 1,100 AU). This result was corroborated by the detection of labeled single cells with fluorescence microscopy (Fig. 6B). In contrast, flow cytometric analysis of the mutant under inducing conditions detected two peaks: one at 1,100 AU, as in the WT, and a second at 750 AU. The accompanying micrographs revealed the presence of fluorescent and nonfluorescent cells (Fig. 6D). Therefore, the low-intensity peak in the flow cytometer represents cells that are unable to produce GFP in large amounts. The C41 (DE3) strain was also tested and was found to be capable of a homogeneously high protein overproduction, as expected (data not shown).

We also tested the overproduction of (i) GFP under the control of the IPTG (isopropyl- β -D-thiogalactopyranoside)-inducible *lac* promoter (pCOLA-P_{*lac*}-*gfp*), (ii) the periplasmic protein DppA fused to the Tat translocation sequence (19) and under the control of the arabinose promoter (pBAD24-RR-*gfp-dppA*), and (iii) the membrane protein LysP fused to a different fluorophore and under the control of an arabinose-inducible promoter (pBAD33-*lysP-mcherry*) (see Table S1 in the supplemental material). The results obtained for the IPTG-inducible GFP reporter were similar to those for the arabinose-controlled system. The *btsSR ypdAB* mutant was hardly able to overproduce the periplasmic DppA or the membrane protein LysP. In summary, the BtsS/BtsR and YpdA/YpdB sensing network helps *E. coli* to cope with the additional metabolic burden imposed by protein overproduction.

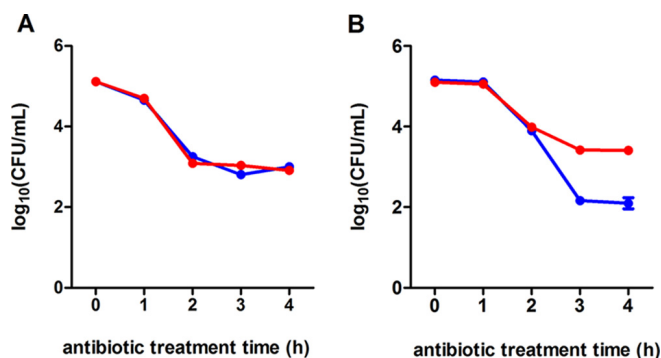


FIG 7 The BtsSR/YpdAB network reduces the proportion of persister cells in populations. Either WT (blue lines) or mutant *btsSR ypdAB* (red lines) cells were grown in LB medium. Before (exponential growth phase) (A) and after (B) activation (post-exponential growth phase) of the systems, the cells were exposed to ampicillin (200 $\mu\text{g/ml}$). Samples were taken and analyzed for CFU. Three independent experiments were performed, and error bars indicate the standard deviations of the means.

The BtsSR/YpdAB network limits the proportion of persister cells in WT populations. We hypothesized that the heterogeneous distribution of the capacity for protein overproduction among the *btsSR ypdAB* mutant population might be related to the presence of a subpopulation of cells that are unable to sense nutrient limitation and consequently fail to activate transporters to acquire needed resources. Persister cells survive exposure to antibiotics owing to their altered metabolic activity and low growth rate, but they can subsequently resume growth to form an antibiotic-sensitive population (20). We were interested to know whether the BtsS/BtsR and YpdA/YpdB network has an influence on persister cell formation. To address this question, we performed population-based studies by exposing growing WT or *btsSR ypdAB* mutant cells to ampicillin and determining the number of CFU. Only cells able to recover from the stress will form CFU. We subdivided a growing culture and exposed cells to ampicillin before and after the natural activation of the signaling systems, namely, at an optical density at 600 nm (OD_{600}) of 0.4 (exponential growth phase) and 1.2 (post-exponential growth phase) (9). After treatment with ampicillin a biphasic time-dependent killing curve was observed, which is typical for persister formation (Fig. 7) (20). When cells were exposed to ampicillin prior to activation of the signaling systems, the two strains exhibited almost identical patterns of response, characterized by a steep initial decrease in CFU, followed by a slower killing rate, revealing persister cells (Fig. 7A). Ampicillin treatment of cells after activation of the signaling systems resulted in a considerably higher level of persister cells in the mutant (2.15%) than the WT (0.14%) population (Fig. 7B).

In parallel, the minimum time taken to kill 99% of the population (MDK_{99}) (21) was determined for both strains after exposure to ofloxacin. The value for the WT was determined to be 0.49 h, and for the *btsSR ypdAB* mutant it was 1.98 h, which is compatible with the higher fraction of persisters in the mutant population (see Fig. S2 in the supplemental material).

These results reveal a novel role for the BtsS/BtsR and YpdA/YpdB signaling network in reducing the percentage of persister cells in a growing population. They are also in accordance with the idea of a contribution of both systems to help individual cells to replenish nutrient resources.

DISCUSSION

BtsS/BtsR (formerly YehU/YehT) is one of the most widespread TCSs in bacteria and is found in many human and plant pathogens. Although most gammaproteobacteria contain this system, some, including *Escherichia*, *Citrobacter*, and *Serratia*, have a second homologous system, YpdA/YpdB (22). Both belong to the LytS/LytTR family. Previous systematic studies failed to identify a function for these TCSs (23, 24). We have now identified the HK BtsS as a high-affinity pyruvate receptor ($K_d = 58.6 \mu\text{M}$) and

YpdA/YpdB as a system that responds to higher levels (>0.6 mM) of the same compound (8, 10). The target genes regulated by the two systems code for the high-affinity pyruvate/H⁺ symporter YjiY (recently renamed BtsT [12]) and a transporter of unknown function, YhjX. However, the biological significance of the BtsS/BtsR and YpdA/YpdB systems has remained unclear.

Therefore, we first investigated the activation of the target genes of each system at the single-cell level using promoter fusions. We found that in clonal populations the chromosomally integrated copies of either P_{yjiY}-*gfp* or P_{yhjX}-*gfp* were heterogeneously activated when grown in LB medium, which is rich in amino acids (Fig. 2), and that induction of P_{yjiY}-*gfp* was slightly more variable than that of P_{yhjX}-*gfp*. In both cases, a predominantly unimodal Gaussian distribution of activation levels was observed, and only a very small percentage of cells remained in the OFF state. This pattern of activation differs markedly from the “all-or-nothing,” switch-like gene expression described for the *lac* or *ara* promoter (25, 26). However, the heterogeneous, but unimodal activation of *yhjX* and *yjiY* can, in principle, be explained by the multiple factors known to affect their expression: (i) binding of the respective transcriptional activators BtsR and YdpB (27), (ii) the influence of the cAMP/CRP protein (P_{yjiY}), (iii) fine-tuning by the carbon starvation regulator CsrA (Fig. 1), and (iv) variations in the physiological state between cells (see below).

YpdA/YpdB-mediated activation of P_{yhjX} was found to be dependent on the concentration of pyruvate in the medium and became homogenous when cells were grown in minimal medium containing pyruvate (20 mM) as the sole carbon source (Fig. 3). In contrast, under all tested conditions BtsS/BtsR-mediated activation of P_{yjiY} was characterized by high cell-to-cell variability, which was virtually unaffected by the amount of pyruvate in the medium (Fig. 4). It is important to note that the BtsS/BtsR systems, whose target gene codes for a high-affinity pyruvate transporter, is only activated by external pyruvate when cells concurrently face nutrient limitation (Fig. 4) (10). The high degree of heterogeneity might reflect variations in the nutritional state of individual cells and differing needs for the high-affinity pyruvate transporter YjiY. Therefore, the BtsS/BtsR system responds only when cells are in need of a high-affinity uptake transporter to scavenge traces of available nutrients, e.g., pyruvate.

It has been proposed that cellular metabolism is both inherently stochastic and a generic source of phenotypic heterogeneity (28). In this general context, the results of our single-cell studies can be accommodated by the following model for the role of the two LytS/LytTR-type systems in *E. coli*. Under certain conditions, e.g., during growth in LB medium, cells excrete pyruvate due to overflow metabolism. Subsequently, other nutrients are depleted, and cells sense the availability of pyruvate. Depending on the external pyruvate concentration and their particular nutritional needs, individual *E. coli* cells activate either the high-affinity BtsS/BtsR and/or the low-affinity YpdA/YpdB system upon entry into the post-exponential growth phase. The interplay between transporters with different affinities for the same substrate has already been described, and this seems to be a successful strategy under nutrient limitation (29).

By using a reporter for the rate of ribosome synthesis, we found that only populations of reporter cells harboring the nutrient-sensing network exhibited unimodal activation of the *rrnB* P1 promoter, whereas the *btsSR ypdAB* mutant was characterized by a bimodal expression pattern (Fig. 5). The heterogeneous activation of either P_{yjiY} or P_{yhjX} in individual WT cells allows uptake of nutrients, e.g., pyruvate, according to the individual requirement of the cells. This results in a unimodal distribution of the activation level of the *rrnB* P1 promoter characteristic of growing cells. It should be noted that previous physiological studies revealed that *E. coli* has more than one pyruvate transporter (30), although only YjiY has thus far been characterized as high-affinity pyruvate transporter (12). Therefore, we assume that individuals within the population of the *btsSR ypdAB* mutant can cope with the lack of the sensing/transport of pyruvate and have normal ribosome synthesis. In addition, we imposed a metabolic burden by forcing cells to overproduce particular proteins. This is a natural scenario, since many pathogens have to produce virulence factors, exoenzymes, siderophores,

TABLE 1 Bacterial strains and plasmids used in this study

Strain or plasmid	Relevant genotype or description ^a	Source or reference
<i>E. coli</i> strains		
MG1655	F ⁻ λ ⁻ <i>ilvG rfb50 rph-1</i>	35
ST18	S17Ipir Δ <i>hemA</i>	36
DH5α	<i>fhuA2 lacΔU169 phoA glnV44 φ80' lacZΔM15 gyrA96 recA1 relA1 endA1 thi-1 hsdR17</i>	37
MG 35	MG1655 Δ <i>btsSR YpdAB</i>	This study
MG 2	MG1655 Δ <i>yehUT</i> = Δ <i>btsSR</i>	7
MG 20	MG1655 Δ <i>ypdAB</i>	8
MG1655 P _{<i>yhjX</i>} - <i>gfp</i>	Integration of P _{<i>yhjX</i>} - <i>gfp</i> at the native locus in <i>E. coli</i> MG1655	This study
MG1655 P _{<i>yjiY</i>} - <i>gfp</i>	Integration of P _{<i>yjiY</i>} - <i>gfp</i> at the native locus in <i>E. coli</i> MG1655	This study
MG1655 P _{<i>rrnB P1</i>} - <i>gfp</i>	Integration of P _{<i>rrnB P1</i>} - <i>gfp</i> at the native locus in <i>E. coli</i> MG1655	This study
MG 35 P _{<i>rrnB P1</i>} - <i>gfp</i>	Integration of P _{<i>rrnB P1</i>} - <i>gfp</i> at the native locus in <i>E. coli</i> MG 35	This study
Plasmids		
pRed/ET	λ-RED recombinase in pBAD24; Amp ^r	Gene Bridges
pCP20	FLP-recombinase, λcl 857 ⁺ , λpR Rep ^{ts} ; Amp ^r Cm ^r	38
pNPTS138-R6KT	<i>mobRP4⁺ ori-R6K sacB</i> , suicide plasmid; Kan ^r	13
pNPTS138-R6KT-P _{<i>yhjX</i>} - <i>gfp</i>	300 bp of P _{<i>yhjX</i>} fused to <i>gfp</i> and cloned into EcoRI/PspOMI sites of pNPTS138-R6KT; Kan ^r	This study
pNPTS138-R6KT-P _{<i>yjiY</i>} - <i>gfp</i>	300 bp of P _{<i>yjiY</i>} fused to <i>gfp</i> and cloned into EcoRI/PspOMI sites of pNPTS138-R6KT; Kan ^r	This study
pNPTS138-R6KT-P _{<i>rrnB P1</i>} - <i>gfp</i>	300 bp of P _{<i>rrnB P1</i>} fused to <i>gfp</i> and cloned into EcoRI/PspOMI sites of pNPTS138-R6KT; Kan ^r	This study
pXGSF	<i>gfp</i> under the control of a vegetative synthetic promoter	G. Klauck and R. Hengge, unpublished data
pBAD24	Arabinose-inducible P _{BAD} promoter, pBR322 ori; Amp ^r	39
pBAD24- <i>gfp</i>	<i>gfp</i> cloned in the EcoRI and NcoI sites of pBAD24	26
pBAD24-RR- <i>gfp</i>	<i>gfp-mut2</i> cloned in the NheI and HindIII sites of pBAD24 (p8754 derivative)	19
pBAD24-RR- <i>gfpmut-dppA</i>	<i>dppA</i> cloned in the HindIII site of pBAD24-RR- <i>gfpmut2</i>	This study
pCOLA Duet-1	Expression vector, CoLA ori; Kan ^r	Merck
pCOLA-P _{<i>lac</i>} - <i>gfp</i>	<i>gfp</i> under the control of the IPTG-inducible <i>lac</i> promoter cloned in the BamHI and HindIII sites of pCOLA-Duet-1	This study
pBAD33- <i>lysP</i>	<i>lysP</i> in pBAD33; Cm ^r	40
pBAD33- <i>lysP-mcherry</i>	<i>mcherry</i> cloned in the XbaI and Sall sites of pBAD33- <i>lysP</i> ; Cm ^r	This study

^aCm^r, chloramphenicol resistance; Kan^r, kanamycin resistance; Amp^r, ampicillin resistance.

etc., in large amounts. Although all WT cells managed to cope with this burden, about 50% of the mutant cells failed to overproduce the test protein, GFP, a pattern which we also observed for the activation of the *rrnB P1* promoter (Fig. 6). It should be noted that the evolved *E. coli* C41(DE3) strain, which has been optimized for protein overproduction, has a point mutation in *btsS* that leads to stimulus-independent expression of *yjiY* (18). In light with the results presented here, the constitutive expression of the high-affinity pyruvate transporter YjiY in strain C41 guarantees a sufficient uptake of pyruvate in all cells independent from external or internal factors. Finally, a population-based persister assay revealed that *btsSR ypdAB* populations contain a higher percentage of antibiotic-tolerant persister cells (dormant cells) than do WT populations (Fig. 7).

Taking these results into account, the model described above can be further extended. Sensing of external pyruvate by the BtsS/BtsR and YpdA/YpdB systems and the tight regulation of expression of the two transporters YjiY and YhjX depending on the needs of the individual cell ensures an optimization of the physiological state within the whole population to withstand upcoming metabolic stress. These findings are important not only in light of the host colonization of pathogenic species and their persistence but also for metabolic engineering.

MATERIALS AND METHODS

Bacterial strains and growth conditions. The *E. coli* strains, including their genotypes, and the plasmids used in this study are listed in Table 1. Mutants were constructed using an *E. coli* Quick-and-Easy gene deletion kit (Gene Bridges) and a BAC modification kit (Gene Bridges), as previously reported (31). Both kits rely on the Red/ET recombination technique (31). The oligonucleotide sequences are available on request.

E. coli MG1655 strains (Table 1) were grown overnight in lysogeny broth (LB; 10 g/liter NaCl, 10 g/liter tryptone, 5 g/liter yeast extract). After inoculation, bacteria were routinely grown in LB medium under agitation (200 rpm) at 37°C. For solid medium, 1.5% (wt/vol) agar was added. Where appropriate, media were supplemented with antibiotics (kanamycin sulfate, 50 µg/ml; ampicillin sodium salt, 100 µg/ml). For the "low-nutrient environment" experiments, cells from an overnight culture in LB were inoculated into 0.1× diluted LB at a starting OD₆₀₀ of 0.05 and grown for 1 h. Pyruvate was then added to the cultures to a final concentration of 0.01, 0.05, 0.1, 0.2, 1, or 20 mM.

E. coli MG1655 strains were also grown overnight in M9 minimal medium with 0.5% (wt/vol) glucose as sole carbon source. Bacteria were then inoculated into M9 minimal medium supplemented with increasing concentrations of pyruvate (0.3, 0.6, 1, 2, and 10 mM), and the total carbon source concentration was adjusted to 20 mM using succinate. The conjugation strain *E. coli* ST18 was grown in the presence of 50 µg/ml 5-aminolevulinic acid.

Construction of fluorescence reporters. Molecular manipulations were carried out according to standard protocols (32). Plasmid DNA and genomic DNA were isolated using a HiYield plasmid minikit (Sued-Laborbedarf) and a DNeasy blood and tissue kit (Qiagen), respectively. DNA fragments were purified from agarose gels using a HiYield PCR cleanup and gel extraction kit (Sued-Laborbedarf). Q5 DNA polymerase (New England Biolabs) was used according to the supplier's instructions. Restriction enzymes and other DNA-modifying enzymes were also purchased from New England Biolabs and used according to the manufacturer's directions. Replicative plasmids were transferred into *E. coli* strains using competent cells prepared as described previously (33).

For construction of the promoter-*gfp* fusions, 300-bp segments of the region immediately upstream of the coding sequence were amplified using oligonucleotide pairs containing EcoRI/PspOMI restriction sites. The resulting promoter fragments were ligated into the γ -origin-dependent vector pNPTS138-R6KT-*gfp* after restriction with EcoRI/PspOMI. Chromosomal insertions of promoter-*gfp* into the designated *E. coli* strains were achieved by integrating the resultant suicide vectors pNPTS138-R6KT-P_{yjiV}-*gfp* and pNPTS138-R6KT-P_{yjiX}-*gfp* via RecA-mediated single homologous recombination as described previously (13). The donor strain *E. coli* ST18, containing the required plasmids, was cultivated together with the recipient *E. coli* MG1655 strain in LB medium, supplemented with additives as described, to an OD₆₀₀ of about 0.8. Recombination-positive clones were selected on kanamycin plates, and correct chromosomal integration was checked by PCR and sequencing. To prevent duplication instability, the reporter strains were always cultivated in the presence of kanamycin.

Single-cell fluorescence microscopy and analysis. To measure promoter activity in individual cells of the reporter strains, cells were cultivated as described above in a rotary shaker. Samples were taken (10 µl) and analyzed on an agarose pad (0.5% [wt/vol] agarose in phosphate-buffered saline [PBS; pH 7.4]), which was placed on a microscope slide and covered with a coverslip.

Images were taken on a Leica microscope (DMI 6000B) equipped with a Leica DFC 365 Fx camera (Andor, 12 bit). An excitation wavelength of 460 nm and a 512-nm emission filter with a 75-nm bandwidth were used for visualization of GFP fluorescence, and an excitation wavelength of 546 nm and a 605-nm emission filter with the same bandwidth were used for visualization of red fluorescence. At least 200 cells per condition were analyzed. The digital images were analyzed using Fiji (34), and statistical analysis was performed using Prism version 5.03 for Windows (GraphPad Software, La Jolla, CA). The background fluorescence was subtracted from each field of view.

The noise was calculated by dividing the standard deviation by the mean. The higher the noise value the more heterogeneous the distribution. The percentage of dark cells was determined from the number of cells whose fluorescence levels overlapped with the negative control (before activation) and the total number of cells quantified. The frequency distributions depict the fraction of values which lie within the range of values that define the bin. The bin range was kept constant at 20 AU. Propidium iodide (Invitrogen, Eugene, OR) was added to the cell cultures at a final concentration of 5 µM to stain dead cells (red fluorescence).

Overproduction experiments. Overnight cultures of *E. coli* MG1655 transformed with the plasmid pBAD24-*gfp* were diluted 100-fold in 20 ml of fresh LB medium supplemented with 100 µg/ml of ampicillin sodium salt and incubated aerobically at 37°C until an OD₆₀₀ was reached 0.6 (early exponential phase). The cells were induced with L-arabinose 0.2% (wt/vol) for 1 h. Before and after induction, 100-µl samples were taken, diluted 1:1,000 in PBS, and analyzed in a BD Accuri C6 flow cytometer equipped with a solid-state laser (488-nm emission; 20 mW). The green fluorescence emission from GFP was collected by the FL1 filter (BP 533/30 filter). Forward-angle light scatter (FSC) and side-angle light scatter (SSC) were collected in the FSC detector and SSC filter (BP 488/10 filter), respectively. The detection threshold was adjusted for FSC to eliminate noise, and the gate was set on the FSC-SSC dot plot to exclude debris. The sheath flow rate was 14 µl/min, and no more than 100 events/s were acquired. For each sample run, a maximum of 2,000 events were collected. Analysis of data was carried out using Cytospec software (http://www.cyto.purdue.edu/Purdue_software).

Persister cell assay. To determine the number of persister cells, the number of CFU per ml was measured after exposure of the culture to 200 µg/ml ampicillin. Overnight cultures were diluted 100-fold in 20 ml of fresh LB medium and incubated aerobically at 37°C until the OD₆₀₀ reached 0.4 or 1.2. Aliquots were then transferred to a new 100-ml flask (final OD₆₀₀ = 1), and the antibiotic was added. Every hour during antibiotic treatment, samples were taken, serially diluted in PBS, plated on LB agar, and incubated at 37°C for 16 h. CFU were counted as a measure of surviving persister cells. Persisters were calculated as the surviving fraction by dividing the number of CFU per milliliter in the culture after incubation with the antibiotic by the number of CFU per milliliter in the culture before addition of the antibiotic. Each experiment was repeated on three different days.

For calculation of the minimum duration of killing (MDK_{99}), the procedure described above was performed using ofloxacin (at a final concentration of 5 $\mu\text{g/ml}$) as the antibiotic. The MDK_{99} value corresponds to the time (in hours) needed to kill 99% of the initial population.

SUPPLEMENTAL MATERIAL

Supplemental material for this article may be found at <https://doi.org/10.1128/JB.00536-17>.

SUPPLEMENTAL FILE 1, PDF file, 0.2 MB.

ACKNOWLEDGMENTS

We thank Nicola Lorenz and Tobias Bauer for strain construction and Lena Stelzer for excellent technical assistance. We thank Regine Hengge and Gisela Klauk for providing plasmids.

This study was financially supported by the Deutsche Forschungsgemeinschaft grants SPP1617 and Exc114/2 and projects JU270/13-2 (K.J.) and KO 4537/1-2 (D.K.).

The funders had no role in study, design, data collection and interpretation, or the decision to submit the work for publication.

REFERENCES

- Mascher T, Helmann JD, Unden G. 2006. Stimulus perception in bacterial signal-transducing histidine kinases. *Microbiol Mol Biol Rev* 70:910–938. <https://doi.org/10.1128/MMBR.00020-06>.
- Stock AM, Robinson VL, Goudreau PN. 2000. Two-component signal transduction. *Annu Rev Biochem* 69:183–215. <https://doi.org/10.1146/annurev.biochem.69.1.183>.
- Sidote DJ, Barbieri CM, Wu T, Stock AM. 2008. Structure of the *Staphylococcus aureus* AgrA LytTR domain bound to DNA reveals a beta fold with an unusual mode of binding. *Structure* 16:727–735. <https://doi.org/10.1016/j.str.2008.02.011>.
- Qin X, Singh KV, Weinstock GM, Murray BE. 2000. Effects of *Enterococcus faecalis* *fsr* genes on production of gelatinase and a serine protease and virulence. *Infect Immun* 68:2579–2586. <https://doi.org/10.1128/IAI.68.5.2579-2586.2000>.
- Shimizu T, Shima K, Yoshino K, Yonezawa K, Shimizu T, Hayashi H. 2002. Proteome and transcriptome analysis of the virulence genes regulated by the VirR/VirS system in *Clostridium perfringens*. *J Bacteriol* 184:2587–2594. <https://doi.org/10.1128/JB.184.10.2587-2594.2002>.
- Rood JI. 1998. Virulence genes of *Clostridium perfringens*. *Annu Rev Microbiol* 52:333–360. <https://doi.org/10.1146/annurev.micro.52.1.333>.
- Kraxenberger T, Fried L, Behr S, Jung K. 2012. First insights into the unexplored two-component system YehU/YehT in *Escherichia coli*. *J Bacteriol* 194:4272–4284. <https://doi.org/10.1128/JB.00409-12>.
- Fried L, Behr S, Jung K. 2013. Identification of a target gene and activating stimulus for the YpdA/YpdB histidine kinase/response regulator system in *Escherichia coli*. *J Bacteriol* 195:807–815. <https://doi.org/10.1128/JB.02051-12>.
- Behr S, Fried L, Jung K. 2014. Identification of a novel nutrient-sensing histidine kinase/response regulator network in *Escherichia coli*. *J Bacteriol* 196:2023–2029. <https://doi.org/10.1128/JB.01554-14>.
- Behr S, Kristofcova I, Witting M, Breland EJ, Eberly AR, Sachs C, Schmitt-Kopplin P, Hadjifrangiskou M, Jung K. 2017. Identification of a high-affinity pyruvate receptor in *Escherichia coli*. *Sci Rep* 7:1388. <https://doi.org/10.1038/s41598-017-01410-2>.
- Pao SS, Paulsen IT, Saier MH. 1998. Major facilitator superfamily. *Microbiol Mol Biol Rev* 62:1–34.
- Kristofcova I, Vilhena C, Behr S, Jung K. 2017. BtsT: a novel and specific pyruvate/H⁺ symporter in *Escherichia coli*. *J Bacteriol* <https://doi.org/10.1128/JB.00599-17>.
- Fried L, Lassak J, Jung K. 2012. A comprehensive toolbox for the rapid construction of *lacZ* fusion reporters. *J Microbiol Methods* 91:537–543. <https://doi.org/10.1016/j.mimet.2012.09.023>.
- Shah D, Zhang Z, Khodursky A, Kaldalu N, Kurg K, Lewis K. 2006. Persisters: a distinct physiological state of *Escherichia coli*. *BMC Microbiol* 6:53. <https://doi.org/10.1186/1471-2180-6-53>.
- Bartlett MS, Gourse RL. 1994. Growth rate-dependent control of the *rrnB* P1 core promoter in *Escherichia coli*. *J Bacteriol* 176:5560–5564. <https://doi.org/10.1128/jb.176.17.5560-5564.1994>.
- Shan Y, Gandt AB, Rowe SE, Deisinger JP, Conlon BP, Lewis K. 2017. ATP-dependent persister formation in *Escherichia coli*. *mBio* 8:1–14. <https://doi.org/10.3391/mbi.2017.8.1.01>.
- Miroux B, Walker JE. 1996. Overproduction of proteins in *Escherichia coli*: mutant hosts that allow synthesis of some membrane proteins and globular proteins at high levels. *J Mol Biol* 260:289–298.
- Schlegel S, Genevaux P, de Gier JW. 2015. De-convoluting the genetic adaptations of *Escherichia coli* C41(DE3) in real time reveals how alleviating protein production stress improves yields. *Cell Rep* 10:1758–1766. <https://doi.org/10.1016/j.celrep.2015.02.029>.
- Santini CL, Bernadac A, Zhang M, Chanal A, Ize B, Blanco C, Wu LF. 2001. Translocation of jellyfish green fluorescent protein via the Tat system of *Escherichia coli* and change of its periplasmic localization in response to osmotic up-shock. *J Biol Chem* 276:8159–8164. <https://doi.org/10.1074/jbc.C000833200>.
- Lewis K. 2010. Persister cells. *Annu Rev Microbiol* 64:357–372. <https://doi.org/10.1146/annurev.micro.112408.134306>.
- Brauner A, Fridman O, Gefen O, Balaban NQ. 2016. Distinguishing between resistance, tolerance, and persistence to antibiotic treatment. *Nat Rev Microbiol* 14:320–330. <https://doi.org/10.1038/nrmicro.2016.34>.
- Behr S, Brameyer S, Witting M, Schmitt-Kopplin P, Jung K. 2017. Comparative analysis of LytS/LytTR-type histidine kinase/response regulator systems in γ -proteobacteria. *PLoS One* 12:e0182993. <https://doi.org/10.1371/journal.pone.0182993>.
- Oshima T, Aiba H, Masuda Y, Kanaya S, Sugiura M, Wanner BL, Mori H, Mizuno T. 2002. Transcriptome analysis of all two-component regulatory system mutants of *Escherichia coli* K-12. *Mol Microbiol* 46:281–291. <https://doi.org/10.1046/j.1365-2958.2002.03170.x>.
- Zhou L, Lei X-H, Bochner BR, Wanner BL. 2003. Phenotype microarray analysis of *Escherichia coli* K-12 mutants with deletions of all two-component systems. *J Bacteriol* 185:4956–4972. <https://doi.org/10.1128/JB.185.16.4956-4972.2003>.
- Ozbudak EM, Thattai M, Lim HN, Shraiman BI, Van Oudenaarden A. 2004. Multistability in the lactose utilization network of *Escherichia coli*. *Nature* 427:737–740. <https://doi.org/10.1038/nature02298>.
- Megerle JA, Fritz G, Gerland U, Jung K, Rädler JO. 2008. Timing and dynamics of single cell gene expression in the arabinose utilization system. *Biophys J* 95:2103–2115. <https://doi.org/10.1529/biophysj.107.127191>.
- Behr S, Heermann R, Jung K. 2016. Insights into the DNA-binding mechanism of a LytTR-type transcription regulator. *Biosci Rep* 36:e00326. <https://doi.org/10.1042/BSR20160069>.
- Kiviet DJ, Nghe P, Walker N, Boulineau S, Sunderlikova V, Tans SJ. 2014. Stochasticity of metabolism and growth at the single-cell level. *Nature* 514:376–379. <https://doi.org/10.1038/nature13582>.
- Levy S, Kafri M, Carmi M, Barkai N. 2011. The competitive advantage of a dual-transporter system. *Science* 334:1408–1412. <https://doi.org/10.1126/science.1207154>.

30. Kreth J, Lengeler JW, Jahreis K. 2013. Characterization of pyruvate uptake in *Escherichia coli* K-12. *PLoS One* 8:6–12. <https://doi.org/10.1371/journal.pone.0067125>.
31. Heermann R, Zeppenfeld T, Jung K. 2008. Simple generation of site-directed point mutations in the *Escherichia coli* chromosome using Red(R)/ET(R) Recombination. *Microb Cell Fact* 7:14. <https://doi.org/10.1186/1475-2859-7-14>.
32. Sambrook J, Fritsch EF, Maniatis T. 1989. *Molecular cloning: a laboratory manual*. Cold Spring Harbor Laboratory Press, New York, NY.
33. Inoue H, Nojima H, Okayama H. 1990. High-efficiency transformation of *Escherichia coli* with plasmids. *Gene* 96:23–28. [https://doi.org/10.1016/0378-1119\(90\)90336-P](https://doi.org/10.1016/0378-1119(90)90336-P).
34. Schindelin J, Arganda-Carreras I, Frise E, Kaynig V, Longair M, Pietzsch T, Preibisch S, Rueden C, Saalfeld S, Schmid B, Tinevez J-Y, White DJ, Hartenstein V, Eliceiri K, Tomancak P, Cardona A. 2012. Fiji: an open-source platform for biological-image analysis. *Nat Methods* 9:676–682. <https://doi.org/10.1038/nmeth.2019>.
35. Blattner FR, Plunkett G, Bloch CA, Perna NT, Burland V, Riley M, Collado-Vides J, Glasner JD, Rode CK, Mayhew GF, Gregor J, Davis NW, Kirkpatrick HA, Goeden MA, Rose DJ, Mau B, Shao Y. 1997. The complete genome sequence of *Escherichia coli* K-12. *Science* 277:1453–1462. <https://doi.org/10.1126/science.277.5331.1453>.
36. Thoma S, Schobert M. 2009. An improved *Escherichia coli* donor strain for diparental mating. *FEMS Microbiol Lett* 294:127–132. <https://doi.org/10.1111/j.1574-6968.2009.01556.x>.
37. Taylor RG, Walker DC, McInnes RR. 1993. *E. coli* host strains significantly affect the quality of small-scale plasmid DNA preparations used for sequencing. *Nucleic Acids Res* 21:1677–1678. <https://doi.org/10.1093/nar/21.7.1677>.
38. Cherepanov PP, Wackernagel W. 1995. Gene disruption in *Escherichia coli*: TcR and KmR cassettes with the option of FIp-catalyzed excision of the antibiotic-resistance determinant. *Gene* 158:9–14. [https://doi.org/10.1016/0378-1119\(95\)00193-A](https://doi.org/10.1016/0378-1119(95)00193-A).
39. Guzman LM, Belin D, Carson MJ, Beckwith J. 1995. Tight regulation, modulation, and high-level expression by vectors containing the arabinose pBAD promoter. *J Bacteriol* 177:4121–4130. <https://doi.org/10.1128/jb.177.14.4121-4130.1995>.
40. Tetsch L, Koller C, Haneburger I, Jung K. 2008. The membrane-integrated transcriptional activator CadC of *Escherichia coli* senses lysine indirectly via the interaction with the lysine permease LysP. *Mol Microbiol* 67: 570–583. <https://doi.org/10.1111/j.1365-2958.2007.06070.x>.

Chapter 5

Concluding discussion

Bacteria are living in constantly fluctuating environments in which they need to keep balance of important nutrients. For this purpose they evolved TCSs to sense various stimuli and respond by rapid alteration of gene expression.

Under carbon limitation, *E. coli* monitors extracellular concentration of pyruvate by the TCS BtsS/BtsR (previously named YehU/YehT) (**Chapter 2**). It was biochemically shown, that the HK BtsS is as a specific receptor for extracellular pyruvate. The activation of BtsS/BtsR leads to upregulation of the transporter BtsT (previously named YjiY). Transport assays with intact cells and proteolosomes demonstrated that BtsT is a specific and high-affinity pyruvate/H⁺ symporter (**Chapter 3**).

Overall the TCS BtsS/BtsR fine tunes pyruvate uptake by BtsT to match its demand. These results led us to formulate the biological role of the TCS BtsS/BtsR. Together with the TCS YpdA/YpdB, which also responds to extracellular pyruvate with different affinity, they contribute to a balanced physiological state of the individual cells within a population (**Chapter 4**).

5.1 Role of the TCS BtsS/BtsR upon carbon starvation

During exponential growth in a nutrient rich environment, *E. coli* can utilize many available carbon sources. To avoid the carbon accumulation in fast growing cells, several intermediates (mainly acetate and pyruvate) are released into the environment, by the process named as overflow metabolism or Crabtree effect (Paczia *et al.*, 2012). Acetate overflow especially occurs under conditions of high glucose concentrations in comparison to pyruvate overflow, which is mainly derived from amino acid metabolism. Extracellular accumulation of pyruvate or acetate is later on followed by a decline of an intracellular nutrient concentration in bacteria. To survive prolonged periods of starvation, *E. coli* coordinates nutrient scavenging and retrieves excreted by-products as alternative substrates (Peterson *et al.*, 2005). When *E. coli* depletes all available carbon sources, bacterial growth rate decelerates and soon enter a stationary phase.

E. coli grown in mixtures of amino acids consumes serine as the first amino acid (Prub *et al.*, 1994). It was shown that the TCS BtsS/BtsR responds to such depletion (**Chapter 2**). Concomitantly, the HK BtsS senses the extracellular pyruvate (step 1) and activates BtsR (step 2) to induce expression of *btsT* (step 3), which codes for the pyruvate transporter BtsT (steps 4,5). BtsT is therefore very advantageous for circumventing the carbon limitation by taking up pyruvate (step 6). Collectively these findings establish a comprehensive model of pyruvate sensing and transport by the TCS BtsS/BtsR in *E. coli* (steps 1-6 in **Fig. 5.1**).

The regulatory role at the transition from exponential to stationary phase has been also described for the LytS/LytTR-like TCS AgrC/AgrA in *Staphylococcus aureus*. To adapt to an environment that does not support anymore a fast growth, bacteria can autoactivate synthesis of signaling molecules (AIP). After a threshold concentration of AIP in the environment, bacteria will regulate expression of virulence genes by the TCS AgrC/AgrA (Novick and Geisinger, 2008).

In addition, the growth of *E. coli* is limited not just by carbon, but also nitrogen and phosphorus. The ratio between all three elements is different in each environment. For all these types of starvation, *E. coli* developed scavenging strategies. However, if scavenging is insufficient, bacteria enter the stationary phase (Peterson *et al.*, 2005). The regulatory role

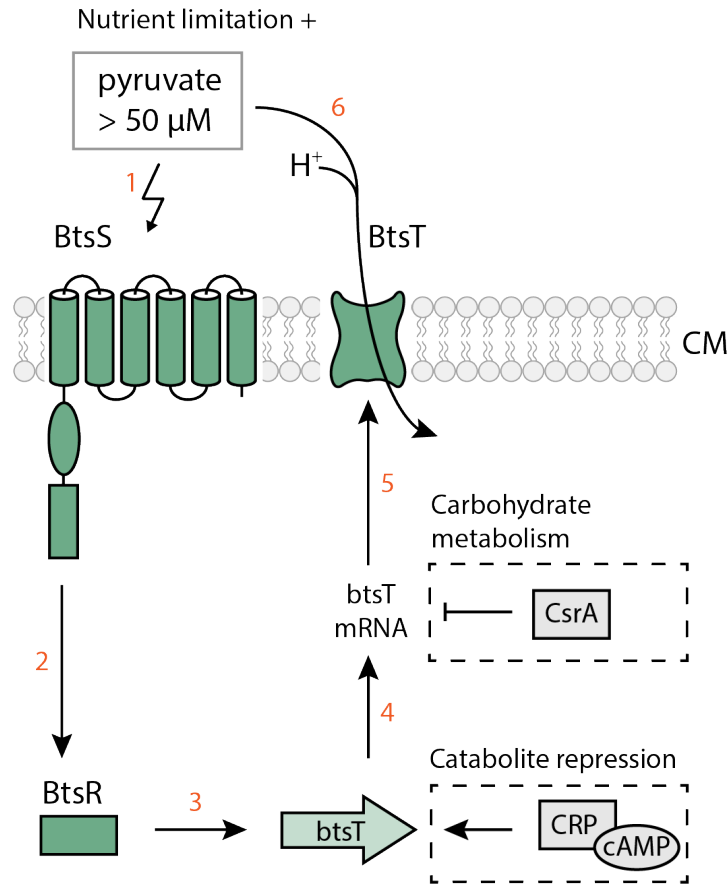


Figure 5.1: Fine-tuning of pyruvate levels in *E. coli* by BtsS/BtsR two-component system. The scheme summarizes the perception of pyruvate by BtsS under nutrient limitation (⚡), signal transduction within the TCS BtsS/BtsR, an influence of global regulators CsrA and CRP, and a symport of pyruvate/H⁺ by BtsT. CM, cytoplasmic membrane.

of TCSs during nutrient scavenging is well described. A TCS PhoR/PhoB surveys inorganic phosphate levels by a Pst transporter system. Upon diminished activity of the Pst transporter, the TCS PhoR/PhoB activates sRNA transcription to stimulate translation of *rpoS* mRNA (Wanner, 1990). RpoS is a master regulator of general stress response, which regulates under direct or indirect control up to 10% of the *E. coli* genes (Weber *et al.*, 2005). On the other hand the TCS NtrB/NtrC analyzes the nutrient status of *E. coli* through the intracellular metabolite glutamine and thus monitors the levels of the nitrogen starvation. However, if and how the TCS NtrB/NtrC regulates RpoS is unclear (Peterson *et al.*, 2005).

It has been shown that the TCS BtsS/BtsR responds to carbon limitation (**Chapter 2**) however how it surveys the carbon levels is unknown. It was proposed that the TCS

BtsS/BtsR senses a low intracellular serine concentration since serine is able to delay response to activate promoter of *btsT* in growing *E. coli*. However, the effect was shown to be indirect by *in vivo btsT* expression studies under nutrient-limiting conditions (**Chapter 2**). Furthermore, it remains unclear if the TCS BtsS/BtsR serves just for pyruvate uptake or also initiate the stationary phase if carbon scavenging is insufficient for the cells. The possibility that BtsS/BtsR affects transcription of *rpoS* should be addressed in order to fully understand the role of the TCS BtsS/BtsR upon carbon starvation in *E. coli*.

5.2 Function of the histidine kinase BtsS

Based on biochemical studies, it has been revealed that BtsS is a high-affinity sensor for pyruvate (**Chapter 2**). Pyruvate binding has been observed to an external side of the transmembrane domain of BtsS. The pyruvate binding to BtsS is very specific with a dissociation constant of 58 μM .

These protein-ligand interaction results have been obtained by a rapid method differential radial capillary action of ligand assay (DRaCALA) (Roelofs *et al.*, 2011). Since BtsS is a membrane protein, DRaCALA is a very advantageous method enabling usage of membrane vesicles with overproduced BtsS, with no requirement of further protein solubilization.

The identification of pyruvate as a substrate sensed by BtsS may bring insights into stimuli perceived by the whole family of LytS-like HKs. Recently, another LytS/LytTR-like TCS, LytS/LytT in *B. subtilis*, has also been shown to be essential for growth on pyruvate (van den Esker *et al.*, 2017). DRaCALA can be as well used for proving the pyruvate binding to the HK LytS in *B. subtilis*. It is worth to mention that the TCS LytS/LytT is proposed to have similar function as the TCS BtsS/BtsR. In nutrient rich environments both *B. subtilis* and *E. coli* release pyruvate into the environment, in the process of overflow metabolism. It is possible that pyruvate receptors in bacteria monitor the external pyruvate levels and such bacteria reflect an available growth condition. Additionally, it is suggested that LytT regulates *ysbA* transcription to produce YsbA, a putative transporter for pyruvate (van den Esker *et al.*, 2017).

The putative binding site for pyruvate in BtsS was not yet elucidated (**Chapter 2**). Actually, pyruvate was once copurified and crystallized with an extracytoplasmic domain

of KinD in *B. subtilis* however its relevance was not yet understood (Wu *et al.*, 2013). A comparison of the structures of KinD in complex with pyruvic acid to a predicted structure of BtsS did not detect any similarities (unpublished observation). Further research should concentrate on determining the pyruvate binding site of BtsS.

In addition, the understanding of how BtsS perceives external pyruvate might help to gain insights into how BtsS generates an intracellular response. Up to now *in vitro* phosphorylation of BtsS has not been observed (Kraxenberger *et al.*, 2012). The reason why is often attributed to an incomplete ATP-binding domain of BtsS lacking amino acids that are usually conserved in other LytS-like HKs in *E. coli* (BtsS lacks the first region of characteristic DxGxG and GxG motif for nucleotide binding) (Kraxenberger *et al.*, 2012). Therefore, it has been hypothesized that the signalling within the TCS BtsS/BtsR is mediated by protein-protein interactions. Indeed it was proved that BtsS interacts with the RR BtsR by *in vivo* protein-protein interaction assays (Behr *et al.*, 2014). For some TCSs, e.g. AmiC/AmiR in *P. aeruginosa*, the signal transduction is achieved via a ligand-induced release of the RR AmiR rather than usual phosphorylation (O’Hara *et al.*, 1999). Therefore, it could be speculated, that also pyruvate has an effect on the strength of protein-protein interactions between BtsS and BtsR, and thus we could get further insights into the signal transduction within the TCS BtsS/BtsR. A ligand influencing the regulatory interplay has already been reported in *E. coli*. Here, lysine is transferred from a co-sensor LysP to a pH sensor CadC and thus induces lysine-dependent adaptation under acidic stress (Rauschmeier *et al.*, 2014).

Last but not least, the HK BtsS might have another ligand binding site. It is possible that a ligand binds to an intracellular site of BtsS, which might answer the question of how the TCS BtsS/BtsR monitors levels of carbon starvation. Such dual sensor has already been observed in *E. coli* to balance extracellular and intracellular K⁺ concentration (Schramke *et al.*, 2016). However, for this purpose the method DRaCALA is not suitable. A limitation of DRaCALA is the requirement of radioactive ligand, which does not enable rapid screening of unknown ligands related to the stationary phase or carbon metabolism. For this reason, e.g. thermofluor-based binding assay (Ericsson *et al.*, 2006) should be used to identify if the HK BtsS also contains the intracellular binding site for a specific ligand. It has been proposed that a GAF domain of BtsS might be involved in such binding, since in other proteins the GAF is capable to bind amino acids, ions and nucleotides (Zoraghi *et al.*, 2004).

5.3 Importance of the pyruvate transporter BtsT

The transporter BtsT has been extensively investigated for its transport activity (**Chapter 3**). Based on the transport studies in intact cells, BtsT is a specific pyruvate transporter with an apparent K_m of $16 \mu\text{M}$. Reconstitution of a purified BtsT into *E. coli* proteoliposomes revealed that BtsT functions as a pyruvate/ H^+ symporter.

BtsT represents the first pyruvate transporter to be identified in *E. coli*. The characterization of other pyruvate transporters in *E. coli* might be tricky since pyruvate is located in a central node of a carbon metabolism and its cellular concentration is tightly controlled (Vemuri *et al.*, 2006). Pyruvate plays an important role in amino acid catabolism (**Fig. 5.2**). During aerobic growth, pyruvate is converted to acetyl-CoA, which enters tricarboxylic acid (TCA) cycle. In addition, pyruvate is a precursor for amino acids (Ala, Ile, Leu and Val). Under anaerobic conditions, pyruvate is converted to lactate and ethanol.

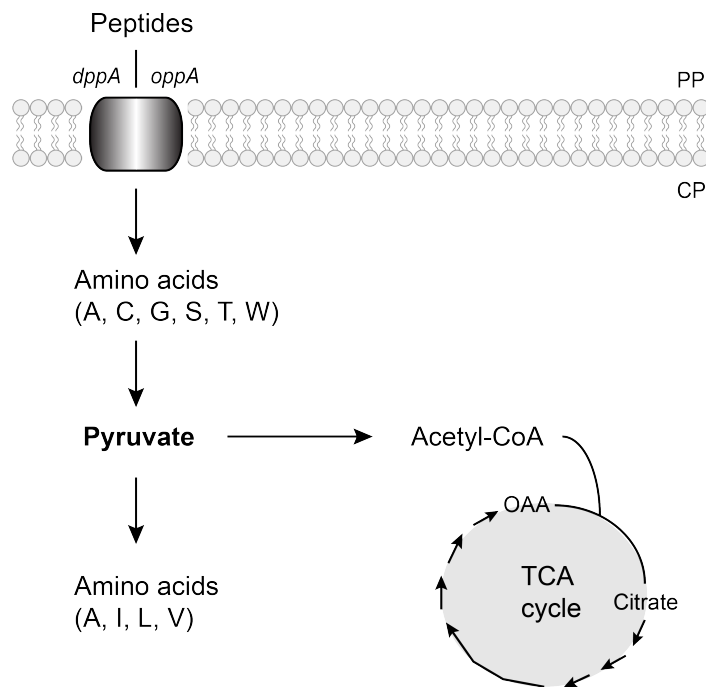


Figure 5.2: Central role of pyruvate in *E. coli* carbon metabolism. Figure summarizes import of peptides by *E. coli* into the cytoplasm, their degradation into amino acids. Amino acids alanine, cysteine, glycine, serine, threonine and tryptophan are directly converted to pyruvate. Under aerobic conditions, pyruvate is degraded to acetyl-CoA, which enters the tricarboxylic acid cycle. Pyruvate is also a precursor for synthesis of amino acids: alanine, isoleucine, leucine and valine. OAA, oxaloacetate, PP, periplasm, CP, cytoplasm.

Pyruvate transport systems have been predicted since it was shown that bacteria excrete and then retrieve pyruvate under several growth conditions (Kodaki *et al.*, 1981). Considering that pyruvate is an acid of pK_a of 2.5, under physiological conditions the deprotonated molecule cannot diffuse through a bacterial membrane and requires an active transporter. Transport assays in intact cells of *E. coli* claimed that there are active transporters however without their further characterization (Lang *et al.*, 1987). Later on, the knowledge about pyruvate transporters have been expanded by a research suggesting two importers and one exporter in *E. coli* yet also lacking their identification (Kreth *et al.*, 2013).

Since BtsT is the pyruvate transporter, it could help to identify other transporters in *E. coli*. A mutation of BtsT can decrease the pool of pyruvate inside *E. coli* and thus enable easier identification of other systems. Further studies of BtsT should also be focused on the elucidation of the pyruvate binding site, that might help to bioinformatically find possible candidates of other pyruvate transporters.

In addition, BtsT contains putative 18 TM domains and it is unknown which contribute for pyruvate uptake. Currently, we can only speculate that the two conserved 5-TM repeat units in members of the CstA family are essential for this function (Vastermark *et al.*, 2014) (**Fig. 5.3**). Furthermore, in the first TM of the second repeat has been identified a motif (CG-x(2)-SG) in the CstA family, which might be essential for function of these transporters (Vastermark *et al.*, 2014). BtsT contains 8 additional TMs, which can have other structural and/or regulatory function.

It is worth to mention that pyruvate transporters are of increasing physiological importance, mainly in biological fitness and virulence of *Enterobacteriaceae*. In *Yersinia pseudotuberculosis*, the high rate of glycolysis induces pyruvate overflow due to a metabolic bottleneck. It is suggested that high rates of nutrient uptake of easily metabolizable compounds, like pyruvate, provides a competitive advantage with other organisms in the gut environment (Bucker *et al.*, 2014). However, the pyruvate exporter or importer in *Y. pseudotuberculosis* has not yet been elucidated.

Even metabolic engineering is focusing its attention on pyruvate in order to achieve optimized metabolite production in *E. coli*, *C. glutamicum* or *B. subtilis* (Sauer and Eikmanns, 2005). The identification of carbon monocarboxylic acid transporters e.g. for pyruvate might gain further insights into metabolic adjustments within the PEP-pyruvate-oxaloacetate node.

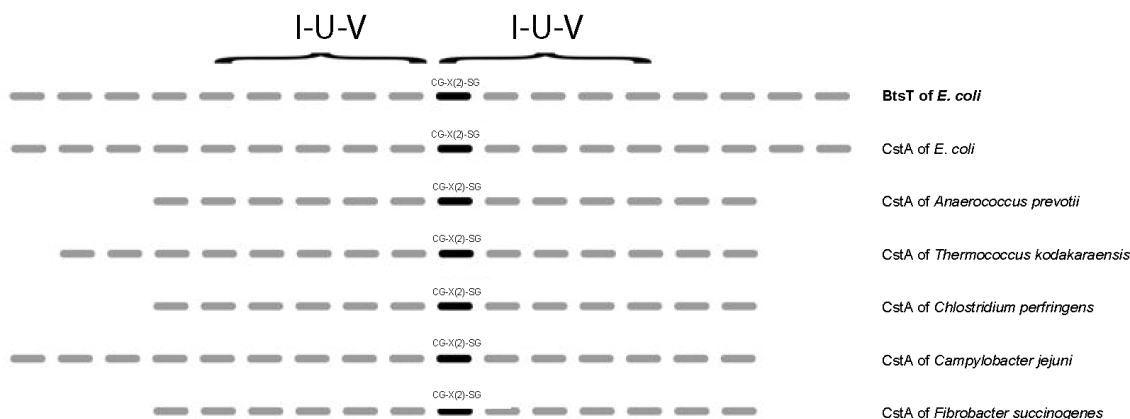


Figure 5.3: Topological prediction of BtsT in *E. coli* and CstA homologues in 6 different bacterial species. The CstA family exhibit 5 TM repeat unit and N- or C- terminal TMs. The I, U, V labels physically look like mentioned letters in 3D structures of APC superfamily proteins and refer to TMs 1, 2-3, 4-5, respectively, in each repeat unit. The location of the CG-x(2)-SG motif is shown. Adopted from (Vastermark *et al.*, 2014).

Indeed, the pyruvate transporter has been identified and characterized in *C. glutamicum*. Biochemical studies revealed that monocarboxylic acid transporter MctC actively take up acetate, propionate and with low affinity pyruvate ($K_{0.5}$ 250 μ M) (Jolkver *et al.*, 2009). For *B. subtilis* nothing is known about pyruvate transport. The function of pyruvate transporter is suggested for YsbA, however, the transporter still awaits its characterization (van den Esker *et al.*, 2017). Nonetheless, to control the carbon flux between the glycolysis and the TCA cycle, further insights into the regulation and characterization of the enzymes and other relevant proteins of the mentioned node are still required.

5.4 Role of the TCS BtsS/BtsR

The TCS BtsS/BtsR plays a role in a nutrient sensing network of *E. coli* and in host colonization.

The TCS BtsS/BtsR forms a functional network with the TCS YpdA/YpdB, which also responds to pyruvate but with a lower affinity (Behr *et al.*, 2014). Single-cell analysis of the activation of their corresponding target genes, *btsT* and *yhjX*, respectively, showed cell-to-cell variability. Comparing the wild-type strain with the *btsSR ypdAB* mutant revealed differences under two metabolically modulated conditions. The *btsSR ypdAB* mutant was

impaired in protein production and had higher percentage of persister cells in a growing population (**Chapter 4**). It suggests, that the mentioned nutrient sensing network in *E. coli* maintain the optimal carbon supply for each individual cell. The similar mechanism is also proposed for other two TCSs. The RRs NarL and NarP regulate two operons depending on the nitrate concentration (Wang and Gunsalus, 2003). Here, a dual adjustment is used to fastly react to environmental changes in levels of nitrate and formate.

The importance of the TCS BtsS/BtsR for pathogenesis has been observed in uropathogenic *E. coli* (UPEC) that colonizes a mammalian bladder. This pathogen accounts for over 85% of urinary-tract infection worldwide (Foxman, 2010). In the UPEC cystitis isolate UTI89, a *btsS/btsR* mutant failed to induce expression of *btsT* however in the wild-type strain *btsT* was transiently expressed. In addition, it was elucidated that BtsS/BtsR is active during both the acute and chronic stages of urinary tract infections (**Chapter 2**).

Actually the bladder of mammals is a nutritionally demanding environment that also contains pyruvate (Foxman, 2010). Metabolic breakdown products, mainly amino acids are degraded to pyruvate or other TCA cycle intermediates (**Fig. 5.2**). Pyruvate is further degraded to acetyl-CoA, which enters the TCA cycle. Both the TCA cycle as well as gluconeogenesis have been shown to be required for UPEC *in vivo* fitness (Foxman, 2010). Therefore, pyruvate plays a central role in UPEC metabolism. It seems like that the TCS BtsS/BtsR responds to pyruvate fluctuations and plays a role in promoting the infections process.

Furthermore, *btsT* was expressed in avian pathogenic *E. coli* (APEC) during the infection in chicken liver and spleen (Tuntufye *et al.*, 2012). This pathogen leads to extraintestinal infections in poultry that cause several diseases known as colibacillosis. During infection, APEC must coordinate genes relevant in virulence, metabolism and regulation. Studies focusing on the influence of BtsS/BtsR in APEC should be carried out to elucidate its importance in pathogenesis.

Last but not least, pyruvate sensing might provide also an advantage in an enteric environment, in intestines. This environment contains high amounts of amino acids (proline, alanine and serine), but also pyruvate (Nagata *et al.*, 2003; Nagata *et al.*, 2007). Therefore, monitoring pyruvate levels can propagate a succesful host colonization of enteric bacteria, e.g. *E. coli*, *S. typhimurium* and *Shigella*, in intestines (Bearson *et al.*, 1997).

5.5 Conclusion and outlook

In this thesis, it was demonstrated how *E. coli* senses and transports pyruvate. Based on several *in vivo* and *in vitro* studies, it was discovered that pyruvate is recognized by the high-affinity HK BtsS of the TCS BtsS/BtsR. Furthermore, it was found out that the target gene of this TCS, BtsT, is a specific pyruvate/H⁺ symporter. Under nutrient limitation, such pyruvate sensing and transport are crucial in carbon scavenging before entry into the stationary phase. Lastly, it was identified that the individual cells use the TCS BtsS/BtsR to optimize their carbon requirements within the population and thus withstand upcoming metabolic stress.

Nevertheless, there are still open questions for future research. Solved structures of BtsS and BtsT, e.g. by 3D-crystallization might bring insights into structural arrangements of pyruvate binding and elucidate the function of other HKs of the LytS family or other transporters of the CstA family, respectively. It is also required to address if the HK BtsS contains an additional binding site for carbon compound and thus monitors carbon limitation. Last but not least, the function of the TCS YpdA/YpdB components should be addressed to fully understand the nutrient sensing network of the TCS BtsS/BtsR and the TCS YpdA/YpdB.

References (Chapter 1. and 4.)

- Allen, B. L., Gerlach, G. F., and Clegg, S. (1991). Nucleotide sequence and functions of *mrk* determinants necessary for expression of type 3 fimbriae in *Klebsiella pneumoniae*. *J Bacteriol.*, 173(2):916–920.
- Alm, E., Huang, K., and Arkin, A. (2006). The evolution of two-component systems in bacteria reveals different strategies for niche adaptation. *PLoS Comput. Biol.*, 2(11):1329–1342.
- Anantharaman, V. and Aravind, L. (2003). Application of comparative genomics in the identification and analysis of novel families of membrane-associated receptors in bacteria. *BMC Genomics*, 4(1):34.
- Anantharaman, V., Balaji, S., and Aravind, L. (2006). The signaling helix: a common functional theme in diverse signaling proteins. *Biol. direct*, 1:25.
- Anetzberger, C., Schell, U., and Jung, K. (2012). Single cell analysis of *Vibrio harveyi* uncovers functional heterogeneity in response to quorum sensing signals. *BMC Microbiol.*, 12(1):209.
- Barakat, M., Ortet, P., and Whitworth, D. E. (2011). P2CS: a database of prokaryotic two-component systems. *Nucleic Acids Res.*, 39:771–776.
- Barrett, J. F. and Hoch, J. A. (1998). Two-component signal transduction as a target for microbial anti-infective therapy. *Antimicrob. Agents Chemother.*, 42(7):1529–1536.
- Bearson, S., Bearson, B., and Foster, J. W. (1997). Acid stress responses in enterobacteria. *FEMS Microbiol. Lett.*, 147(2):173–180.

- Behr, S., Brameyer, S., Witting, M., Schmitt-Kopplin, P., and Jung, K. (2017). Comparative analysis of LytS/LytTR-type histidine kinase/response regulator systems in γ -proteobacteria. *PLoS One*, 12(8):1–14.
- Behr, S., Fried, L., and Jung, K. (2014). Identification of a novel nutrient-sensing histidine kinase/response regulator network in *Escherichia coli*. *J. Bacteriol.*, 196(11):2023–2029.
- Behr, S., Heermann, R., and Jung, K. (2016). Insights into the DNA-binding mechanism of a LytTR-type transcription regulator. *Biosci. Rep.*, 36(2):e00326.
- Beier, D. and Gross, R. (2006). Regulation of bacterial virulence by two-component systems. *Curr. Opin. Microbiol.*, 9(2):143–152.
- Boor, K. J. (2006). Bacterial stress responses: What doesn't kill them can make them stronger. *PLoS Biol.*, 4(1):0018–0020.
- Brown, P. K., Dozois, C. M., Nickerson, C. a., Zuppardo, A., Terlonge, J., and Curtiss, R. (2001). MrA, a novel regulator of curli (AgF) and extracellular matrix synthesis by *Escherichia coli* and *Salmonella enterica* serovar Typhimurium. *Mol. Microbiol.*, 41(2):349–363.
- Brunskill, E. W. and Bayles, K. W. (1996). Identification and molecular characterization of a putative regulatory locus that affects autolysis in *Staphylococcus aureus*. *J. Bacteriol.*, 178(3):611–618.
- Bucker, R., Heroven, A. K., Becker, J., Dersch, P., and Wittmann, C. (2014). The pyruvate-tricarboxylic acid cycle node. A focal point of virulence control in the enteric pathogen *Yersinia pseudotuberculosis*. *J. Biol. Chem.*, 289(43):30114–30132.
- Capra, E. J. and Laub, M. T. (2012). The evolution of two-component signal transduction systems. *Annu Rev Microbiol.*, 66:325–347.
- Checroun, C. and Gutierrez, C. (2004). σ s-dependent regulation of *yehZYXW*, which encodes a putative osmoprotectant ABC transporter of *Escherichia coli*. *FEMS Microbiol. Lett.*, 236(2):221–226.

- Deretic, V., Dikshit, R., Konyecsni, W. M., Chakrabarty, A. M., and Misra, T. K. (1989). The *algR* gene, which regulates mucoidy in *Pseudomonas aeruginosa*, belongs to a class of environmentally responsive genes. *J. Bacteriol.*, 171(3):1278–1283.
- Diep, D. B., Havarstein, L. S., and Nes, I. F. (1996). Characterization of the locus responsible for the bacteriocin production in *Lactobacillus plantarum* C11. *J. Bacteriol.*, 178(15):4472.
- Ericsson, U. B., Hallberg, B. M., DeTitta, G. T., Dekker, N., and Nordlund, P. (2006). Thermofluor-based high-throughput stability optimization of proteins for structural studies. *Anal. Biochem.*, 357(2):289–298.
- Fabret, C., Feher, V. A., and Hoch, J. A. (1994). Two-component signal transduction in *Bacillus subtilis*: How one organism sees its world. *Anal. Biochem.*, 217(2):220–230.
- Foxman, B. (2010). The epidemiology of urinary tract infection. *Nat Rev Urol*, 7(12):653–660.
- Fried, L., Behr, S., and Jung, K. (2013). Identification of a target gene and activating stimulus for the YpdA/YpdB histidine kinase/response regulator system in *Escherichia coli*. *J Bacteriol*, 195(4):807–15.
- Galperin, M. Y. (2005). A census of membrane-bound and intracellular signal transduction proteins in bacteria: bacterial IQ, extroverts and introverts. *BMC Microbiol.*, 5:35.
- Galperin, M. Y. (2006). Structural classification of bacterial response regulators: diversity of output domains and domain combinations. *J. Bacteriol.*, 188(12):4169–4182.
- Gao, R. and Stock, A. M. (2009). Biological insights from structures of two-component proteins. *Annu Rev Microbiol.*, 63:133–154.
- Garai, P., Lahiri, A., Ghosh, D., Chatterjee, J., and Chakravorty, D. (2015). Peptide utilizing carbon starvation gene *yjiY* is required for flagella mediated infection caused by *Salmonella*. *Microbiology*, 162:100–116.
- Gotoh, Y., Eguchi, Y., Watanabe, T., Okamoto, S., Doi, A., and Utsumi, R. (2010). Two-component signal transduction as potential drug targets in pathogenic bacteria. *Curr. Opin. Microbiol.*, 13(2):232–239.

- Grebe, T. W. and Stock, J. B. (1999). The histidine protein kinase superfamily. *Adv. Microb. Physiol.*, 41:139–227.
- Gushchin, I., Melnikov, I., Polovinkin, V., Ishchenko, A., Yuzhakova, A., Buslaev, P., Bourenkov, G., Grudinin, S., Round, E., Balandin, T., Borshchevskiy, V., Willbold, D., Leonard, G., Büldt, G., Popov, A., and Gordeliy, V. (2017). Mechanism of transmembrane signaling by sensor histidine kinases. *Science*, 356(1043).
- Haneburger, I., Fritz, G., Jurkschat, N., Tetsch, L., Eichinger, A., Skerra, A., Gerland, U., and Jung, K. (2012). Deactivation of the *E. coli* pH stress sensor CadC by cadaverine. *J. Mol. Biol.*, 424(1-2):15–27.
- Heermann, R. and Jung, K. (2010). Stimulus perception and signaling in histidine kinases. In Krämar, R. and Jung, K., editors, *Bacterial signalling*, pages 135–161. WILEY-VCH.
- Hemm, M. R., Paul, B. J., Schneider, T. D., Storz, G., and Rudd, K. E. (2008). Small membrane proteins found by comparative genomics and ribosome binding site models. *Mol. Microbiol.*, 70(6):1487–1501.
- Henry, J. and Crosson, S. (2011). Ligand binding PAS domains in a genomic, cellular, and structural context. *Annu Rev Microbiol*, 65:261–286.
- Huhne, K., Axelsson, L., Holck, A., and Krockel, L. (1996). Analysis of the sakacin P gene cluster from *Lactobacillus sake* Lb674 and its expression in sakacin-negative *Lb. sake* strains. *Microbiology*, 142(6):1437–1448.
- Jolkver, E., Emer, D., Ballan, S., Krämer, R., Eikmanns, B. J., and Marin, K. (2009). Identification and characterization of a bacterial transport system for the uptake of pyruvate, propionate, and acetate in *Corynebacterium glutamicum*. *J. Bacteriol.*, 191(3):940–948.
- Jung, K., Fried, L., Behr, S., and Heermann, R. (2012). Histidine kinases and response regulators in networks. *Curr Opin Microbiol*, 15(2):118–24.
- Kodaki, T., Murakami, H., Taguchi, M., Izui, K., and Katsuki, H. (1981). Stringent control of intermediary metabolism in *Escherichia coli*: pyruvate excretion by cells grown on succinate. *J Biochem.*, 90(5):1437–1444.

- Krämer, R. (1999). Multiple roles of prokaryotic cell membranes. In Lengeler, J., Drews, G., and Schlegel, H., editors, *Biology of the prokaryotes*, pages 68–87. London: Blackwell Science Inc.
- Kraxenberger, T., Fried, L., Behr, S., and Jung, K. (2012). First insights into the unexplored two-component system YehU/YehT in *Escherichia coli*. *J Bacteriol*, 194(16):4272–4284.
- Kreikemeyer, B., Boyle, M. D. P., Buttaro, B. A., Heinemann, M., and Podbielski, A. (2001). Group A streptococcal growth phase-associated virulence factor regulation by a novel operon (Fas) with homologies to two-component-type regulators requires a small RNA molecule. *Mol. Microbiol.*, 39(2):392–406.
- Krell, T., Lacal, J., Busch, A., Silva-Jiménez, H., Guazzaroni, M.-E., and Ramos, J. L. (2010). Bacterial sensor kinases: diversity in the recognition of environmental signals. *Annu. Rev. Microbiol.*, 64:539–559.
- Kreth, J., Lengeler, J. W., and Jahreis, K. (2013). Characterization of pyruvate uptake in *Escherichia coli* K-12. *PLoS One*, 8(6):6–12.
- Lang, V. J., Leystra-lantz, C., and Cook, R. A. (1987). Characterization of the specific pyruvate transport system in *Escherichia coli* K-12. *J. Bacteriol.*, 169(1):380–385.
- Lyon, G. J., Mayville, P., Muir, T. W., and Novick, R. P. (2000). Rational design of a global inhibitor of the virulence response in *Staphylococcus aureus*, based in part on localization of the site of inhibition to the receptor-histidine kinase, AgrC. *Proc. Natl. Acad. Sci. U. S. A.*, 97(24):13330–13335.
- Mascher, T. (2014). Bacterial (intramembrane-sensing) histidine kinases: signal transfer rather than stimulus perception. *Trends Microbiol.*, 22(10):559–565.
- Mizuno, T. (1997). Compilation of all genes encoding two-component phosphotransfer signal transducers in the genome of *Escherichia coli*. *DNA Res.*, 4(2):161–168.
- Nagata, K., Nagata, Y., Sato, T., Fujino, M. A., Nakajima, K., and Tamura, T. (2003). L-serine, D- and L-proline and alanine as respiratory substrates of *Helicobacter pylori*:

- correlation between *in vitro* and *in vivo* amino acid levels. *Microbiology*, 149(8):2023–2030.
- Nagata, Y., Sato, T., Enomoto, N., Ishii, Y., Sasaki, K., and Yamada, T. (2007). High concentrations of D-amino acids in human gastric juice. *Amino Acids*, 32(1):137–140.
- Nikolskaya, A. N. and Galperin, M. Y. (2002). A novel type of conserved DNA-binding domain in the transcriptional regulators of the AlgR/AgrA/LytR family. *Nucleic Acids Res.*, 30(11):2453–9.
- Njoroge, J. and Sperandio, V. (2009). Jamming bacterial communication: new approaches for the treatment of infectious diseases. *EMBO Mol. Med.*, 1(4):201–210.
- Novick, R. P. (2003). Autoinduction and signal transduction in the regulation of staphylococcal virulence. *Mol. Microbiol.*, 48(6):1429–1449.
- Novick, R. P. and Geisinger, E. (2008). Quorum sensing in staphylococci. *Annu Rev Genet*, 42:541–564.
- Novick, R. P., Projan, S. J., Kornblum, J., Ross, H. F., Ji, G., Kreiswirth, B., Vandenesch, F., Moghazeh, S., and Novick, R. P. (1995). The *agr* P2 operon: an autocatalytic sensory transduction system in *Staphylococcus aureus*. *Mol. Gen. Genet. MGG*, 248(4):446–458.
- O’Hara, B. P., Norman, R. A., Wan, P. T. C., Roe, S. M., Barrett, T. E., Drew, R. E., and Pearl, L. H. (1999). Crystal structure and induction mechanism of AmiC-AmiR: A ligand-regulated transcription antitermination complex. *EMBO J.*, 18(19):5175–5186.
- O’Keeffe, T., Hill, C., and Ross, R. P. (1999). Characterization and heterologous expression of the genes encoding enterocin A production, immunity, and regulation in *Enterococcus faecium* DPC1146. *Appl. Environ. Microbiol.*, 65(4):1506–1515.
- Okkotsu, Y., Little, A. S., and Schurr, M. J. (2014). The *Pseudomonas aeruginosa* AlgZR two-component system coordinates multiple phenotypes. *Front. Cell. Infect. Microbiol.*, 4(June):82.

- Paczia, N., Nilgen, A., Lehmann, T., Gätgens, J., Wiechert, W., and Noack, S. (2012). Extensive exometabolome analysis reveals extended overflow metabolism in various microorganisms. *Microb. Cell Fact.*, 11(1):122.
- Pestova, E. V., Håvarstein, L. S., and Morrison, D. A. (1996). Regulation of competence for genetic transformation in *Streptococcus pneumoniae* by an auto-induced peptide pheromone and a two-component regulatory system. *Mol. Microbiol.*, 21(4):853–862.
- Peterson, C. N., Mandel, M. J., and Silhavy, T. J. (2005). *Escherichia coli* starvation diets: essential nutrients weigh in distinctly. 187(22):7549–7553.
- Prub, B. M., Nelms, J. M., Park, C., and Wolfe, A. J. (1994). Mutations in NADH:ubiquinone oxidoreductase of *Escherichia coli* affect growth on mixed amino acids. *J. Bacteriol.*, 176(8):2143–2150.
- Quadri, L. E. N., Kleerebezem, M., Kuipers, O. P., De Vos, W. M., Roy, K. L., Vederas, J. C., and Stiles, M. E. (1997). Characterization of a locus from *Carnobacterium piscicola* LV17B involved in bacteriocin production and immunity: evidence for global inducer-mediated transcriptional regulation. *J. Bacteriol.*, 179(19):6163–6171.
- Rasmussen, J. J., Vegge, C. S., Frøkiær, H., Howlett, R. M., Krogfelt, K. A., Kelly, D. J., and Ingmer, H. (2013). *Campylobacter jejuni* carbon starvation protein A (CstA) is involved in peptide utilization, motility and agglutination, and has a role in stimulation of dendritic cells. *J. Med. Microbiol.*, 62(Pt 8):1135–1143.
- Rauschmeier, M., Schüppel, V., Tetsch, L., and Jung, K. (2014). New insights into the interplay between the lysine transporter LysP and the pH sensor CadC in *Escherichia coli*. *J. Mol. Biol.*, 426(1):215–229.
- Roelofs, K. G., Wang, J., Sintim, H. O., and Lee, V. T. (2011). Differential radial capillary action of ligand assay for high-throughput detection of protein-metabolite interactions. *Proc. Natl. Acad. Sci. U. S. A.*, 108(37):15528–33.
- Rumbaugh, K. P., Diggle, S. P., Watters, C. M., Ross-Gillespie, A., Griffin, A. S., and West, S. A. (2009). Quorum sensing and the social evolution of bacterial virulence. *Curr. Biol.*, 19(4):341–345.

- Salis, H., Tamsir, A., and Voigt, C. (2009). Engineering bacterial signals and sensors. *Contrib. Microbiol.*, 16:194–225.
- Sauer, U. and Eikmanns, B. J. (2005). The PEP-pyruvate-oxaloacetate node as the switch point for carbon flux distribution in bacteria. *FEMS Microbiol. Rev.*, 29(4):765–794.
- Schramke, H., Laermann, V., Tegetmeyer, H. E., Brachmann, A., Jung, K., and Altendorf, K. (2017). Revisiting regulation of potassium homeostasis in *Escherichia coli*: the connection to phosphate limitation. *Microbiologyopen*, 6(3):1–16.
- Schramke, H., Tostevin, F., Heermann, R., Gerland, U., and Jung, K. (2016). A dual-sensing receptor confers robust cellular homeostasis. *Cell Rep.*, 16(1):213–221.
- Schultz, J. E. and Matin, A. (1991). Molecular and functional characterization of a carbon starvation gene of *Escherichia coli*. *J. Mol. Biol.*, 218(1):129–140.
- Schumann, W. (2012). Thermosensory stems in eubacteria. In López-Larrea, C., editor, *Sensing in nature*, pages 1–16. Springer US, New York, NY.
- Shimizu, T., Ba-Thein, W., Tamaki, M., and Hayashi, H. (1994). The *virR* gene, a member of a class of two-component response regulators, regulates the production of perfringolysin O, collagenase, and hemagglutinin in *Clostridium perfringens*. *J. Bacteriol.*, 176(6):1616–1623.
- Singh, D., Chang, S.-J., Lin, P.-H., Averina, O. V., Kaberdin, V. R., and Lin-Chao, S. (2009). Regulation of ribonuclease E activity by the L4 ribosomal protein of *Escherichia coli*. *Proc. Natl. Acad. Sci. U. S. A.*, 106(3):864–869.
- Snider, J., Gutsche, I., Lin, M., Baby, S., Cox, B., Butland, G., Greenblatt, J., Emili, A., and Houry, W. A. (2006). Formation of a distinctive complex between the inducible bacterial lysine decarboxylase and a novel AAA⁺ ATPase. *J. Biol. Chem.*, 281(3):1532–1546.
- Staron, A., Sofia, H. J., Dietrich, S., Ulrich, L. E., Liesegang, H., and Mascher, T. (2009). The third pillar of bacterial signal transduction: classification of the extracytoplasmic function (ECF) σ factor protein family. *Mol. Microbiol.*, 74(3):557–581.

- Stewart, R. C. (2010). Protein histidine kinases: assembly of active site and their regulation in signaling pathways. *Curr Opin Microbiol*, 13(2):133–141.
- Stock, A. M., Robinson, V. L., and Goudreau, P. N. (2000). Two-component signal transduction. *Annu Rev Biochem*, 69:183–215.
- Thakor, H., Nicholas, S., Porter, I. M., Hand, N., and Stewart, R. C. (2011). Identification of an anchor residue for CheA-CheY interactions in the chemotaxis system of *Escherichia coli*. *J. Bacteriol.*, 193(15):3894–3903.
- Tuntufye, H. N., Lebeer, S., Gwakisa, P. S., and Goddeeris, B. M. (2012). Identification of avian pathogenic *Escherichia coli* genes that are induced *in vivo* during infection in chickens. *Appl. Environ. Microbiol.*, 78(9):3343–3351.
- Ulrich, L. E., Koonin, E. V., and Zhulin, I. B. (2005). One-component systems dominate signal transduction in prokaryotes. *Trends Microbiol.*, 13(2):52–56.
- van den Esker, M. H., Kovacs, A. T., and Kuipers, O. P. (2017). YsbA and LytST are essential for pyruvate utilization in *Bacillus subtilis*. *Environ. Microbiol.*, 19(1):83–94.
- Vastermark, A., Wollwage, S., Houle, M. E., Rio, R., and Saier, M. H. (2014). Expansion of the APC superfamily of secondary carriers. *Proteins*, 82(10):2797–2811.
- Vemuri, G. N., Altman, E., Sangurdekar, D. P., Khodursky, a. B., and Eiteman, M. a. (2006). Overflow metabolism in *Escherichia coli* during steady-state growth: transcriptional regulation and effect of the redox ratio. *Appl. Environ. Microbiol.*, 72(5):3653–3661.
- Wang, H. and Gunsalus, R. P. (2003). Coordinate regulation of the *Escherichia coli* formate dehydrogenase *fdnGHI* and *fdhF* genes in response to nitrate, nitrite, and formate: roles for NarL and NarP. *J. Bacteriol.*, 185(17):5076–5085.
- Wanner, B. L. (1990). Phosphorus assimilation and control of the phosphate regulon. In Hauska, G. and Thauer, R. K., editors, *The molecular basis of bacterial metabolism*, pages 152–163. Springer Berlin Heidelberg.

- Weber, H., Polen, T., Heuveling, J., Wendisch, V. F., and Hengge, R. (2005). Genome-wide analysis of the general stress response network in *Escherichia coli*: σ^S -dependent genes, promoters, and sigma factor selectivity. *J. Bacteriol.*, 187(5):1591 – 1603.
- Wolanin, P. M., Thomason, P. A., and Stock, J. B. (2002). Histidine protein kinases: key signal transducers outside the animal kingdom. *Genome Biol.*, 3(10).
- Wong, F. H., Chen, J. S., Reddy, V., Day, J. L., Shlykov, M. A., Wakabayashi, S. T., and Saier, M. H. (2012). The amino acid-polyamine-organocation superfamily. *J Mol Microbiol Biotechnol*, 22(2):105–113.
- Wu, R., Gu, M., Wilton, R., Babnigg, G., Kim, Y., Pokkuluri, P. R., Szurmant, H., Joachimiak, A., and Schiffer, M. (2013). Insight into the sporulation phosphorelay: crystal structure of the sensor domain of *Bacillus subtilis* histidine kinase, KinD. *Protein Sci.*, 22(5):564–576.
- Yamamoto, K., Hirao, K., Oshima, T., Aiba, H., Utsumi, R., and Ishihama, A. (2005). Functional characterization *in vitro* of all two-component signal transduction systems from *Escherichia coli*. *J. Biol. Chem.*, 280(2):1448–1456.
- Yu, H., Mudd, M., Boucher, J., Schurr, M. J., and Deretic, V. (1997). Identification of the *algZ* gene upstream of the response regulator *algR* and its participation in control of alginate production in *Pseudomonas aeruginosa*. *J. Bacteriol.*, 179(1):187–193.
- Zoraghi, R., Corbin, J. D., and Francis, S. H. (2004). Properties and functions of GAF domains in cyclic nucleotide phosphodiesterases and other proteins. *Mol. Pharmacol.*, 65(2):267–278.

Supplemental Material - Chapter 2

Supplementary Material:

Identification of a High-Affinity Pyruvate Receptor in *Escherichia coli*

Stefan Behr^a, Ivica Kristoficova^a, Michael Witting^b, Erin J. Breland^c, Allison R. Eberly^d,
Corinna Sachs^a, Philippe Schmitt-Kopplin^b, Maria Hadjifrangiskou^{d,e}, Kirsten Jung^{a*}

^a Munich Center for Integrated Protein Science (CIPSM) at the Department of Microbiology, Ludwig-Maximilians-Universität München, 82152 Martinsried, Germany

^b Helmholtz Zentrum München, Deutsches Forschungszentrum für Gesundheit und Umwelt (GmbH), Research Unit Analytical BioGeoChemistry, 85764 Neuherberg, Germany

^c Departments of Pharmacology, Vanderbilt University Medical Center, Nashville, TN 37232, USA

^{d,e} Departments of Pathology, Microbiology & Immunology ^d and Urologic Surgery ^e, Vanderbilt University Medical Center, Nashville, TN 37232, USA

* To whom correspondence should be addressed: Dr. Kirsten Jung, Ludwig-Maximilians-Universität München, Department Biologie I, Bereich Mikrobiologie, Großhaderner Str. 2-4, 82152 Martinsried, Germany. Phone: +49-89-2180-74500; Fax: +49-89-2180-74520; E-mail: jung@lmu.de

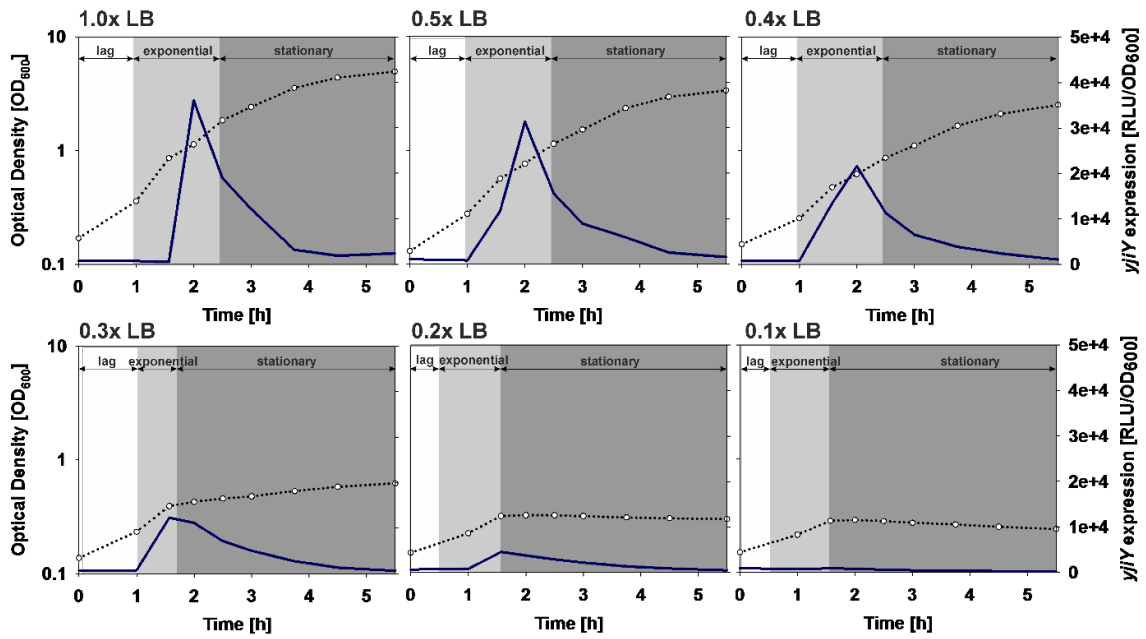


Fig. S1. Characterization of *yjiY* expression in different concentrations of LB medium.

Escherichia coli MG1655 / pBBR *yjiY*-lux was cultivated under aerobic conditions and growth and luminescence were measured over time. Expression of *yjiY* over growth of *E. coli* cells in 1.0x, 0.5x, 0.4x, 0.3x, 0.2x and 0.1x diluted LB. The growth phases of *E. coli* are marked as following: lag phase (white), exponential growth (light grey) and stationary phase (dark grey).

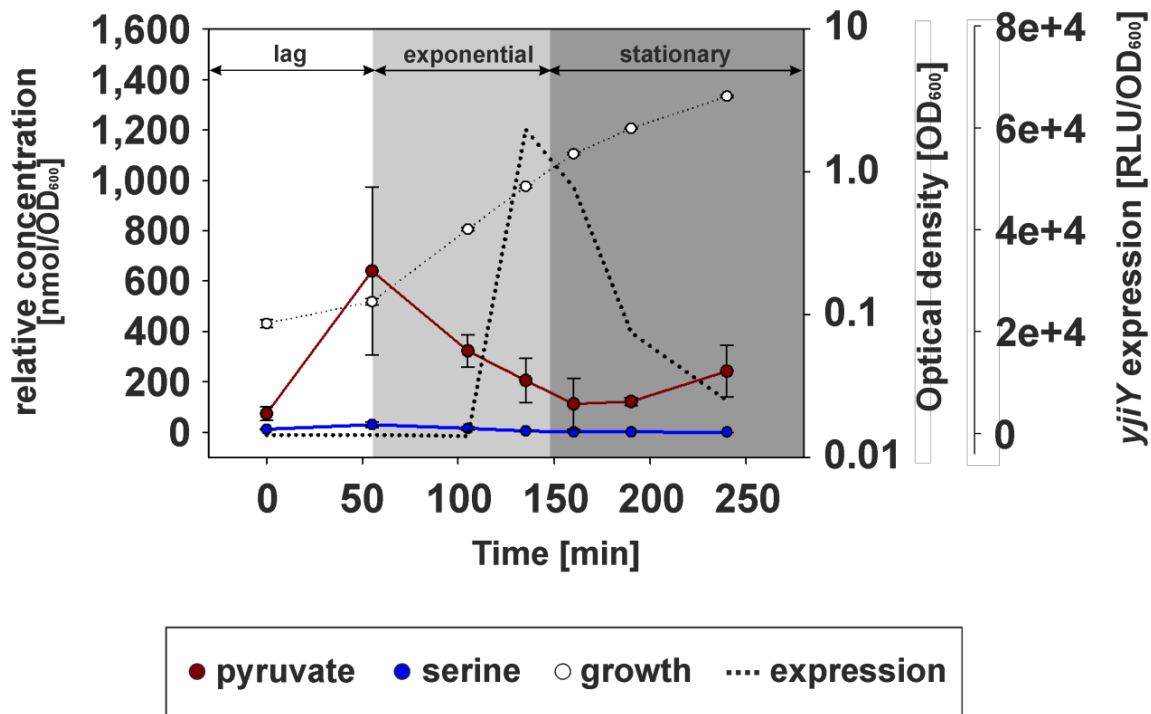


Fig. S2. Determination of changes in intracellular concentrations of serine and pyruvate during growth of *E. coli*. *E. coli* MG1655/pBBR *yjiY-lux* was cultivated in LB medium, and growth (OD₆₀₀) and luminescence were monitored. At the times indicated, cells were harvested, and serine and pyruvate levels were quantified by hydrophilic interaction liquid chromatography. All experiments were performed in triplicate, and the error bars indicate the standard deviation of the means. The growth phases of *E. coli* are marked as following: lag phase (white), exponential growth (light grey) and stationary phase (dark grey).

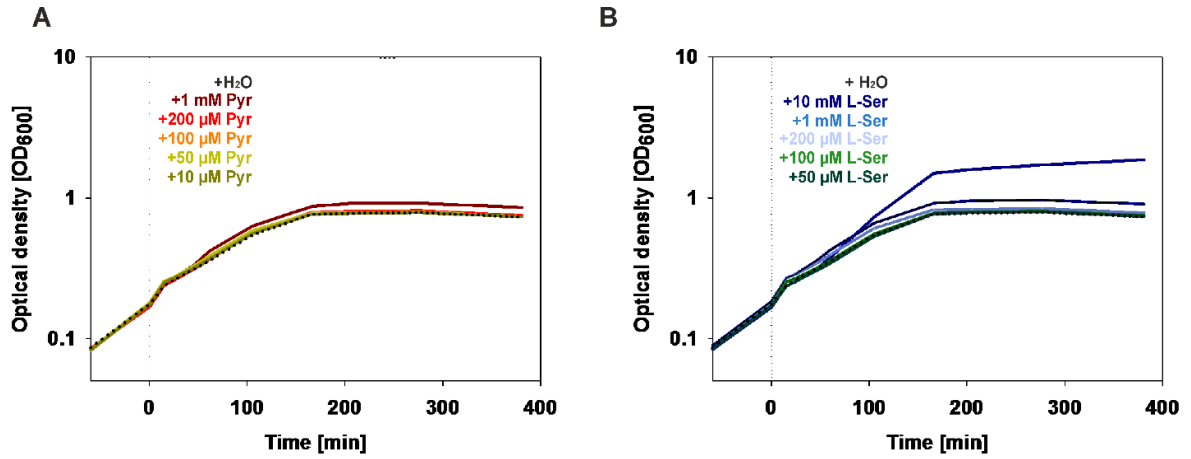


Fig. S3. Corresponding *E. coli* growth curves under nutrient-limiting conditions. *E. coli* MG1655 mutant $\Delta yhjX$ harboring pBBR *yjiY-lux* was cultivated in 0.1x LB medium. After 1 h (time point 0), the indicated concentration of pyruvate (A), or L-serine (B), or the equivalent volume of water was added. Growth was monitored over time.

Table S1. Summary of growth and *yjiY* expression data from *E. coli* cells grown in LB and diluted LB medium Growth rates for each time point (t(x)) were determined with $\mu = [\ln(\text{OD}_{600}(x)) - \ln(\text{OD}_{600}(x-1))] / [t(x) - t(x-1)]$.

Medium	Growth rate μ	max OD ₆₀₀	OD ₆₀₀ at max. <i>yjiY</i> expression	max. <i>yjiY</i> expression [RLU/OD ₆₀₀]
1.0x LB	1.27 h ⁻¹	4.96	1.13	36,009
0.5x LB	1.18 h ⁻¹	3.36	0.76	31,272
0.4x LB	0.95 h ⁻¹	2.53	0.62	21,629
0.3x LB	1.05 h ⁻¹	0.62	0.39	12,315
0.2x LB	0.75 h ⁻¹	0.3	0.28	4,536
0.1x LB	0.63 h ⁻¹	0.24	not detectable	no expression

Supplemental Material - Chapter 3

BtsT - a novel and specific pyruvate/H⁺ symporter in *Escherichia coli*

Ivica Kristoficova, Cláudia Vilhena, Stefan Behr^{*}, Kirsten Jung[#]

Munich Center for Integrated Protein Science (CIPSM) at the Department of Microbiology,
Ludwig-Maximilians-Universität München, 82152 Martinsried, Germany^a

To whom correspondence should be addressed: Dr. Kirsten Jung, Ludwig-Maximilians-Universität München, Department Biologie I, Bereich Mikrobiologie, Großhaderner Str. 2-4, 82152 Martinsried, Germany. Phone: +49-89-2180-74500; Fax: +49-89-2180-74520; E-mail: jung@lmu.de

* Present address: Stefan Behr, Roche Diagnostics GmbH, Nonnenwald 2, 82377 Penzberg

```

E. coli MDTKKIFKHI PWVILGII GA FCLAVVALRR GEHVSALWIV VASVSVYLLVA 50
S. enterica MDTKKIFKHI PWVILGII GA FCLSVVALRR GEHVSALWIV VASVSVYLLVA 50

E. coli YRYYSLYIAQ KVMKLDPTRA TPAVINNDGL NYVPTNRYVL FGHFFAAIAG 100
S. enterica YRYYSLYIAQ KVMKLDPTRA TPAVINNDGL NYVPTNRYVL FGHFFAAIAG 100

E. coli AGPLVGPVLA AQMGYLPGLT WLLAGVVLAG AVQDFMVLFI SSRRNGASLG 150
S. enterica AGPLVGPVLA AQMGYLPGLT WLLAGVVLAG AVQDFMVLFI SSRRNGASLG 150

E. coli EMIKEEMGPV PGTIALFGCF LIMIIILAVL ALIVVKALAE SPWGVFTVCS 200
S. enterica EMIKEEMGTV PGTIALFGCF LIMIIILAVL ALIVVKALAE SPWGVFTVCS 200

E. coli TVPIALFMGI YMRFIRPGRV GEVSVIGIVL LVASIFYGGV IAHDPYWGPA 250
S. enterica TVPIALFMGI YMRFIRPGRV GEVSVIGIVL LVASIFYGGV IAHDPYWGPA 250

E. coli LTFKDDTITF ALIGYAFVSA LLPWLI LAP RDTLATFLKI GVI VGLALGI 300
S. enterica LTFKDDTITF ALIGYAFVSA LLPWLI LAP RDTLATFLKI GVI VGLALGI 300

E. coli VVLNPELKMP AMTQYIDGTG PLWKGALFPF LFIT IACGAV SGFHALISSG 350
S. enterica VILNPELKMP ALTQYVDGTG PLWKGALFPF LFIT IACGAV SGFHALISSG 350

E. coli TTPKLLANEET DARF IGYGAM LME SFVAI MA LVAASIEEPG LYFAMNTPPA 400
S. enterica TTPKLLACEET DARF IGYGAM LME SFVAVMA LVAASIEEPG LYFAMNTPPA 400

E. coli GLGITMPNLH EMGGENAPII MAQLKDVTAH AAATVSSWGF VISPEQILQET 450
S. enterica GLGITMPNLH EMGGENAPLI MAQLKDVTAH AAATVSSWGF VISPEQILQET 450

E. coli AKDIGEPSVL NRAGGAPTLA VGIAHVFHKV LPMADMGFWY HFGILFEALF 500
S. enterica AKDIGEPSVL NRAGGAPTLA VGIAHVFHKV LPMADMGFWY HFGILFEALF 500

E. coli ILTALDAGTR SGRFMLQDLL GNFI PFLKKT DSLVAGIIGT AGCVGLWGYL 550
S. enterica ILTALDAGTR SGRFMLQDLL GNFI PFLKKT DSLVAGIIGT AGCVGLWGYL 550

E. coli LYQGVVDPLG GVKSLWPLFG ISNQMLAAVA LVLGTVVLIK MKRTQYI WVT 600
S. enterica LYQGVVDPLG GVKSLWPLFG ISNQMLAAVA LVLSTVVLIK MQRTKYI WVT 600

E. coli VVPVWLLIC TTWALGLKLF STNPQMEGFF YMASQYKEKI ANGTDLT AQQ 650
S. enterica VIPVWLLIC TTWALGLKLF SANPQMEGFF YMANLYKEKI ANGTDLT AQQ 650

E. coli IANMNHIVVN NYTNAGLSIL FLIVVYSIIF YGFKTWLAVR NSDKRTDKE T 700
S. enterica IANMNHIVVN NYTNAGLSIL FLVVVYSIIF YGFTTWMKVR NSDKRTDKE T 700

E. coli PYVP IPEGGV KISSHH 716
S. enterica PYVP VPEGGV KISSHH 716

```

Figure S1. Comparison of the BtsT consensus sequences of *E. coli* and *S. enterica*. A consensus-based approach sequence comparison was used. 148 sequences of BtsT of *E. coli* and 122 sequences of BtsT of *S. enterica* were aligned and consensus sequences for each bacterium were generated by using the CLC Main Workbench software. Subsequently, both consensus sequences were aligned. The amino acids were colored based on their polarity (red - acidic and polar; blue - basic and polar; green - neutral and polar; black - neutral and nonpolar). Red background color was used to highlight deviating amino acids.

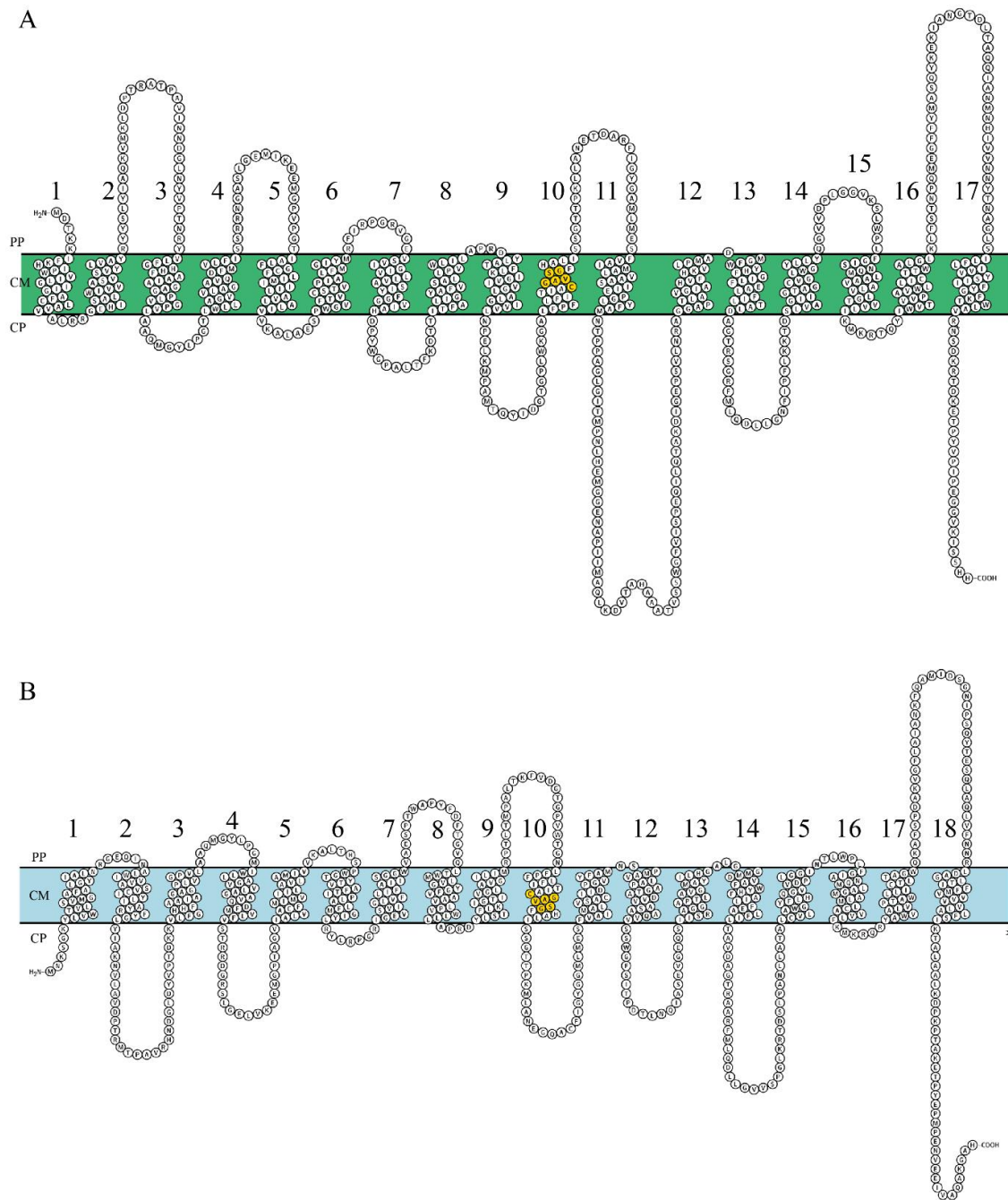


Figure S2. Schematic models of the secondary structure of (A) *E. coli* BstT and (B) *E. coli* CstA. Both models are based on the analysis of the secondary structure using the Uniprot program (1) and visualized with the Protter tool (2). Transmembrane domains (TMs) are numbered with numerals. The conserved motif CG-x(2)-SG with a high degree of sequence

conservation within CstA homologues is marked in yellow (3). PP periplasm, CM cytoplasmic membrane, CP cytoplasm.

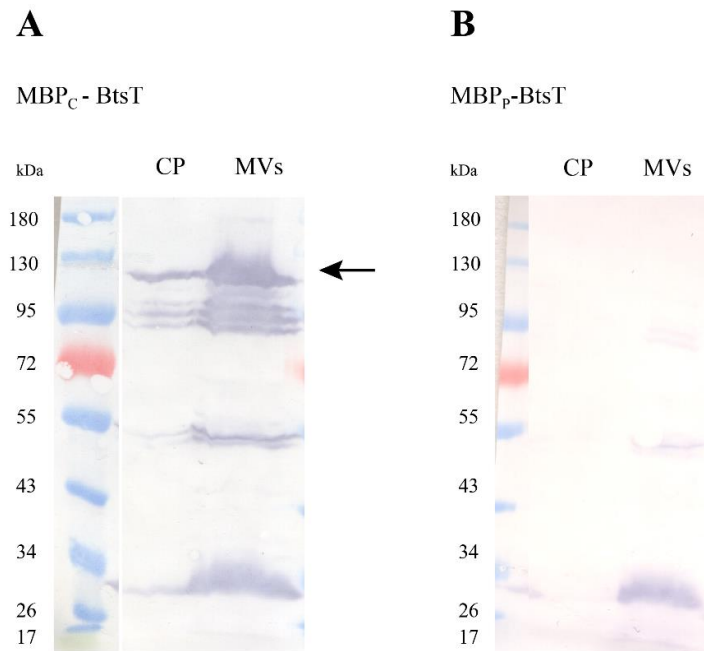


Figure S3. Localization of maltose-binding protein (MBP) hybrids. *malE* without or with leader sequence was fused to the 5' end of *btsT* encoding hybrid proteins with either a putative cytoplasmically located MPB (MBP_C-BtsT) (A) or a periplasmically located MBP (MBP_P-BtsT) (B), respectively. Cells with overproduced hybrids were fractionated to separate cytoplasm (CP) and membrane vesicles (MVs). Both fractions were adjusted to the same volume and separated by 12.5% (w/v) SDS-polyacrylamide gel electrophoresis and immunoblotted using a penta-His antibody for detection. The arrow indicates MBP_C-BtsT (about 120 kDa).

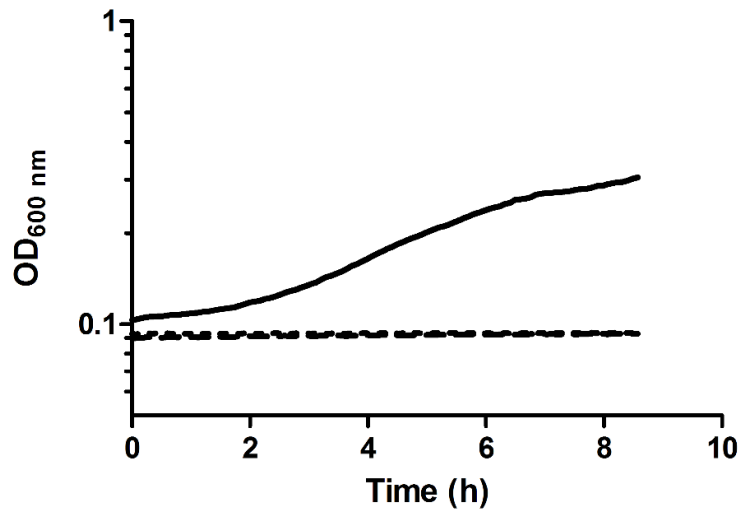


Figure S4. Complementation of *E. coli* MM39 with different MBP-BtsT hybrid proteins. *malE* deficient *E. coli* MM39 cells were transformed with plasmids pMAL-p2x (solid line), pMAL_P-*btsT* (dotted line) and pMAL_C-*btsT* (dashed line), and their growth was monitored over time on maltose as the sole carbon source.

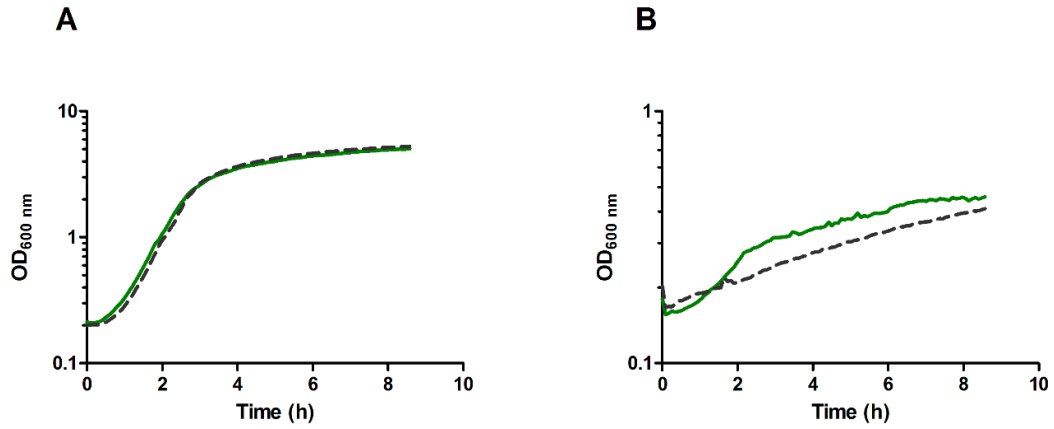


Figure S5. Growth of *E. coli* MG1655 and the *bstT* mutant in different media. *E. coli* MG1655 (green line) and *E. coli* MG1655 $\Delta bstT$ (dotted black line) were cultivated in LB medium (A) or in M9 minimal medium supplemented with pyruvate as carbon source (20 mM) (B). Samples were taken and analyzed every 5 min (A) or 2 hours (B).

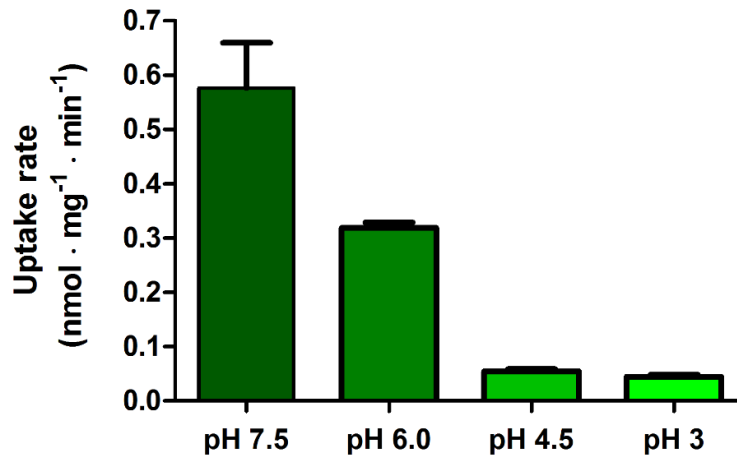


Figure S6. Rates of ¹⁴C-pyruvate uptake by BtsT-producing strain *E. coli* MG1655 $\Delta btsT$ pBAD24-*btsT* at various external pH values. ¹⁴C pyruvate was added at a final concentration of 10 μM .

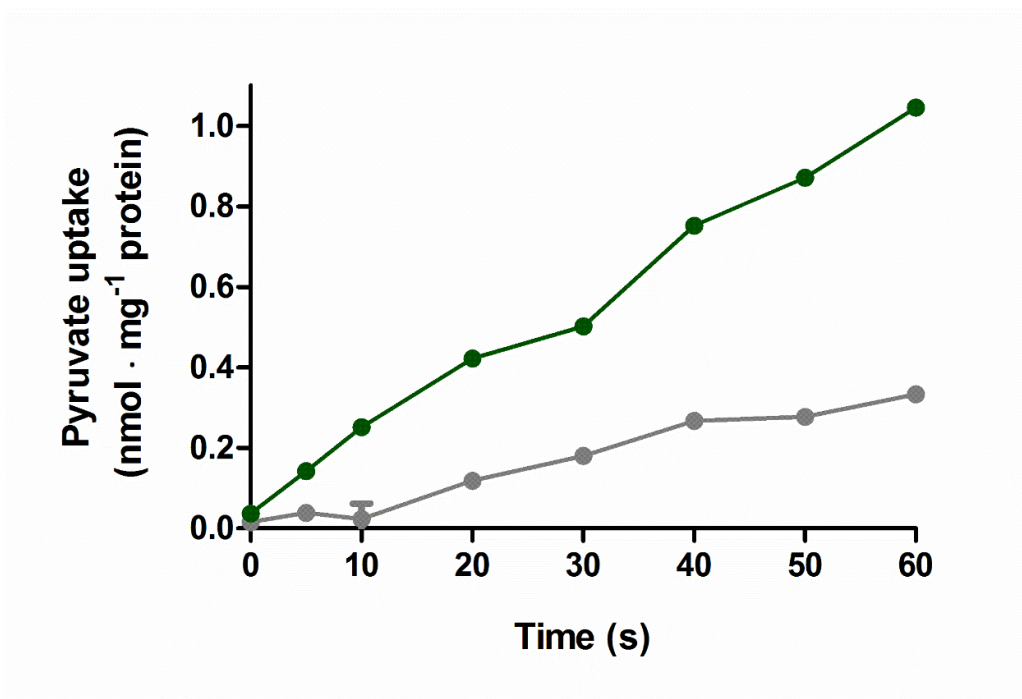


Figure S7. Time course of pyruvate uptake by *E. coli* YYC202. ¹⁴C-Pyruvate uptake was determined at a final pyruvate concentration of 10 μ M at 15°C. Rates of uptake accumulation: BtsT producing strain *E. coli* YYC202 pBAD24-*btsT* (green), control strain *E. coli* YYC202 pBAD24 (grey). Standard deviations are estimated from three biological replicates.

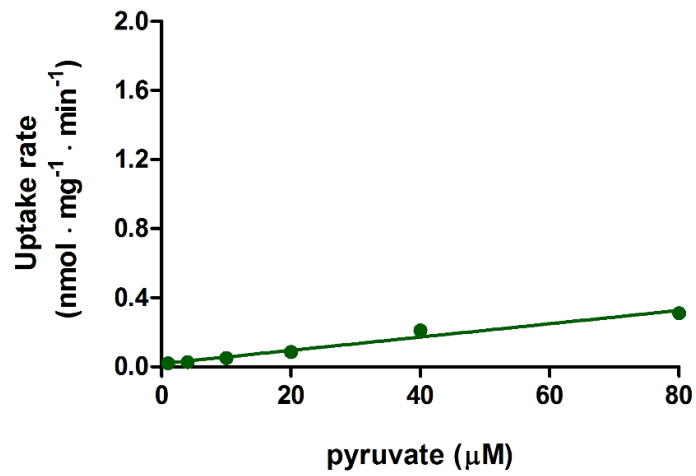


Figure S8. Pyruvate diffusion in intact *E. coli* cells. Uptake of ¹⁴C-pyruvate by *E. coli* MG1655 $\Delta btsT$ transformed with pBAD24 was determined in the presence of increasing pyruvate concentrations. The best-fit line was determined by linear regression. Error bars represent standard error of the mean.

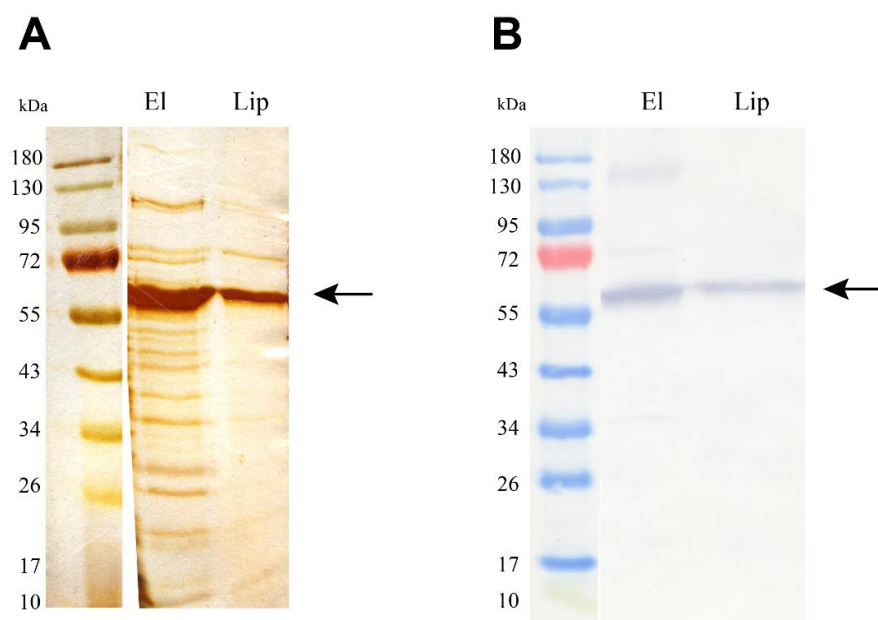


Figure S9. Purification of His-tagged BtsT. Membrane vesicles were prepared from *E. coli* cells after overproduction of BtsT-6His. Membrane proteins were then solubilized with 1.5% (w/v) n-dodecyl β -D-maltoside. The His-tagged BtsT was purified as described in Materials and Methods. El, BtsT eluted from the column with 300 mM imidazole (8.75 μ g of protein). Lip, BtsT reconstituted into *E. coli* liposomes (10 μ g of protein). Proteins were separated using 12.5% (w/v) SDS-polyacrylamide gel electrophoresis and stained with silver (A) or immunodetected by using a penta-His antibody (B). The arrows indicate BtsT-6His. In both images, non-relevant lanes were omitted for clarity.

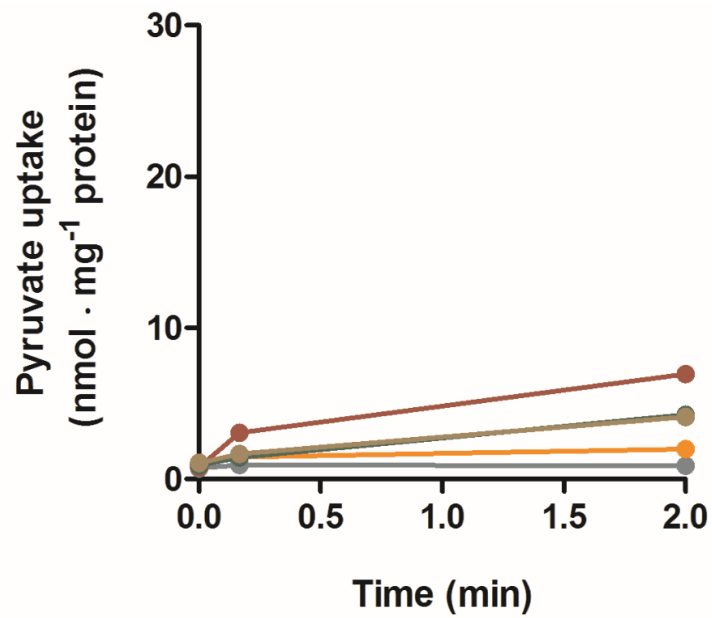


Figure S10. Pyruvate diffusion in *E. coli* liposomes. ^{14}C -pyruvate ($40\ \mu\text{M}$) diffusion was analyzed in liposomes (in the absence of protein). Time course of pyruvate uptake in the presence of artificially imposed $\Delta\tilde{\mu}_{H^+}$ (green), $\Delta\Psi$ (orange), ΔpH (red), $\Delta\tilde{\mu}_{Na^+}$ (brown) or in the absence of any gradient (grey).

REFERENCES

1. The UniProt Consortium. 2017. UniProt: the universal protein knowledgebase. *Nucleic Acids Res* 45:158–169.
2. Omasits U, Ahrens CH, Muller S, Wollscheid B. 2014. Protter: interactive protein feature visualization and integration with experimental proteomic data. *Bioinformatics* 30:884–886.
3. Vastermark A, Wollwage S, Houle ME, Rio R, Saier MH. 2014. Expansion of the APC superfamily of secondary carriers. *Proteins* 82:2797–2811.

Supplemental Material - Chapter 4

SUPPLEMENTARY MATERIAL

A single-cell view of the BtsSR/YpdAB pyruvate sensing network in *Escherichia coli* and its biological relevance

Cláudia Vilhena,^a Eugen Kaganovitch,^b Jae Yen Shin,^{a*} Alexander Grünberger,^{b*} Stefan Behr,^{a*}
Ivica Kristofcova,^a Sophie Brameyer,^{a*} Dietrich Kohlheyer,^b Kirsten Jung,^{a#}

Munich Center for Integrated Protein Science (CIPSM) at the Department of Microbiology, Ludwig-Maximilians-Universität München, Martinsried, Germany^a; Institute for Bio- and Geosciences, IBG-1: Biotechnology, Forschungszentrum Jülich GmbH, Jülich, Germany^b

Running Head: Phenotypic heterogeneity in *E. coli*

#Address correspondence to Kirsten Jung, jung@lmu.de

*Present address: Alexander Grünberger, Multiscale Bioengineering, Bielefeld University, Universitätsstraße 25, 33615 Bielefeld; Stefan Behr, Roche Diagnostics GmbH, Nonnenwald 2 82377 Penzberg; Jae Yen Shin, MPI of Biochemistry, Am Klopferspitz 18 82152 Martinsried; Sophie Brameyer, University College London, Gower Street, WC1E 6EA London

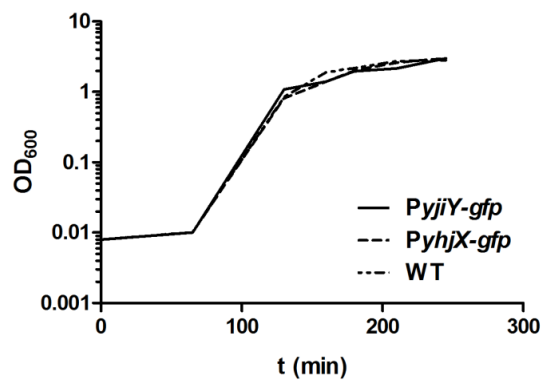


FIG S1 Growth of reporter strains. *E. coli* cells expressing *gfp* under the control of P_{yhjX} or P_{yjiY} and the MG1655 strain (WT, without promoter-*gfp* fusion) were grown in LB medium.

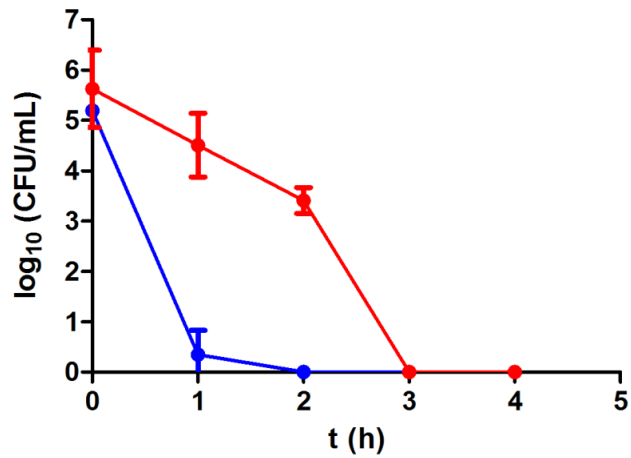


FIG S2 Determination of the minimum duration of killing (MDK) after ofloxacin treatment. *E. coli* cells of either WT (blue line) or mutant *ΔbtsSRypdAB* (red line) were grown in LB-medium. At the post-exponential growth phase cells were challenged with ofloxacin (5 μg/ml). Samples were taken and analyzed for colony forming units (CFUs). The MDK₉₉ value was taken as the time needed to kill 99% of the initial population. Experiments were performed three independent times and error bars indicate the standard deviations of the means.

STRAINS	- INDUCER		+ INDUCER	
	Cells (%)		Cells (%)	
	OFF	ON	OFF	ON
WT GFP (IPTG)	92.7	7.3	3.1	96.9
<i>btsSRypdAB</i> GFP (IPTG)	97.8	2.2	51.0	49.0
WT GFP-DppA (Arabinose)	94.9	5.1	24.4	75.6
<i>btsSRypdAB</i> GFP-DppA (Arabinose)	98.1	1.9	99.4	0.6
WT LysP-mCherry (Arabinose)	97.7	2.3	33.4	66.6
<i>btsSRypdAB</i> LysP-mCherry (Arabinose)	98.2	1.8	98.5	1.5

TABLE S1 The BtsSR/YpdAB network promotes overproduction of proteins. *E. coli* cells of either WT or the *btsSRypdAB* mutant harboring an overproduction vector with IPTG inducible promoter for the overproduction of GFP; an arabinose inducible promoter for the overproduction of DppA-GFP and an arabinose inducible promoter for the overproduction of LysP-mCherry were grown in LB medium. Samples were taken before (- inducer) and after (+ inducer) the addition of the inducer. Flow cytometry was used to count fluorescent cells (maximum of 2000

events), and the percentages of OFF (non-fluorescent cells) and ON cells (fluorescent cells) were calculated from the raw data. Experiments were performed three independent times and standard deviations were below 10%.

Acknowledgements

Looking back almost 4 years since I came to Munich, it was an amazing experience! I would like to thank all people who supported my research and made this thesis possible.

First, I would like to acknowledge the contribution of Prof. Kirsten Jung, who gave me the opportunity of doing scientific research in AG K Jung and for all the patient advice. Thanks goes to my TAC committee members, Prof. Marc Bramkamp and Prof. Jürgen Soll, for all their contribution and help to bring my PhD to its final form. Special thanks also to my thesis committee members, Prof. Wolfgang Enard, Prof. Jörg Nickelsen and Prof. Boshart for generously offering their time to examine my PhD thesis. I would also like to thank Prof. Heinrich Jung for all insightful conversations, and to Francisca Mende and all the members of LSM graduate school.

I am so glad for meeting so many interesting people over 4 years. Thanks to all YehUT team members, Stefan, Florian and all our students, my office mates Wolfram, Ralph and Felix and of course, my friends Ana, Bruno, Yang and Kim. It was an amazing time with you all. I would like to specially thank Cláudia, my YehUT team colleague, office mate, reviewer, secretary, business partner but most importantly, my best friend.

Last but not least, I consider myself very fortunate for all the support of my parents. And my last thanks goes to Stanislav, the one who was there for me all the time.



Ivica Krištofičová

Curriculum Vitae

Education

- 2014–Present **PhD in Microbiology**, *Ludwig Maximilians University, Munich, Germany.*
- Student of The Graduate School Life Science Munich (LSM)
 - Supervisor:
 - Prof. Kirsten Jung
 - PhD. Project:
 - Biochemical characterisation of a two-component system BtsS/BtsR by in vivo and in vitro studies in *Escherichia coli*.
 - Publications:
 - Identification of a High-Affinity Pyruvate Receptor in *Escherichia coli* Sci Rep 2017
- 2011–2013 **Masters of Biochemistry**, *Charles University in Prague, Prague, Czech Republic.*
- Supervisors:
 - Marek Ingr PhD.
 - Doc. Jan Konvalinka
 - Diploma thesis:
 - Study of the cleavage kinetics of Gag polyprotein from HIV-1 virus by the viral protease.
- 2008–2011 **Bachelor of Biochemistry**, *Comenius University, Bratislava, Slovakia.*
- Supervisor:
 - Prof. Jozef Nosek
 - Bachelor thesis:
 - Quorum Sensing - communication of bacteria and its application in synthetic biology.

Work

- 2011–2013 **Scientist**, *Institute of Organic Chemistry and Biochemistry, Prague, Czech Republic.*

I have joined there a research group under the supervision of Doc. Jan Konvalinka, that deals with the analysis, structure, activity and inhibition of proteases and other enzymes that are medically important.

Wurmstraße 58 – Gräfelfing 82166, Germany

☎ +49 176 35363437 • ✉ ivica.kristoficova@gmail.com

📄 [linkedin.com/in/ivicakristoficova](https://www.linkedin.com/in/ivicakristoficova)

Awards

- 2016 Annual Conference 2016 of VAAM at Jena, Germany, Best Poster Presentation
- 2009–2010 Comenius University, Scholarship for excellent study results (top 10 % of students)
- 2008 Comenius University, Scholarship for excellent study results (top 5 % of students)

Skills

- Certificates Purification and Characterization of proteins, Malvern Instruments (2016), Hands-on training course NGS data analysis (2016), Workshop on "Sensory and regulatory RNAs in prokaryotes" (2016), MicroCal Course Advanced Isothermal Titration Calorimetry (2015)
- Soft skills Workshop "Presentation skills (Natural sciences and medical research)" (2015), Workshop "Writing and publishing of papers, reviews and theses in the life sciences" (2015), Workshop " Leadership Skills" (2015)
- Other L^AT_EX, Adobe Illustrator

Academic Meetings

- 2017 Attended SPP1617-progress report meeting in München, Germany
- 2017 Talk at the VAAM conference in Würzburg, Germany
- 2016 Attended SPP1617-progress report meeting in Düsseldorf, Germany
- 2016 Poster at the VAAM conference in Jena, Germany
- 2015 Poster at the 77th Harden Conference: Two Component Signalling in Bacteria: Integrating Approaches and Science in Warwick, UK
- 2015 Attended CAS Conference Synthetic Biology II in München, Germany
- 2015 Poster at the VAAM conference in Marburg, Germany
- 2015 Poster at the Blast XIII conference in Tucson, USA

Languages

- Mothertongue **Slovak**
- Advanced **English, Czech**
- Intermediate **German**

Interests

- Literature
- Movies
- Driving (B category)
- Travelling
- Taking pictures